

1-1-1997

## **Modification, characterization and application of hyperbranched polyarylates.**

Bodan Ma  
*University of Massachusetts Amherst*

Follow this and additional works at: [https://scholarworks.umass.edu/dissertations\\_1](https://scholarworks.umass.edu/dissertations_1)

---

### **Recommended Citation**

Ma, Bodan, "Modification, characterization and application of hyperbranched polyarylates." (1997).  
*Doctoral Dissertations 1896 - February 2014*. 958.  
<https://doi.org/10.7275/p8mh-gz81> [https://scholarworks.umass.edu/dissertations\\_1/958](https://scholarworks.umass.edu/dissertations_1/958)

This Open Access Dissertation is brought to you for free and open access by ScholarWorks@UMass Amherst. It has been accepted for inclusion in Doctoral Dissertations 1896 - February 2014 by an authorized administrator of ScholarWorks@UMass Amherst. For more information, please contact [scholarworks@library.umass.edu](mailto:scholarworks@library.umass.edu).

UMASS/AMHERST



312066 0264 0664 8

# MODIFICATION, CHARACTERIZATION AND APPLICATION OF HYPERBRANCHED POLYARYLATES

A Dissertation Presented

by

BODAN MA

Submitted to the Graduate School of the  
University of Massachusetts Amherst in partial fulfillment  
of the requirements for the degree of

DOCTOR OF PHILOSOPHY

May 1997

Department of Polymer Science and Engineering

© Copyright by Bodan Ma 1997

All Rights Reserved

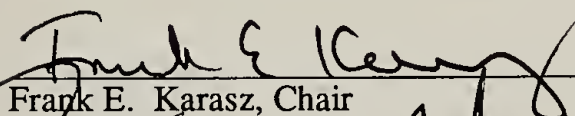
# MODIFICATION, CHARACTERIZATION AND APPLICATION OF HYPERBRANCHED POLYARYLATES

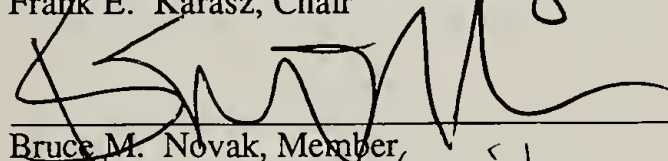
A Dissertation Defense Presented

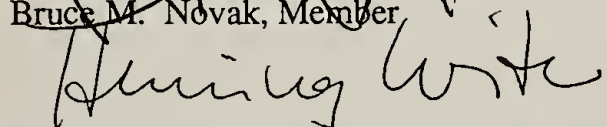
by

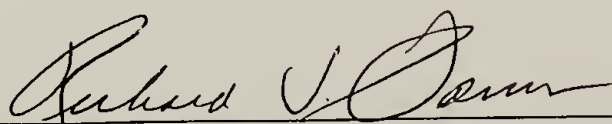
BODAN MA

Approved as to style and content by:

  
Frank E. Karasz, Chair

  
Bruce M. Novak, Member

  
Henning H. Winter, Member

  
Richard J. Farris, Department Head  
Polymer Science and Engineering

Dedicated to my family, whose unconditional love and support  
made all the hard work and endurance worthwhile.

## ACKNOWLEDGMENTS

I wish to express my deepest gratitude for the mentorship of Professor Karasz. Your patience and inspiration throughout my residency has not only enriched my knowledge, but also brightened my understanding of life.

I would like to extend my appreciation to Professor Novak and Professor Winter for your time and your interest in serving in my committee. Your high academic standard has been tremendously beneficial to my education.

The memories I shall cherish most are of the friendships which were nurtured here. There are truly some special friendships I am honored to acknowledge: Dave, you have been a true friend to me. I can not imagine how I could have adjusted to life in America without your generous help, and I wish you the best of everything. Michael, you have been like a brother to me throughout the years, and I wish you and your newly expanded family all the happiness in the world.

I would like to acknowledge Dr. Charles Dickinson for his guidance on NMR experiments. I would like to thank Dr. Lothar Franke of Lark Enterprise for performing preparative GPC. I would like to extend my appreciation to Dr. Wolfgang Wedler for the guidance on the rheology experiments. I would like to acknowledge Dr. Zhou Yang for his guidance and discussion on synthesis of etherimide.

I would like to thank my fellow students, Thomas Hahn, Mike Chen, Marian Mours, Zhaohui Su, Andrew Bushelman, Yuanqiao Rao and Xin Jin for the help you offered during my research and the completion of this thesis. I would like to thank all the members in Karasz research group for the wonderful time we had together.

Finally, I would like to thank my beloved family: my grandmother and aunt, who brought me up and taught me the first lessons of life; my parents, who are always my role models and the source of continuous support; and my brother, who is always there for me. Moment by moment in the years to come, I hope I can give back all you have given me.

## ABSTRACT

### MODIFICATION, CHARACTERIZATION AND APPLICATION OF HYPERBRANCHED POLYARYLATES

MAY 1997

BODAN MA, B.S., TSINGHUA UNIVERSITY

M.S., UNIVERSITY OF MASSACHUSETTS AMHERST

Ph.D., UNIVERSITY OF MASSACHUSETTS AMHERST

Directed by: Professor Frank E. Karasz

Hyperbranched polymers are polymers with highly branched, yet non-crosslinked structures. In this work, the existing laboratory polymerization procedure was scaled up by a suspension method to synthesize hyperbranched poly(5-acetoxy isophthalic acid) of high molecular weight. A method of modifying the residual acyl groups of this polymer with different reagents was also established. Especially, the synthesis of monofunctional etherimide facilitated the compatibilization of the hyperbranched polyarylate with commercial polyetherimide. All modified polymers were characterized by FTIR,  $^1\text{H}$  and  $^{13}\text{C}$  NMR, elemental analysis and DSC. Through this modification route, hyperbranched polymers with glass transition temperatures ranging from  $-50^\circ\text{C}$  to  $188^\circ\text{C}$  were prepared. Using fractionation techniques, samples with different molecular weights were obtained.

The structural profiles of hyperbranched polyarylate were then investigated. The measurement of the degree of branching indicated that these macromolecules had uniform chemical structures. Solution static light scattering revealed that the hyperbranch polyarylates had very compact structures, the dimension of which remained stable regardless of different polymer-solvent interactions. Light scattering, NMR with LSR (Lanthanide Shift Reagent) as well as molecular simulation showed that molecules such as LSR ( $d \sim 10 \text{ \AA}$ ) and solvent could penetrate most part of the

structure. Thus, these molecules should be treated as hard porous particles with small pore sizes.

n-Butyl hyperbranched polyarylate and its linear analog poly(1,4-butylene isophthalate) were employed to investigate the effect of hyperbranching topology on blend properties. Under all experimental conditions, including a wide range of annealing temperature, molecular weight and blend composition, the blends were found always immiscible by the observation of glass transitions using DSC. Entropically, the compact nature of the hyperbranched polymer prevented itself from mixing with its linear analog at segmental scale. However, TEM revealed that the domain size of the phase separation was around 400 to 600 Å, indicating good compatibility. A modified Flory-Huggins theory was introduced to explain the immiscibility.

The rheological properties of hyperbranched polymer and its blends presented the most promising aspect for future applications. The relaxation spectrum of hyperbranched polyarylate did not exhibit a plateau zone that is an indication of chain entanglement for linear polymers. This observation was true even for samples with molecular weight over  $10^5$ . Zero shear viscosity of hyperbranched polyarylate was generally one magnitude lower than that of its linear analog with comparable molecular weight. Furthermore, the viscosities of their blends showed negative deviations from the so-called “log-additivity rule”. This finding showed a true opportunity for hyperbranched polymers to be used as rheology modifiers.

Finally, the mechanical property of blends of etherimide modified hyperbranched polyarylate and polyetherimide was investigated. While the tensile modulus of the material was enhanced, the toughness was drastically reduced due to the lack of entanglement between the macromolecules. Possible methods for improving this drawback were proposed.

# TABLE OF CONTENTS

	Page
ACKNOWLEDGMENTS.....	v
ABSTRACT.....	vi
LIST OF TABLES .....	x
LIST OF FIGURES.....	xi
CHAPTER	
1. INTRODUCTION.....	1
References .....	9
2. PREPARATION OF HYPERBRANCHED POLYARYLATES WITH NARROW MOLECULAR WEIGHT DISTRIBUTION.....	13
Introduction .....	13
Experimental .....	15
Synthesis and Modification of Poly(5-acetoxysisophthalic acid).....	15
Fractionation.....	18
Characterization.....	18
Results and Discussion.....	19
Suspension Polymerization .....	19
Modification .....	20
Fractionation.....	20
Conclusions .....	21
References .....	27
3. MOLECULAR PARAMETERS OF HYPERBRANCHED POLYARYLATES.....	28
Introduction .....	28
Experimental .....	30
Nuclear Magnetic Resonance (NMR) .....	30
Static Light Scattering.....	31
Molecular Simulation.....	31
Dynamic Mechanical Measurement.....	31
Results and Discussion.....	32
Degree of Branching .....	32
Effect of Lanthanide Shift Reagent.....	34
Static Light Scattering.....	35

	Molecular Simulation .....	39
	Dynamic Mechanical Analysis.....	40
	Conclusion.....	41
	References .....	54
4.	BLEND OF N-BUTYL HYPERBRANCHED POLYARYLATE AND POLY(1,4-BUTYLENE ISOPHTHALATE).....	56
	Introduction .....	56
	Experimental .....	58
	Sample Preparation.....	58
	Differential Scanning Calorimetry (DSC).....	58
	Transmission Electron Microscopy (TEM).....	59
	Dynamic Mechanical Analysis.....	59
	Results and discussion.....	60
	Miscibility of BuHP/PBuI Blends.....	60
	Morphology of BuHP/PBuI blends .....	63
	Dynamic mechanical analysis .....	64
	Conclusion.....	65
	References .....	77
5.	ETHERIMIDE MODIFIED HYPERBRANCHED POLYARYLATE.....	78
	Introduction .....	78
	Results and Discussion.....	79
	Synthesis of [AB] Type Polyetherimide .....	79
	Thermal Analysis .....	84
	Morphology of Blend .....	84
	Mechanical Properties .....	84
	Experimental .....	86
	Synthesis.....	86
	Blend Sample Preparation .....	89
	Thermal Analysis .....	89
	Transmission Electron Microscopy.....	89
	Mechanical Testing .....	90
	Conclusion.....	90
	References .....	100
6.	CONCLUSIONS AND SUGGESTED FUTURE WORK.....	101
	Conclusions .....	101
	Suggested future work.....	104
	BIBLIOGRAPHY .....	106

## LIST OF TABLES

Table	Page
1.1 Comparison among highly branched polymers with different topology.....	7
2.1 Fractionation results of hyperbranched polyarylates.....	26
3.1 dn/dc values for static light scattering.....	31
3.2 Polymer-solvent interaction parameters.....	36
3.3 $\psi$ values for different polymer-solvent interactions.....	39
5.1 DSC of EIHP/PEI 50/50 wt% blend.....	84
5.2 Tensile properties of EIHP/PEI blend.....	85

## LIST OF FIGURES

Figure		Page
1.1	Scheme I, formation of hyperbranched structure .....	1
1.2	Scheme II, condensation of benzyl chloride .....	2
1.3	Structure of amylopectin .....	2
1.4	Structure of dendritic polymer .....	3
1.5	Structure of microgel.....	4
2.1	Scheme I, condensation of 5-acetoxyisophthalic acid.....	13
2.2	Scheme II, formation and hydrolysis of anhydride .....	14
2.3	Scheme III, modification of poly(5-acetoxyisophthalic acid).....	14
2.4	<sup>1</sup> H NMR of MeHP .....	22
2.5	<sup>1</sup> H NMR of PhHP .....	23
2.6	<sup>1</sup> H NMR of BuHP.....	24
2.7	<sup>1</sup> H NMR of EhHP .....	25
3.1	Structure of Eu(fod) <sub>3</sub> .....	30
3.2	<sup>1</sup> H NMR peak identification of aromatic protons of EhHP.....	42
3.3	Dependence of degree of branching on degree of polymerization.....	43
3.4	Effect of LSR on <sup>1</sup> H NMR of EhHP (M <sub>n</sub> =21,400).....	44
3.5	Dependence of root mean square radius of gyration $\langle R_g^2 \rangle^{1/2}$ on weight average molecular weight (M <sub>w</sub> ) (measured in dioxane at 15°C) .....	45
3.6	Dependence of root mean square radius of gyration $\langle R_g^2 \rangle^{1/2}$ on weight average molecular weight (M <sub>w</sub> ) (Measured with MeHP at 15°C) .....	46
3.7	Dependence of the second virial coefficient (A <sub>2</sub> ) on weight average molecular weight (M <sub>w</sub> ) (measured in dioxane at 15°C) .....	47
3.8	Dependence of the second virial coefficient (A <sub>2</sub> ) on weight average molecular weight (M <sub>w</sub> ) (measured with MeHP at 15°C).....	48
3.9	Molecular simulation results .....	49
3.10	Mastercurves of BuHP and PBuI (T <sub>ref</sub> =T <sub>g</sub> +80°C) .....	50
3.11	Dynamic viscosity of BuHP and PBuI (T <sub>ref</sub> =T <sub>g</sub> +80°C).....	51

3.12	Relaxation spectra of BuHP and PBuI .....	52
3.13	Mastercurves of BuHP of $M_w=16,500$ and $283,000$ ( $T_{ref}=120^\circ\text{C}$ ) .....	53
4.1	DSC traces for BuHP/PBuI blends of different compositions .....	66
4.2	DSC traces for BuHP/PBuI (50/50) blend with BuHP of different molecular weight .....	67
4.3	Modified lattice model .....	68
4.4	Micrograph of BuHP/PBuI 20/80 (wt%) blend.....	69
4.5	Micrograph of BuHP/PBuI 40/60 (wt%) blend.....	70
4.6	Micrograph of BuHP/PBuI 60/40 (wt%) blend.....	71
4.7	Mastercurve of BuHP/PBuI 50/50 (wt%) blend.....	72
4.8	Relationship between $G'$ and $G''$ .....	73
4.9	Dependence of frequency reduction parameter $a_T$ on temperature $T$ .....	74
4.10	Dependence of $\eta_0$ on blend composition.....	75
4.11	Dependence of fractional free volume $f$ on blend composition .....	76
5.1	Scheme I, commercial polyetherimide and its synthesis.....	80
5.2	Structures of monomer I and monomer II.....	80
5.3	Scheme II, synthesis of monomer I.....	81
5.4	Scheme III, in-situ condensation polymerization of monomer I.....	81
5.5	Scheme III, synthesis of AB type polyetherimide.....	82
5.6	Structure of side product (1') .....	83
5.7	TEM micrograph of 40/60 EIHP/PEI blend.....	91
5.8	$^{13}\text{C}$ NMR of monomer I.....	92
5.9	FTIR of polymerization of monomer I.....	93
5.10	$^{13}\text{C}$ NMR of intermediate (1).....	94
5.11	$^{13}\text{C}$ NMR of intermediate (2).....	95
5.12	$^{13}\text{C}$ NMR of monomer II.....	96
5.13	FTIR of polymerization of monomer II .....	97

5.14	$^{13}\text{C}$ NMR of AB type polyetherimide.....	98
5.15	GPC trace of fractionation of EIHP .....	99

# CHAPTER 1

## INTRODUCTION

Hyperbranched polymer is a group of branched polymers based on  $AB_x$  ( $x \geq 2$ ) type monomers in which A may condense with B, but reactions between like functional groups are forbidden as is shown in Figure 1.1 for a polymer of  $AB_2$  type monomer.

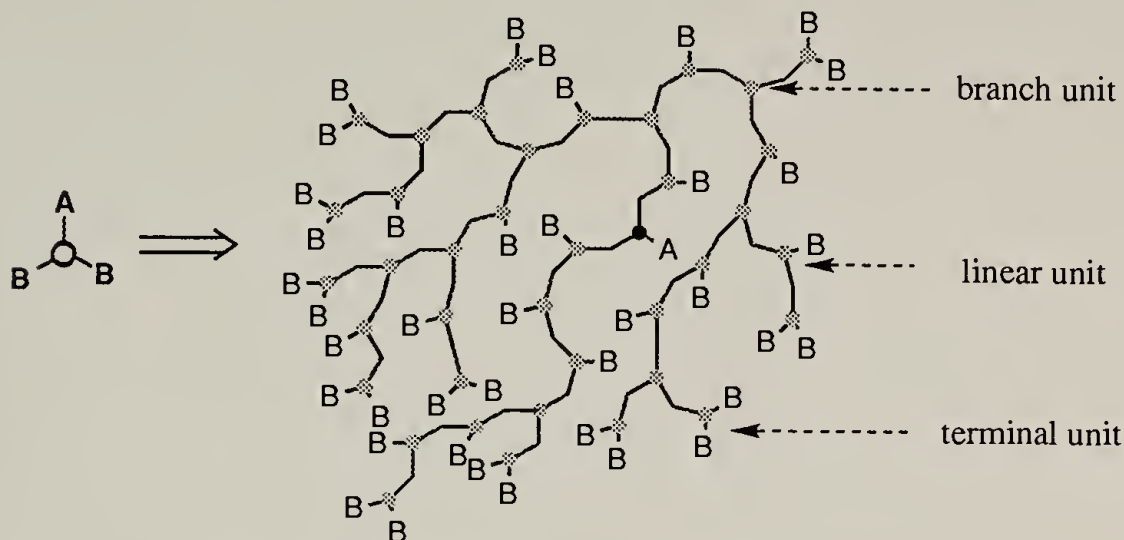


Figure 1.1: Scheme I, formation of hyperbranched structure

Three major units can be identified in the above hyperbranched structure, namely branch unit, linear unit and terminal unit. The term “Degree of Branching”<sup>1</sup> was used to quantify the branching density of the structure.

$$\text{Degree of Branching} = \frac{\text{branch units} + \text{terminal units}}{\text{branch units} + \text{terminal units} + \text{linear units}}$$

Although the terminology “hyperbranch” did not appear in literature until the early 90s, the history of this polymer group is just as long as polymer science itself. As early as 1885, Friedel and Crafts<sup>2</sup> observed the condensation of benzyl chloride in the presence of aluminum chloride. Part of the polymer obtained by this reaction was described as soluble resinlike material. It was later found<sup>3</sup> that this material was non-crystalline, and immiscible with pyroxylin, cellulose acetate, polyvinyl acetate,

polyvinyl chloride or with glyptyl resins. The structure of this polymer was doubtlessly described as

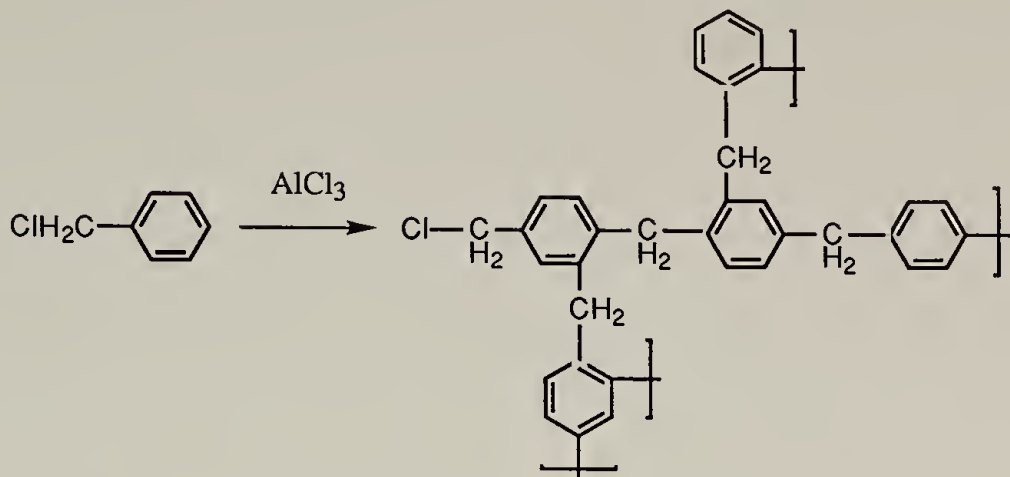


Figure 1.2: Scheme II, condensation of benzyl chloride

Hyperbranched structures are also abundant in natural polymers. In the amylopectin fraction of starch, for example, most of the units are bifunctional 1,4- $\alpha$ -anhydroglucose, but one unit in every 15 to 20 consists of a trifunctional 1,4,6- $\alpha$ -glucose branched unit. The structure of amylopectin according to Meyer<sup>4</sup> is shown in Figure 1.3.

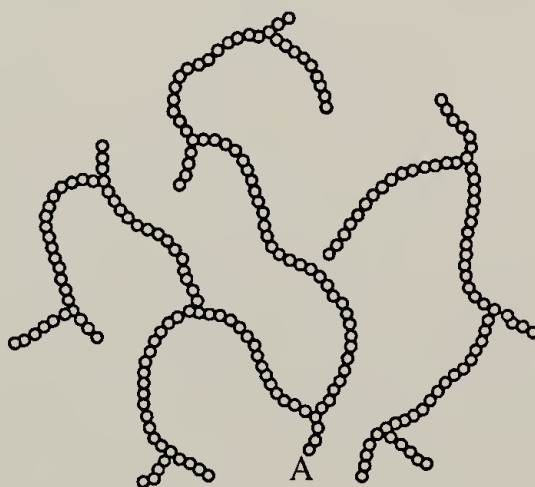


Figure 1.3: Structure of amylopectin

The single reducing end group is indicated by A; all other terminal units are attached at 1-position only.

In the early 50s, Flory<sup>5</sup> recognized the special feature of these polymers and statistically calculated the molecular weight and its distribution of such a system. Although the concept has long been in existence, hyperbranching molecular topology was not investigated as a way to design new material until recently due to the development of dendritic polymers and microgels. These three polymer groups share some common characteristics such as submicron size and highly branched structure. In the meantime, each of them has its own special features. Dendritic polymers are synthesized via such a controlled strategy<sup>6,7</sup> that they have a generationalized perfect structure shown in Figure 1.4. The degree of branching of a dendritic polymer according to the previous definition is always 100%. There is no linear unit in the structure. Because of this highly controlled topology, there exists a molecular weight limit above which the perfect growth of an additional generation can not be sustained.

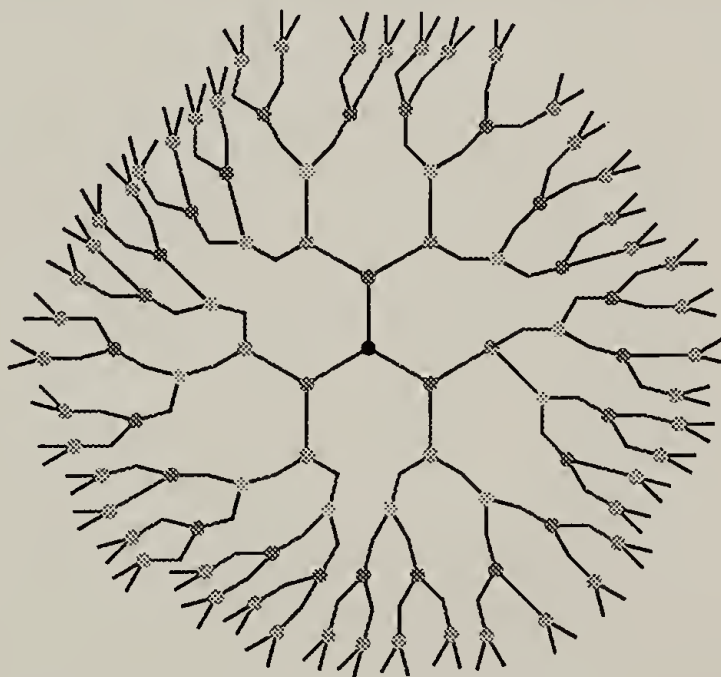


Figure 1.4: Structure of dendritic polymer

Microgels (shown in Figure 1.5) are crosslinked polymer networks synthesized by emulsion polymerization process<sup>8</sup>. Because of the presence of a network, unlike the other two polymer groups, the branch unit content is always greater than the terminal unit content. There is also no limit for the growth of an individual microgel particle.



Figure 1.5: Structure of microgel

Similar to dendritic polymers, hyperbranched polymers do not have network formation. However, they can have an infinite growth of molecular weight just like microgels.

All these three groups of highly branched, highly functionalized polymers are perceived to have extensive applicational potentials as drug delivery systems<sup>7,9,10,11</sup>, catalytic group carriers<sup>12,13,14,15</sup> for chemical reactions, and rheology modifiers in coating<sup>7,16</sup> and polymer processing<sup>17</sup>. Compared with dendrimers and microgels, hyperbranched polymers have the advantage of requiring no special treatment during polymerization process, such as the protecting-deprotecting synthesis of dendrimers and the emulsion polymerization of microgels. The polymerization can be completed in one step. Therefore, it will be both interesting in academics and important in application to study in detail the properties of this unique group of new material.

Unlike the tremendous efforts in dendritic polymer synthesis<sup>18-44</sup>, only a few  $AB_2$  type monomers have been polymerized to form hyperbranched polymers. These polymers are polyarylates<sup>45-49</sup>, polyethers<sup>50,51</sup>, polyamines<sup>52</sup>, poly(siloxysilanes)<sup>53</sup>, polyphenylenes<sup>54</sup>, polycarbozoles<sup>55</sup> and poly(acrylic acid)s<sup>56</sup>. Amongst them, poly(aryl ester)s or polyarylates based on 5-acetoxisophthalic acid and 3,5-diacetoxybenzoic acid are getting most of the attention. There have been even fewer publications on the

properties of hyperbranched polymers. In addition to the glass transition temperatures ( $T_g$ ) of hyperbranched polyarylates, Turner et al<sup>47</sup> reported an  $\alpha$  value smaller than 0.5 in the Mark-Houwink equation  $[\eta]=KM^\alpha$ , indicating that the macromolecule had a compact structure. Kim et al<sup>57</sup> and Connolly et al<sup>58</sup> found the  $T_g$  of a hyperbranched polymer was affected to a large extent by the terminal groups. Blends of hyperbranched polymer and linear polymers were also studied. Kim et al<sup>54</sup> investigated the blend of hyperbranched polyphenylene and linear polystyrene up to 5 wt% hyperbranched polymer content. The viscosity of the polystyrene was reduced while the modulus was increased. Massa et al<sup>59</sup> reported that hyperbranched polyarylates were immiscible with poly(acetoxystyrene) and poly(vinylphenol). The tensile moduli of these blends were higher than the linear polymers while the toughnesses of the materials were compromised. The above text has covered all publications on hyperbranched polymers up to date.

To systematically study hyperbranched polymers, some fundamental questions have to be addressed. They are (1) Are these particles compact? (2) If they are compact, to what extent? Do they behave like impenetrable spheres? (3) What are the implications of the compactness on the properties of the material, such as rheology and miscibility with other polymers?

These questions have been approached to some extent in the research of dendritic polymers and microgels by a variety of experimental techniques. Intrinsic viscosity measurements on dendritic poly(amidoamine)<sup>60</sup> and polyether<sup>61</sup> were in basic agreement with Lescanec and Muthukumar's<sup>62</sup> simulation results which predicted a density maximum in the center of the dendrimer. However, small angle neutron scattering (SANS)<sup>63</sup> of poly(amidoamine) showed the profile of a sphere of uniform density. Static light scattering of polycyanurate microgels<sup>64</sup> revealed that the molecular parameters, such as molecular weight and radius of gyration followed the prediction of

three dimensional percolation theory. The degree of swelling for such a randomly crosslinked structure was also low.

Nuclear Magnetic Resonance (NMR) techniques were employed to investigate the molecular structure of dendritic polymers. Meltzer et al<sup>65,66</sup> measured the  $^2\text{H}$  and  $^{13}\text{C}$  relaxation parameters of poly(amidoamine) dendrimers.  $T_1$  of the terminal nuclei was found decreasing with the order of generation while  $T_1$  of the branch nuclei became independent of molecular weight after the second generation, indicating an agreement with Lescanec and Muthukumar's<sup>62</sup> prediction. Newkome<sup>67,68</sup> and coworkers studied dendritic polyamide using diffusion ordered spectroscopy ( $^1\text{H}$  DOSY NMR). The hydrodynamic radius of the polymer was found to respond to the stimulus of a pH change.

Photophysical studies involving probe molecules were conducted to investigate the intramolecular structure of dendrimers and microgels. Hawker et al<sup>69</sup> used a solvatochromic molecule to probe a polyether dendrimer. They found, for solvents of low polarity, a dramatic change in the adsorption on going from generation 3 to generation 4. The authors correlated this result to a transition in the shape of the dendritic macromolecule from an extended to a more globular structure. Pankasem et al<sup>70</sup> used fluorescent probes to investigate the size contraction of poly(N-isopropyl acrylamide) microgels with increasing temperature. Their findings were in basic agreement with independent light scattering results.

The melt viscosity of a polystyrene microgel was studied by Antonietti et al<sup>71</sup>. Comparing the data of the linear polystyrene, they reported a very similar molecular weight dependence but a reduced viscosity by a factor of 200. The emergence of the plateau zone which has been traditionally attributed to chain entanglements happened at much higher molecular weight. Since reptation motion was hardly possible in this system, the reason for the existence of the plateau zone was still to be determined.

Copolymers and blends of dendrimers have been reported. Gitsov et al<sup>72</sup> studied linear-dendritic polyether copolymers. Their results showed that the block copolymers were able to form mono- and multi-molecular micelles. The linear blocks were able to crystallize in different structural forms depending on the experimental condition. Connolly et al<sup>73</sup> found the addition of a dendritic poly(aryl ester) in a polycarbonate reduced the glass transition temperature of the polycarbonate while maintaining the  $\beta$  transition which is considered to be responsible for the toughness of the material.

In summary, the characteristics of dendritic polymer, hyperbranched polymer and microgel can be presented in the following Table 1.1.

Table 1.1 Comparison among highly branched polymers with different topology

Topology	Dendritic polymer	Hyperbranched polymer	Microgel
Structure	DB=100% [branch]=[terminal]	DB<100% [branch]≤[terminal]	[branch]>[terminal]
Synthesis	AB <sub>2</sub> monomer via protection-deprotection route	AB <sub>2</sub> monomer via one step polymerization	emulsion polymerization with crosslinking reagent
Investigated Properties	Intramolecular structure, low dendritic polymer content blend	little studied	fractal dimension, rheology

As already indicated, compared with dendrimers and microgels, hyperbranched polymers offer special application interests while their characterization and properties are far from clear and thorough. The mission of this thesis is to characterize hyperbranched polyarylates from different perspectives to achieve better understanding of this new and unique material. The objectives include (1) modifying in large quantity hyperbranched poly(5-acetoxy isophthalic acid) with different terminal groups; (2) studying the interaction between the hyperbranched polyarylate with other molecules, such as solvent, NMR shift reagent; (3) investigating the miscibility and the dynamic mechanical properties of the blends of the hyperbranched polyarylate and its linear analog; (4) modifying the hyperbranched polyarylate with etherimide terminal groups

and studying the mechanical properties of the blend of this polymer with a linear polyetherimide for application considerations.

## References

1. Hawker, C. J. and Frechet, J. M. J., J. Am. Chem. Soc. **112**, 7638 (1990)
2. Friedel, and Crafts, Bull. Soc. Chim., **43**, 53 (1885)
3. Jacobson, R. A., J. Am. Chem. Soc., **54**, 1513 (1932)
4. Meyer, K. H., Natural and Synthetic Polymers, 2nd ed., pp.456 ff.(Interscience Publishers, New York-London, 1950)
5. Flory, P. J., J. Am. Chem. Soc., **74**, 2718 (1952)
6. Tomalia, D.A., Baker, H., Dewald, J., Hall, M., Kallos, G., Martin, S., Roeck, J., Ryder, J. and Smith, P., Polym. J., **17**, 117 (1985)
7. Newkome, G. R., Yao, Z., Baker, G. R., Gupta, V. K., J. Org. Chem., **50**, 2004 (1985)
8. Murry, M. J. and Snowden, M. J., Adv. Colloid Interface Sci., **54**, 73 (1995)
9. Kawaguchi, H., Colloid Polym. Sci., **270**, 53 (1992)
10. Tomalia, D. A., Naylor, A. M. and Goddard, W. A., III., Angew. Chem. Int. Ed. Engl., **29**, 138 (1990)
11. Snowden, M. J. and Booty, M. T., in Karsa, D. (Ed.), Encapsulation and Cotrolled Release., Royal Society of Chemistry, p.141 (1993)
12. Lee, J. J., Ford, W. T., Moore, J. A. and Li, Y. F., Macromol., **27**, 4632 (1994)
13. Evans D. J., Kanagasooriam, A., Williams, A. and Pryce, R. J., J. Molecul. Catal., **85**, 21 (1993)
14. Stacey K. A., Weatherhead R. H. and Williams, A., Makromol. Chem., **181**, 2517 (1980)
15. Harun, G. and Williams, A., Polymer, **22**, 916 (1981)
16. Aihara, T. and Nakayama Y., Prog. Org. Coat., **14**, 103 (1986)
17. Bromley, C. W. A., J. Coat. Tech., **61**, 768 (1989)
18. Duan, R. G., Miller, L. L. and Tomalia, D. A., J. Am. Chem. Soc., **117**, 10783 (1995)
19. Wooley, K. L., Hawker, C. J. and Frechet, J. M. J., J. Am. Chem. Soc., **113**, 4252 (1991)

20. Gitsov, I., Wooley, K. L., Hawker, C. J., Ivanova, P. T. and Frechet, J. M. J., Macromol., **26**, 5621 (1993)
21. Hawker, C. J., Wooley, K. L. and Frechet, J. M. J., J. Chem. Soc., Chem. Commun., **8**, 925 (1994)
22. Newkome, G. R., Hu, Y., Saunders, M. J. and Fronczek, F. R., Tetrahedron Lett., **32**, 1133 (1991)
23. Newkome, G. R., Moorefield, C. N., Baker, G. R., Johnson, A. J. and Behera, R. K., Angew. Chem., Int. Ed. Engl., **30**, 1176 (1991)
24. Newkome, G. R., Behera, R. K., Moorefield, C. N. and Baker G. R., J. Org. Chem., **56**, 7162 (1991)
25. Newkome, G. R. and Lin, X., Macromol., **24**, 1443 (1991)
26. Miller, T. M. and Neenan, T. X., Chem. Mater., **2**, 346 (1990)
27. Miller, T. M., Kwock, E. W. and Neenan, T. X., Macromol., **25**, 3143 (1992)
28. Moore, J. S. and Xu, Z., Macromol., **24**, 5894 (1991)
29. Xu, Z. and Moore, J. S., Angew. Chem. Int. Ed. Engl., **32**, 246 (1993)
30. Kawaguchi, T. K., Walker, K. L., Wilkins, C. L. and Moore, J. S., J. Am. Chem. Soc., **117**, 2159 (1995)
31. Morikawa, A., Kakimoto, M. and Imai, Y., Macromol., **24**, 3469 (1991)
32. Morikawa, A., Kakimoto, M. and Imai, Y., Macromol., **25**, 3247 (1992)
33. Morikawa, A., Kakimoto, M. and Imai, Y., Macromol., **26**, 6324 (1993)
34. van Hest, J. C. M., delnoye, D. A. P., Baars, M. W. P. L., van Genderen. M. H. P. and Meijer, E. W., Science, **268**, 1592 (1995)
35. Kremers, J. A. and Meijer, E. W., J. Org. Chem., **59**, 4202 (1994)
36. Percec, V. and Kawasami, M., Macromol., **25**, 3843 (1992)
37. Percec, V., Chu, P., Ungar, G. and Zhou, J., J. Am. Chem. Soc., **117**, 11440 (1995)
38. Mekelburger, H., Rissanen, K. and Vogtle, F., Chem. Ber., **126**, 1161 (1993)
39. Lange, P., Schier, A. and Schmidbaum H., Inorg. Chem., **35**, 637 (1996)
40. Suzuki, H., Kimata, Y., Satoh, S. and Kuriyama, A., Chem. Lett., **4**, 293 (1995)

41. Seyferth, D., Son, D. Y., Rheingold, A. L. and Ostrander, R. L., Organometallics, **13**, 2682 (1994)
42. Lapierre, J., Skobridis, K. and Seebach, D., Helvetica Chimica Acta, **76**, 2419 (1993)
43. Slany, M., Bardaji, M., Casanove, M., Caminade, A., Majoral, J. and Chaudet, B., J. Am. Chem. Soc., **117**, 9764 (1995)
44. Rao, C. and Tam, J. P., J. Am. Chem. Soc., **116**, 6975 (1994)
45. Hawker, C. J., Lee, R. and Frechet, J. M. J., J. Am. Chem. Soc., **113**, 4583 (1991)
46. Turner, S. R., Voit, B. I. and Mourey, T. H., Macromol., **26**, 4617 (1993)
47. Turner, S. R., Walter, F., Voit, B. I. and Mourey, T. H., Macromol., **27**, 1611 (1994)
48. Kricheldorf, H. R. and Stober, O., Macromol. Rapid Commun., **15**, 87 (1994)
49. Kricheldorf, H. R., Stober, O. and Lubers, D., Macromol., **28**, 2118 (1995)
50. Uhrich, K. E., Hawker, C. J., Frechet, J. M. J. and Turner, S. R., Macromol., **25**, 4583 (1992)
51. Miller, T. M., Neenan, T. X., Kwock, E. W. and Stein, S. M., J. Am. Chem. Soc., **115**, 356 (1993)
52. Suzuki, M., Ii, A. and Saegusa, T., Macromol., **25**, 7071 (1992)
53. Mathias, L. J. and Carothers, T. W., J. Am. Chem. Soc., **113**, 4043 (1991)
54. Kim, Y. H. and Webster, O. W., Macromol., **28**, 3214 (1995)
55. Zhang, Y., Wang, L., Wada, T. and Sasabe, H., J. Polym. Sci., Part A: Polym. Chem., **34**, 1359 (1996)
56. Zhou, Y., Bruening, M. L., Bergbreiter, D. E., Crooks, R. M. and Wells, M., J. Am. Chem. Soc., **118**, 3773 (1996)
57. Kim, Y. H. and Beckerbauer, R., Macromol., **27**, 1968 (1994)
58. Connolly, J. M., Ma, B., Wedler, W., Winter, H. H. and Karasz, F. E., to be published.
59. Massa, D. J., Shriner, K. A., Turner, S. R. and Voit, B. I., Macromol., **28**, 3214 (1995)
60. Mansfield, M. L. and Klushin, L. I., private communication.

61. Mourey, T. H., Turner, S. R., Rubinstein, M., Frechet, J. M. J., Hawker, C. J. and Wooley, K. L., Macromol., **25**, 2401 (1992)
62. Lescanec, R. L. and Muthukumar, M., Macromol., **24**, 4892 (1991)
63. Bauer, B. J., Briber, B. M. and Hammouda, B., Polym. Prep., **2**, 476 (1992)
64. Bauer, J. and Burchard, W., Macromol., **26**, 3103 (1993)
65. Meltzer, A. D., Tirrell, D. A., Jones, A. A., Inglefield, P. T., Hedstrand, D. M. and Tomalia, D. A., Macromol., **25**, 4541 (1992)
66. Meltzer, A. D., Tirrell, D. A., Jones, A. A. and Inglefield P. T., Macromol., **25**, 4549 (1992)
67. Newkome, G. R., Young, J. K., Baker, G. R., Potter, R. L., Audoly, L., Cooper, D. and Weis, C. D., Macromol., **26**, 2394 (1993)
68. Young, J. K., Baker, G. R., Newkome, G. R., Morris, K. F. and Johnson, C. S., Jr., Macromol., **27**, 3464 (1994)
69. Hawker, C. J., Wooley, K. L. and Frechet, J. M. J., J. Am. Chem. Soc., **115**, 4375 (1993)
70. Pankasem, S., Thomas, J. K., Snowden, M. J. and Vincent B., Langmuir, **10**, 3023 (1994)
71. Antonietti, M., Pakula, T. and Bremer, W., Macromol., **28**, 4227 (1995)
72. Gitsov, I. and Frechet, J. M. J., Macromol., **26**, 6536 (1993)
73. Connolly, J. M., Ma, B. and Karasz, F. E., to be published.

## CHAPTER 2

### PREPARATION OF HYPERBRANCHED POLYARYLATES WITH NARROW MOLECULAR WEIGHT DISTRIBUTION

#### Introduction

Among the available hyperbranched polymers, hyperbranched polyarylates based on monomers 5-acetoxyisophthalic acid and 3,5-diacetoxybenzoic acid have attracted most attention<sup>1-5</sup> so far due to their straight-forward synthesis strategy. In addition to the synthesis advantage, aromatic polyesters are thermally stable up to 220°C which affords a wide temperature window for our subsequent property study. Turner et al<sup>2,3</sup> used a melt polymerization to carry out the transesterification reaction shown in Figure 2.1.

Scheme I

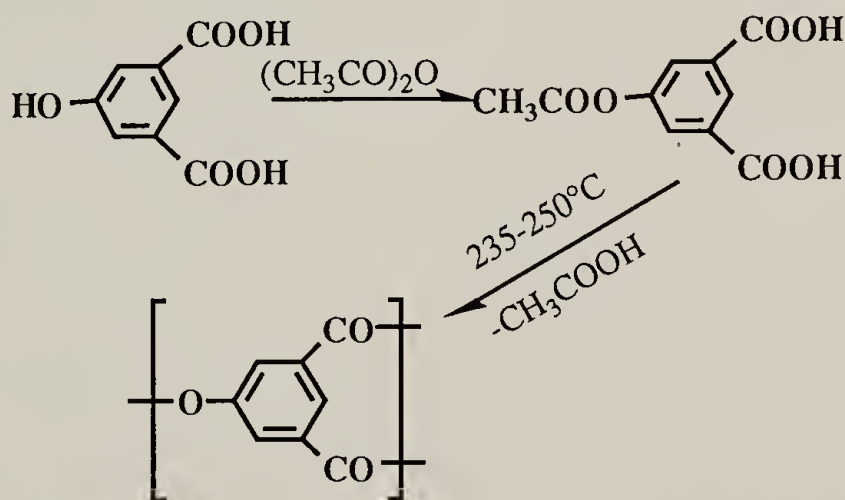


Figure 2.1: Scheme I, condensation of 5-acetoxyisophthalic acid

Due to the 1:1 reaction ratio between the acetoxy and the carboxyl groups, at the late stage of the polymerization, half of the carboxyl groups were to be unreacted with almost all the acetoxy groups being reacted. The high concentration of the carboxyl groups caused an anhydride formation which crosslinked the whole system. This side reaction together with the release of acetic acid and water made foaming and solidification inevitable. Although the anhydride linkages could be hydrolyzed to

recover the carboxyl groups, however, once the foam was formed, the heat transfer and the uniformity of the final product became hard to control over a prolonged reaction time. So the productivity and the yield of the melt process was limited.

Scheme II

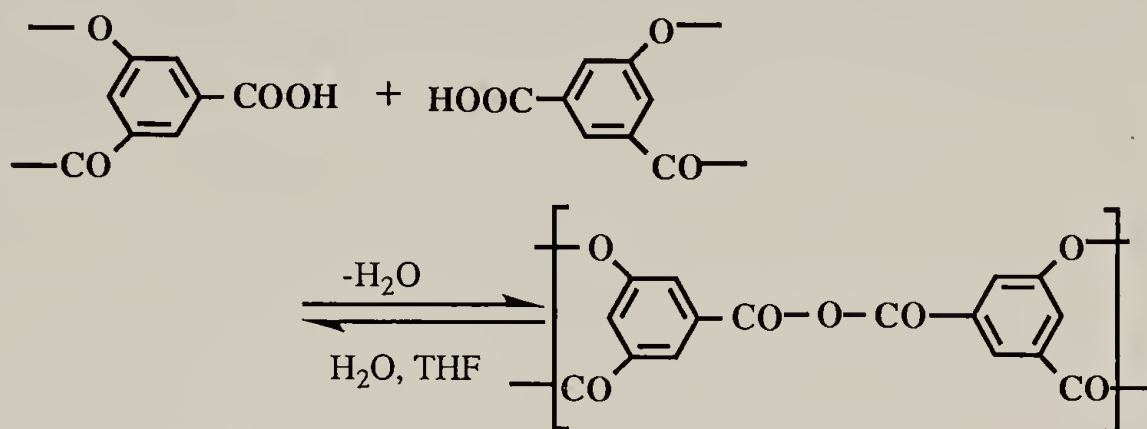


Figure 2.2: Scheme II, formation and hydrolysis of anhydride

For the purpose of our investigation, a large quantity of sample was required. To achieve this goal and to avoid the heat transfer problem, a suspension polymerization was used instead of the melt process.

The residual carboxyl groups remaining in hyperbranched structure were the sites for further modification through acyl chloride intermediate as shown in Scheme III.

Scheme III

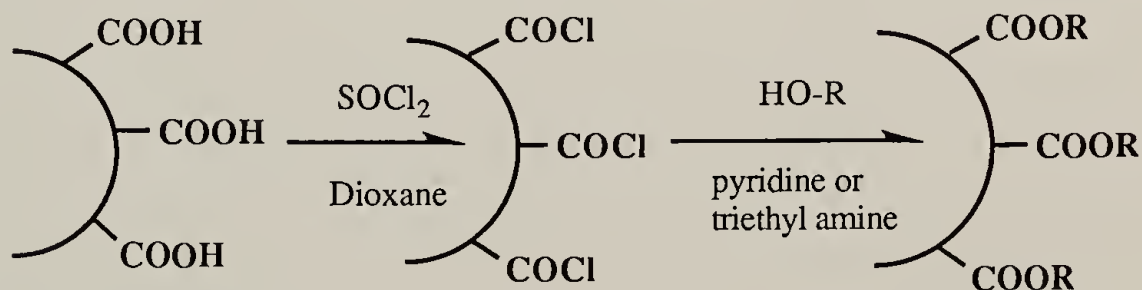


Figure 2.3: Scheme III, modification of poly(5-acetoxysophthalic acid)

Several modified products were made with this procedure. Only methyl, phenyl, n-butyl and 2-ethylhexyl hyperbranched polyarylates (abbreviated as MeHP,

PhHP, BuHP and EhHP respectively) will be reported here due to the relevancy of these materials for further characterizations.

Fractionations<sup>6</sup> of the above polyarylates were carried out by two methods based on the requirements of experiments. MeHP, PhHP and BuHP samples were prepared by the precipitation fractionation method which utilized the solubility difference between polymers of different molecular weights. It used less solvent and the procedure was convenient. The major drawback of this method was the low resolution on fractions with either very low or very high molecular weight. EhHP sample was prepared by the preparative GPC method which took advantage of the hydrodynamic volume difference between polymers of different molecular weight. While it offered high resolution, the operation was quite cumbersome because of the large quantity of solvent involved.

### Experimental

#### Synthesis and Modification of Poly(5-acetoxyisophthalic acid)

General Procedure. All solvents were reagent grade unless otherwise indicated. 5-hydroxyisophthalic acid and other reagents were purchased from Aldrich. All products and intermediates were dried at 60°C under house vacuum of about 30 torr for 48 hours.

Monomer Synthesis (5-acetoxyisophthalic acid). 5-hydroxyisophthalic acid (0.25 mol, 45.5g) was heated in 102g of acetic anhydride (1mol) to reflux. The acid dissolved after about 30 minutes of reflux and the reflux was continued overnight. The excess acetic anhydride was removed in vacuum and the crude white product was recrystallized twice from a chloroform/toluene mixture and yielded 48g (86%) with a melting point of 230°C. <sup>1</sup>H NMR (DMSO-*d*<sub>6</sub>),  $\delta$  in ppm: 2.25 (s, 3H), 7.8 (s, 2H), 8.2 (s, 1H), 13.4 (br, 2H, COOH). Elemental analysis for C<sub>9</sub>H<sub>8</sub>O<sub>6</sub>: C, 53.57; H, 3.57. Found: C, 53.44; H, 3.61.

Suspension Polymerization of 5-Acetoxyisophthalic acid. An 1000ml 4-neck flask was equipped with a mechanical stirrer, a nitrogen inlet, a thermometer and a Dean condenser. 300ml high boiling point silicone oil was added and purged with nitrogen for 10 minutes before 50g 5-acetoxyisophthalic acid was added. The temperature of the suspension was gradually raised to 235°C under nitrogen in 1 hour during which the monomer melted into droplets and subsequently solidified into beads as acetic acid was collected. The size of the beads depended on the stirring rate. Temperature was then raised to 250°C and a vacuum of 30torr was applied for 4 hours. The product beads were filtered and washed with hexane. 200ml THF:H<sub>2</sub>O solution was used to hydrolyze the anhydride and to dissolve the beads. Poly(5-acetoxyisophthalic acid) was precipitated in water, taken up in THF and reprecipitated in ether. Elemental analysis by ash found no silicon trace. <sup>1</sup>H NMR (DMSO-*d*<sub>6</sub>),  $\delta$  in ppm: 7-9 (br, ArH), 13.4 (br, COOH).

Acyl Chloride of Poly(5-acetoxyisophthalic acid). 20g of poly(5-acetoxyisophthalic acid) was dissolved in 100ml dry dioxane. 20g thionyl chloride was added gradually to the solution. The solution was refluxed for 4 hours. Residual thionyl chloride and dioxane were distilled on a rotary evaporator. The acyl chloride was further dried under 3 torr vacuum at 60°C for 2 days. FTIR showed complete shift of carbonyl stretching band from 1700 to 1780 cm<sup>-1</sup>.

Methyl Hyperbranched Polyarylate (MeHP). 10g acyl chloride of poly(5-acetoxyisophthalic acid) and 10ml absolute methanol were dissolved in 200 ml dry THF. The reaction was kept at 50°C for 3 hours after the gradual addition of 10g pyridine. The polymer was precipitated in methanol, taken up in THF and reprecipitated in methanol. <sup>1</sup>H NMR (chloroform-*d*),  $\delta$  in ppm: 3.95 (b, CH<sub>3</sub>), 8.09-8.10 (bd, ArH), 8.18 (b, ArH), 8.30 (b, ArH), 8.41 (b, ArH), 8.58 (b, ArH), 8.80 (b, ArH), 8.98 (b, ArH), as shown in Figure 2.4. Elemental analysis for (C<sub>9</sub>H<sub>6</sub>O<sub>4</sub>)<sub>n</sub>: C, 60.67; H,

3.37. Found: C, 60.74; H, 3.31. Glass transition temperature ( $T_g$ ) of MeHP was measured to be 165°C.

Phenyl Hyperbranched Polyarylate (PhHP). 10g acyl chloride of poly(5-acetoxyisophthalic acid) and 10g anhydrous phenol were dissolved in 200 ml dry THF. 10g pyridine was added gradually to the solution and the reaction was kept at 50°C for 3 hours after the addition of pyridine. The polymer was precipitated in methanol, taken up in THF and reprecipitated in methanol.  $^1\text{H}$  NMR (chloroform- $d$ ),  $\delta$  in ppm: 7.1-7.4 (bm, ArH), 8.36 (b, ArH), 8.95 (b, ArH), as shown in Figure 2.5. Elemental analysis for  $(\text{C}_{14}\text{H}_8\text{O}_4)_n$ : C, 70.00; H, 3.33. Found: C, 69.88; H, 3.41.  $T_g$  of PhHP was measured to be 175°C.

n-Butyl Hyperbranched Polyarylate (BuHP). 10g acyl chloride of poly(5-acetoxyisophthalic acid) and 10ml n-butanol were dissolved in 200ml dry THF. 0.5ml allyl alcohol was also added to facilitate future TEM investigation. The reaction was kept at 50°C for 3 hours after a gradual addition of 10g pyridine. The product was precipitated in methanol, taken up in THF and reprecipitated in methanol.  $^1\text{H}$  NMR (chloroform- $d$ ),  $\delta$  in ppm: 0.98 (b,  $\text{CH}_3$ ), 1.34-1.50 (b,  $\text{CH}_2$ ), 4.35 (b,  $\text{CH}_2$ ), 7.82-7.98 (bm, ArH), 8.08-8.10 (bd, ArH), 8.20 (b, ArH), 8.31 (b, ArH), 8.45 (b, ArH), 8.61 (b, ArH), 8.80 (b, ArH), 9.02 (b, ArH), as shown in Figure 2.6. Elemental analysis for  $(\text{C}_{12}\text{H}_{12}\text{O}_4)_n$ : C, 65.45; H, 5.45. Found: C, 65.42; H, 5.41.  $T_g$  of BuHP was 65 °C.

2-Ethylhexyl Hyperbranched Polyarylate (EhHP). 10g acyl chloride of poly(5-acetoxyisophthalic acid) and 10g 2-ethylhexanol were dissolved in 200ml dry THF. 10ml pyridine was added dropwise to the solution. The mixture was kept at 50°C for 3 hours after all the pyridine was added. The product was precipitated in methanol, taken up in THF and reprecipitated in methanol.  $^1\text{H}$  NMR (chloroform- $d$ ),  $\delta$  in ppm: 0.95 (b,  $\text{CH}_3$ ), 1.34-1.50 (b,  $\text{CH}_3$ ), 1.75 (b, CH), 4.35 (b,  $\text{CH}_2$ ), 7.82-7.98 (bm, H), 8.08-8.10 (bd, ArH), 8.20 (b, ArH), 8.31 (b, ArH), 8.44 (b, ArH), 8.62 (b, ArH), 8.82 (b, ArH), 9.01 (b,

ArH), as shown in Figure 2.7. Elemental analysis for  $(C_{16}H_{20}O_4)_n$ : C, 69.57; H, 7.25. Found: C, 69.48; H, 7.31.  $T_g$  of EhHP was 47°C.

### Fractionation

Precipitation Fractionation of MeHP, PhHP and BuHP. 5g sample was dissolved in 500g dioxane at 25°C in an 1 l Erlenmeyer flask. Water was added in 10ml increments to the solution until the solution, under steady stirring, turned cloudy and did not recover in two minutes. Additional 10ml water was added to the solution and the temperature was raised to 30°C in a water bath. The solution was transferred to an 1 l separatory funnel to settle at 25°C overnight. The bottom layer of the concentrated high molecular weight solution was collected as the first fraction. The solvent was evaporated on a rotary evaporator. The top layer was transferred back to the Erlenmeyer flask and additional 10ml water was added again and the procedure of heating and settling was repeated to collect the next portion until no cloudiness was observable after additional water was added to the solution.

Preparative Gel Permeation Chromatography (GPC). The operation was performed on a Waters GPC system set up with 5cm x120cm Styragel 10E03 and 10E04 preparative GPC columns using THF as solvent. Trials were carried out to determine the best resolution and productivity. These were proved to be at 20ml/min flow rate and 30mg/ml sample concentration. Portions of eluent with different retention times were collected separately. Samples with the same retention time were accumulated through a number of runs. Finally, the solvent in each fraction was evaporated on rotavap and polymers were dried at 60°C for 2 days under a house vacuum of 30 torr.

### Characterization

FID files of NMR were obtained on a Bruker AC200 200MHz instrument. Fourier transform and the follow-up data processing were conducted using WINNMR software from Bruker. FTIR analysis was done on an IBM IR20 instrument. Elemental

Analysis was accomplished in the Microanalysis Lab at University of Massachusetts. Molecular weight information was obtained by GPC with two Plgel mixed-bed 7.5mm i.d.x300mm 10 $\mu$ m particle diameter columns (Polymer Laboratories, Amherst, MA). The system was equipped with an on-line refractometer. Glass transition temperatures were measured on a Perkin-Elmer DSC7 instrument. The reported data were based on the second run with a 20°C/min heating rate.

## Results and Discussion

### Suspension Polymerization

In order to get consistent data in the study of physical properties, all samples should be from the same batch of reaction. For this requirement, a large quantity of poly(5-acetoxysophthalic acid) was needed. Suspension polymerization<sup>7</sup> method was one way to fulfill this requirement. It eliminated the heat transfer problem by introducing certain suspension medium which dispersed the reacting melt into small droplets. The key to this successful suspension polymerization was to identify the proper suspension medium. Several conventional suspension fluids such as mineral oil, wax, and high carbon number alkanes were tried. All were found to partially dissolve the monomer at high temperature so that the suspension could not be obtained. High boiling point silicone oil was chosen at last because of its ability to form stable suspension and to endure high temperature and vacuum for a prolonged period of time. After the reaction was completed, most of the silicone oil were recovered and reused. There had been some concern<sup>8</sup> that the Si-O bonds may rearrange under slightly acidic condition at high temperature interfering with the condensation polymerization. The elemental analysis and NMR spectrum on final product showed that this process was insignificant to the formation of polyarylate. However, after a number of repeated uses of the silicone oil, its viscosity was found to increase slightly, presumably due to the partial crosslinking caused by the rearrangement.

## Modification

The transformations of acyl chlorides to esters, using methanol, n-butanol, phenol and 2-ethylhexyl alcohol were completed to 100% as detected by NMR spectroscopy. From a certain perspective, this indicated that the backbone of hyperbranched polyarylate had enough free space allowing the modifying agents to penetrate the structure to react with all the residual groups. In other words, small molecules still treated these structures as porous.

The glass transition temperatures of hyperbranched polyarylates were sensitive to the nature of modifying groups. Of all the reported<sup>9</sup> modified polyarylates,  $T_g$  ranged from 188°C to -50°C. This offered a way of creating a variety of hyperbranched polymers with different thermal and mechanical properties without ever changing the backbone structure of the polymer.

## Fractionation

Fractionation results are listed in Table 2.1. EhHP samples had the narrowest molecular weight distribution due to the good performance of preparative GPC. In the meantime, reasonably good results were obtained on low and middle molecular weight MeHP, PhHP and BuHP samples. The distribution of high molecular weight fractions were not as satisfactory.

Unlike linear polymers, hyperbranched polymers do not necessarily have the same molecular structure even if all the molecules have the same molecular weight. Hyperbranched polymers with the same molecular weight may have different degrees of branching. This feature adds an additional dimension to the polydispersity of these polymers. None of the available fractionation theories and techniques is capable of making such a distinction. It is generally assumed in the following chapters that this structural polydispersity does not have any significant effect on determining the macroscopic properties of the material.

## Conclusions

Hyperbranched poly(5-acetoxyisophthalic acid) was synthesized in large quantity with one-batch condensation method. Residual carboxyl groups were modified to ester groups through an acyl chloride intermediate. Chemical structures of all products were characterized by  $^1\text{H}$  NMR and other analytic techniques. Glass transition temperatures of modified polyarylates were dependent of modifying groups. Samples with narrow molecular weight distribution were prepared by fractionation techniques for further characterization.

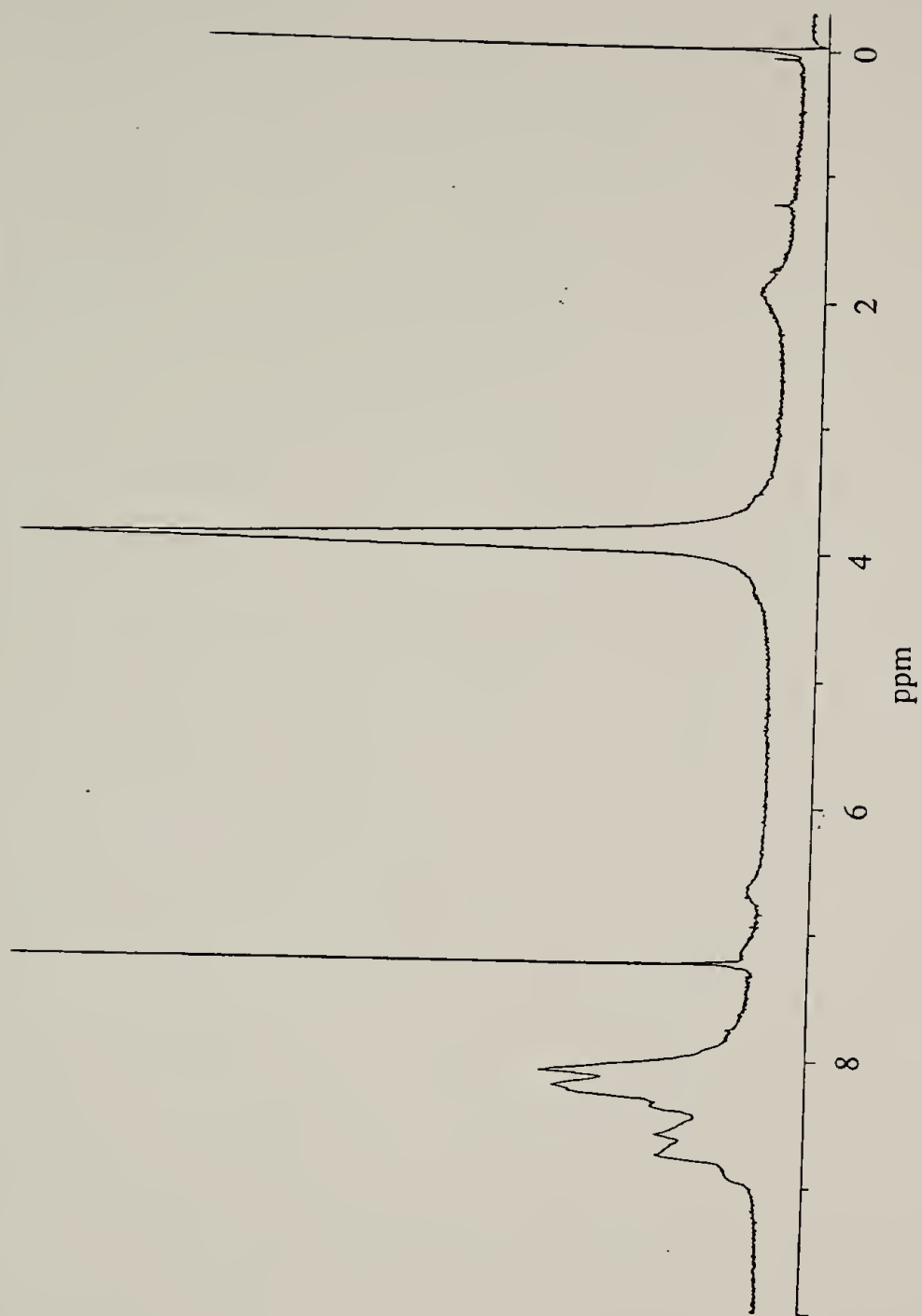


Figure 2.4:  $^1\text{H}$  NMR of MeHP

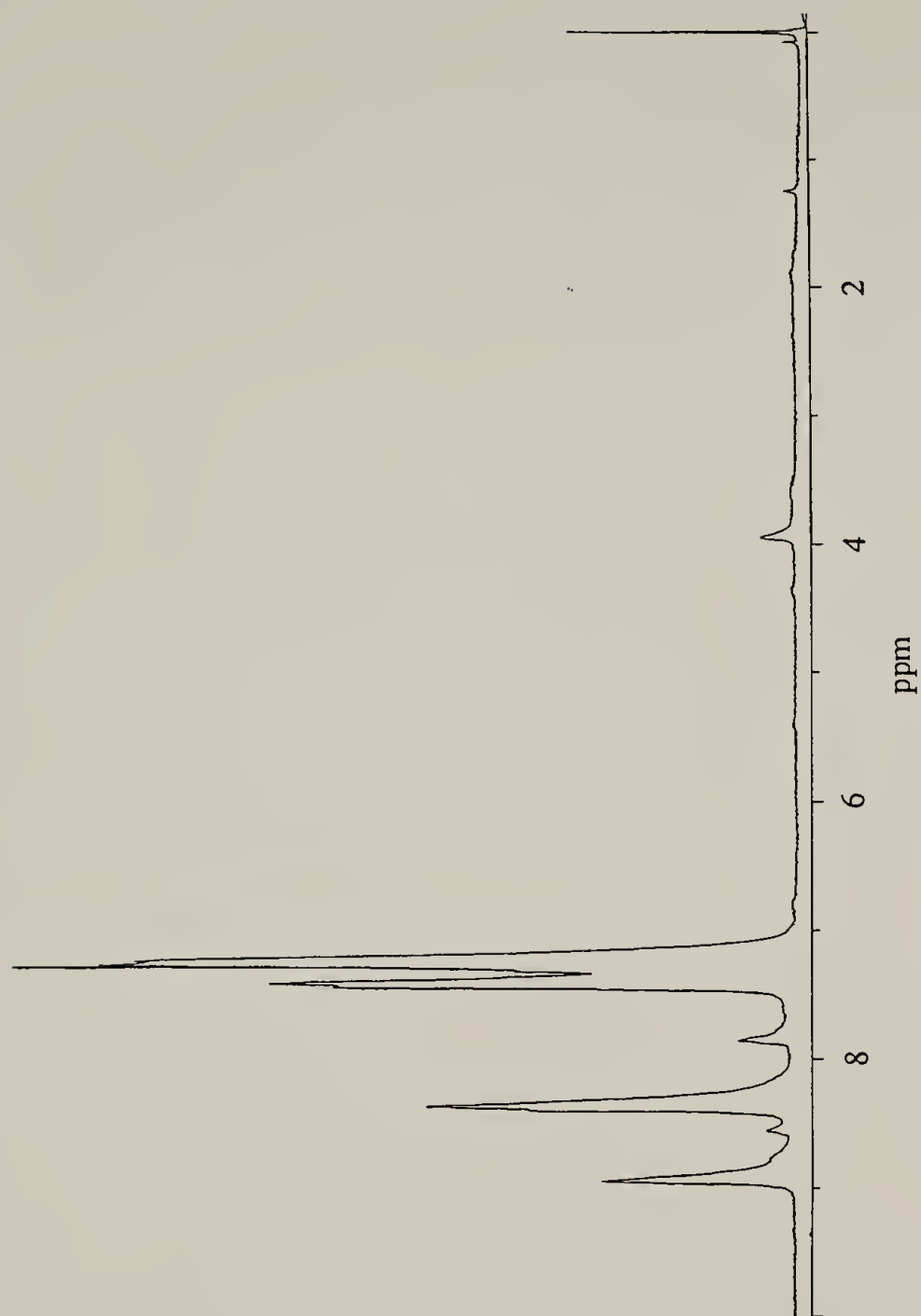


Figure 2.5:  $^1\text{H}$  NMR of PhHP

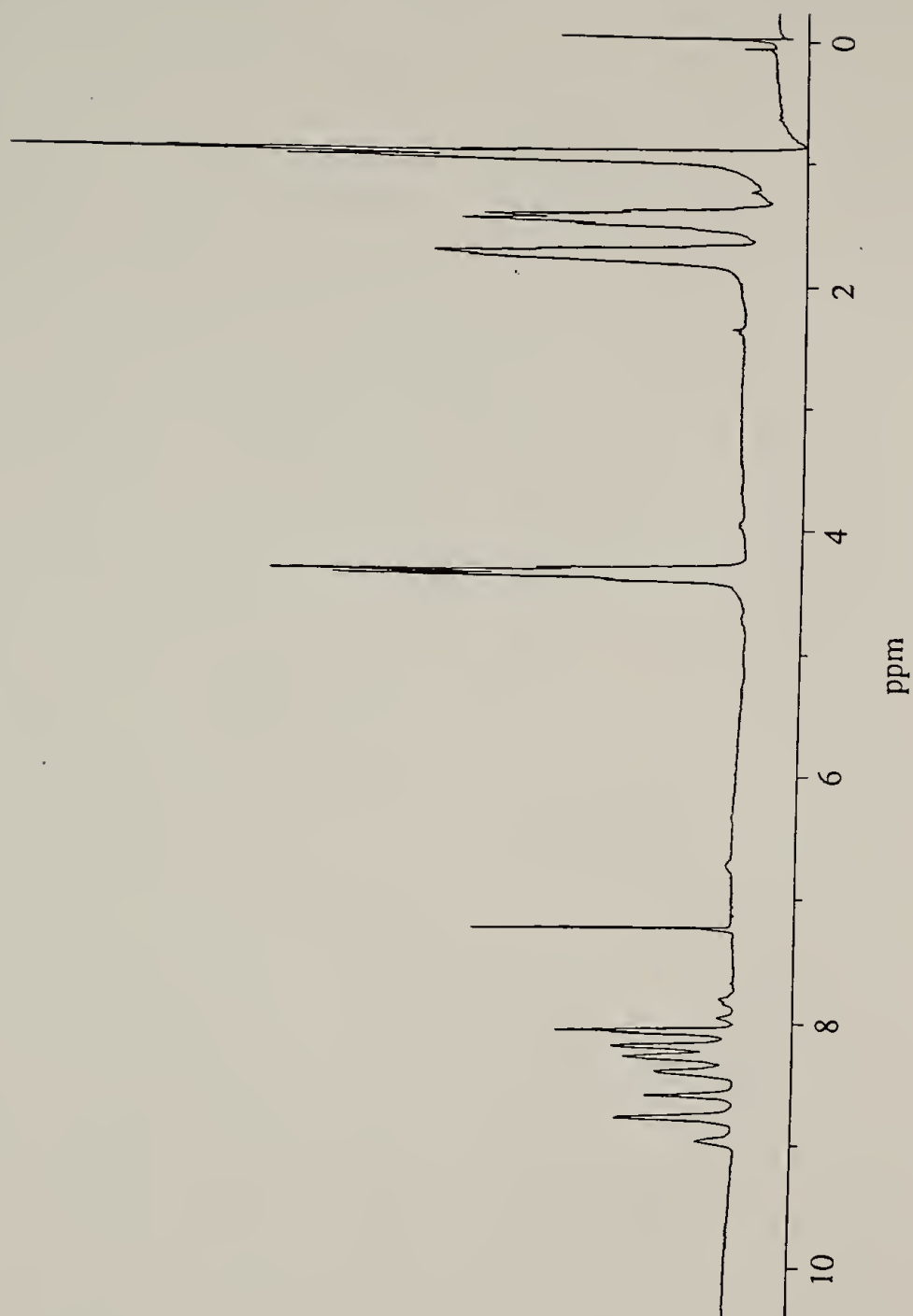


Figure 2.6:  $^1\text{H}$  NMR of BuHP

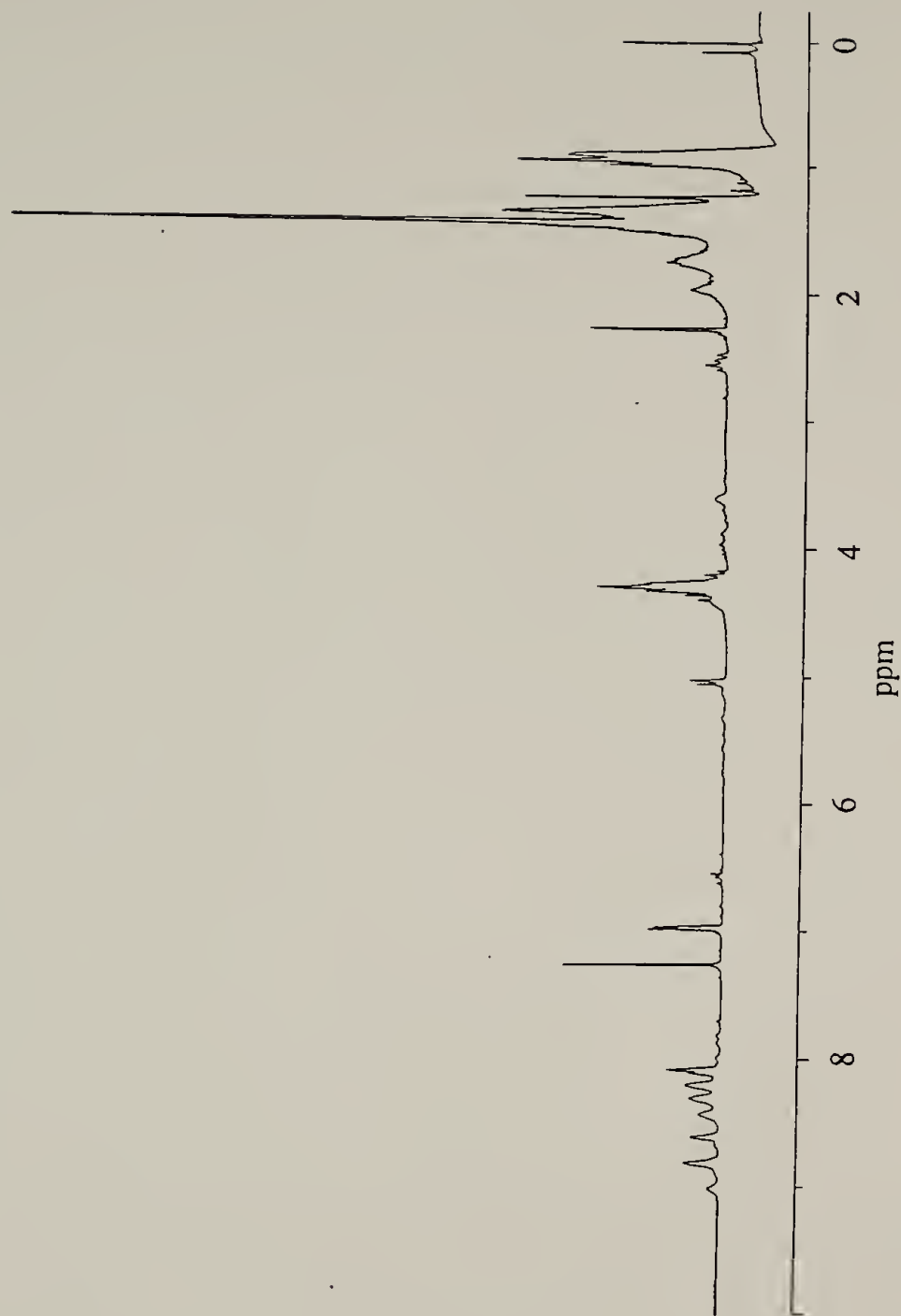


Figure 2.7:  $^1\text{H}$  NMR of EhHP

Table 2.1: Fractionation results of hyperbranched polyarylates<sup>a</sup>

Sample No.	2-Ethylhexyl Ester <sup>b</sup>		Phenyl Ester <sup>c</sup>		Methyl Ester <sup>c</sup>		n-Butyl Ester <sup>c</sup>	
	$M_n (\times 10^4)$	PDI	$M_n (\times 10^4)$	PDI	$M_n (\times 10^4)$	PDI	$M_n (\times 10^4)$	PDI
1	0.126	1.16	3.58	1.23	4.28	1.29	0.235	1.39
2	0.251	1.19	6.51	1.30	6.35	1.24	0.363	1.44
3	0.437	1.33	7.64	1.35	9.71	1.27	0.647	1.37
4	0.603	1.34	10.5	1.26	10.3	1.33	0.724	1.43
5	0.832	1.37	14.2	1.36	15.5	1.36	0.775	2.13
6	1.12	1.27	21.1	1.51	40.7	1.58	2.68	2.58
7	1.41	1.29	26.0	1.73	50.4	1.85	5.84	2.85
8	1.91	1.32	34.2	1.82	82.6	2.06	9.24	3.06
9	2.14	1.34	47.3	2.06	103	3.35	12.6	4.35
10	2.40	2.19	55.0	2.43	126	3.57	17.3	4.57
11	3.47	2.78	108	3.56				
12	13.8	2.83	183	4.48				
13	17.8	3.42	294	4.57				

a. Starting condition:  $PDI = M_w/M_n > 10.0$

b. By preparative GPC method

c. By precipitation method

## References

1. Hawker, C. J., Lee, R. and Frechet, J. M. J., J. Am. Chem. Soc., **113**, 4583 (1991)
2. Turner, S. R., Voit, B. I. and Mourey, T. H., Macromol., **26**, 4617 (1993)
3. Turner, S. R., Walter, F., Voit, B. I. and Mourey, T. H., Macromol., **27**, 1611 (1994)
4. Kricheldorf, H. R. and Stober, O., Macromol. Rapid Commun., **15**, 87 (1994)
5. Kricheldorf, H. R., Stober, O. and Lubers, D., Macromol., **28**, 2118 (1995)
6. Cantow, M. J. R., Polymer Fractionation, (Academic Press: New York) (1967)
7. Mark, H. F., Bikales, R. M., Overbrerger, C. G. and Menges, G., ed., Encyclopedia of Polymer Science and Engineering, 2nd ed., (Wiley: New York) (1990)
8. Clarson, S. J., Siloxane Polymers, (New Jersey: PTR Prentice Hall) (1993)
9. Connolly, J. M., Ma, B. and Karasz, F. E., to be published.

## CHAPTER 3

### MOLECULAR PARAMETERS OF HYPERBRANCHED POLYARYLATES

#### Introduction

The main objective of this chapter is to characterize the intramolecular structure of hyperbranched polyarylates from different perspectives. The central question to be addressed is how compact these polymers are.

As indicated in Chapter I, the question about the compactness of the hyperbranched polymer has never been approached systematically. Even for the better studied dendritic polymers, the answer is not totally clear. Theoretically, de Gennes and Hervet<sup>1</sup> suggested that there existed a limit at which the branching pattern would be interrupted by an over-crowding of the terminal groups. Maciejewski<sup>2</sup> proposed that large dendritic molecules should be capable of forming an outer barrier that restricted the access to the interior of the molecules. No experimental data has been published to support this model.

By simulating the growth of dendritic molecules, Lescanec and Muthukumar<sup>3</sup> suggested that there was an increase in monomer density in the interior of the molecules as molecular weight increases owing to the folding back of chains into the interior of the molecule. Meltzer et al.<sup>4,5</sup>'s NMR relaxation measurement on poly(amido amine) and Mansfield et al.<sup>6</sup>'s intrinsic viscosity measurement seemed to support this prediction. However, neutron scattering<sup>7,8</sup> suggested a uniform structure. For the hyperbranched polyarylates that we were interested in, this question was approached by studying the dependence of the degree of branching on molecular weight, by observing the effect of NMR shift reagent as well as by using molecular simulation.

The compactness of a particle can also be measured from the scaling relationship between the radius of gyration and molecular weight, in other words, the fractal dimension. The branching process governing the growth of hyperbranched polymer, Cayley tree branching<sup>9</sup>, has been the repeated topic of theoretical

investigations. The percolative behavior of the Cayley tree (or Bethe lattice) was intensively studied as a model system to describe various natural critical phenomena, including polymer gelation. de Gennes<sup>10</sup>, by improving Zimm and Stockmeyer<sup>11</sup>'s treatment, predicted that for a three dimensional branch system, the exponent  $\nu$  in the relation  $R_g \propto M^\nu$  was 0.5 for a swelled gel and 0.4 for an unswelled gel. Studies on several randomly branched polymers, such as polycyanurates by Bauer and Burchard<sup>12</sup>, polystyrenes by Antonietti et al<sup>13</sup> and epoxy resins by Wachenfeld-Eisele et al.<sup>14</sup> revealed  $\nu=0.44 - 0.48$  in good solvents. They attributed the discrepancy between theory and experiment to a partial swelling of the gel. In the investigation of hyperbranched polyarylates,  $\nu$  were examined by static light scattering of fractionated samples. Before our work, the above prediction had never been applied to hyperbranched polymers.

If hyperbranched polymers are indeed as compact as have been perceived, there should be a lack of entanglement between the macromolecules. Thus they should have different dynamic mechanical response from that of linear polymers. A typical dynamic-mechanical response of linear polymers of high molecular weight, in which segments can interpenetrate and entangle, can be classically separated into a glass zone, a transition zone, a plateau zone and a terminal zone (in the order of decreasing frequencies)<sup>15</sup>. This relaxation curve was not only qualitatively explained by the reptation model but the theory also resulted in a quantitative explanation of the plateau modulus as a function of entanglement length. Antonietti et al<sup>16</sup> studied the rheology of small spherical polystyrene microgels and found that the emergence of plateau zone happened at much higher molecular weight than linear polymers, indicating a lack of entanglement. However, the fact that the plateau zone still existed in this system was the indication of some relaxation mechanism other than reptation. Just like microgels,

the highly branched structure of hyperbranched polymer makes it harder for the molecule to reptate. The investigation into their dynamic mechanical properties would shed new light on the dynamic properties of polymers in general.

### Experimental

#### Nuclear Magnetic Resonance (NMR)

FID files of NMR studies were done on a Bruker AC200 instrument. Fourier transform and the follow-up data processing were performed by WINNMR software from Bruker. Chloroform-*d* was the solvent. In addition to the routine operation which measured the degree of branching, Lanthanide Shift Reagent, specifically tris-(6,6,7,7,8,8,8-heptafluoro-2,2-dimethyl-3,5-octanedione)europium(III), shorthand as  $\text{Eu}(\text{fod})_3$ , was used as a probe to test the permeability of the probe in a hyperbranched polyarylate.  $\text{Eu}(\text{fod})_3$  as shown in Figure 3.1 was dried over  $\text{P}_4\text{O}_{10}$  in 3 torr vacuum for 2 days before use.

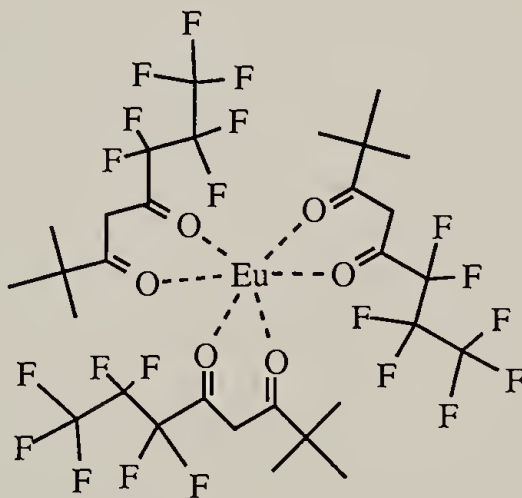


Figure 3.1: Structure of  $\text{Eu}(\text{fod})_3$

To keep the polymer concentration constant, two solutions were prepared prior to the experiment. Solution 1 contained only the hyperbranched polymer. Solution 2 contained  $\text{Eu}(\text{fod})_3$  and the same concentration of the polymer as in solution 1. A series of solutions of different  $[\text{LSR}]/[\text{carbonyl}]$  ratios were obtained by mixing solution 1 and

2 in different volumetric fractions. Measurements were conducted 2 hours after all the solutions were prepared to ensure that an equilibrium state was obtained.

### Static Light Scattering

Light scattering was conducted on an Otsuka DLS-700 instrument with a He-Ne laser beam of 632.8nm. The operational temperature range of the instrument was 5°C ~ 60°C. The experiments were performed with fractionated MeHP and PhHP in cyclohexane, dioxane and benzonitrile at 15°C. The refractive index increments of all solutions were measured with a RM-102 differential refractometer and the results are listed in Table 3.1. The concentrations of the sample solutions ranged between 0.05g/l and 3g/l. The solutions were filtered through Millipore 0.2μm PTFE filters before being poured into optical cells. Weight average molecular weight ( $M_w$ ), mean square root radius of gyration ( $\langle R_g^2 \rangle^{1/2}$ ) and the second virial coefficient ( $A_2$ ) were calculated with Zimm plot.

Table 3.1: dn/dc values for static light scattering

dn/dc	dioxane	benzonitrile	cyclohexane
MeHP	0.094	0.113	0.148
PhHP	0.106	0.082	0.164

### Molecular Simulation

Simulation was accomplished with Biosim's Dreiding II Molecular Simulation program. Compared with other available programs, it had the advantage of predicting accurate geometries with less difficulty for large molecules by ignoring long range interactions. The simulation process started with a single monomer unit and the total energy was minimized after every new unit was added to the structure.

### Dynamic Mechanical Measurement

Samples tested were BuHP of  $M_w=16,500$  and  $283,000$ . To make a comparison, linear poly(1,4-butylene isophthalate) of  $M_w=18,300$  which was purchased from Sp<sup>2</sup> Scientific Polymer Products, Inc. was also tested. Measurements of storage and loss

shear modulus  $G'$ ,  $G''$  were conducted on a Rheometrics RMS800 rheometer. By compression molding at 170°C, disks with a diameter of 30mm were prepared to fit the geometry of a 25mm plate/plate rheometer. This treatment and the subsequent measurement did not affect the original molecular weight distribution as checked by GPC. The temperature of testing ranged from 80°C to 170°C and the frequency from 1 rad/s to 464 rad/s.

## Results and Discussion

### Degree of Branching

A hyperbranched polyarylate has three kinds of basic structural units, namely branch unit, linear unit and terminal unit. Hawker and Frechet<sup>17</sup> defined the degree of branching as

$$DB = \frac{\text{branch units} + \text{terminal units}}{\text{branch units} + \text{terminal units} + \text{linear units}}$$

They also offered a method to measure this parameter based on the <sup>1</sup>H NMR peaks of the H-2 on the aromatic ring. Since the 2-ethylhexyl ester of hyperbranched polyarylate had a better resolved spectrum, we were able to identify the rest of the aromatic peaks as shown in Figure 3.2 so that an alternative calculation of DB based on these peaks could be defined. Thus,

$$\begin{aligned} DB &= \frac{\text{Area of } d_b + \text{Area of } d_t}{\text{Area of } d_b + \text{Area of } d_t + \text{Area of } d_l} && \text{(Hawker and Frechet's method)} \\ &= \frac{\text{Area of } d_w + \text{Area of } d_z}{\text{Area of } d_w + \text{Area of } d_x + \text{Area of } d_y + \text{Area of } d_z} \end{aligned}$$

In Figure 3.2, a term “initial unit” was given to the only unit of which the acetoxy group was not substituted. This unit was detectable up to  $M_n = 34,700$ . Following the above definition, we measured the DB of the fractionated hyperbranched polyarylate 2-ethylhexyl esters and the results are shown in Figure 3.3. The

measurement of  $M_n$  was based on the GPC result with polystyrene as standard. Degree of polymerization (N) was calculated based on the average molecular weight of the three basic units. DB only changed at small molecular size and became invariant after the degree of polymerization exceeded 15 when the molecule could be considered polymeric. This finding indicated that during the formation of the hyperbranched structure, the monomer attached to the initial structure experienced the same environment as the ones attached later. This was only possible when the structure has a uniform segmental density. In the case of a dendritic polymer, the segmental density changes within the molecule, the infinite growth of molecular weight is not possible.

Figure 3.3 also shows the curve for an ideally random condensation process of  $AB_2$  type monomer. For a hyperbranched polymer with degree of polymerization N formed by such a process, the possibility of a B group being reacted with an A group, p, is

$$p = \frac{N-1}{2N}$$

The possibilities of a unit being branch ( $P_b$ ), linear ( $P_l$ ) and terminal ( $P_t$ ) are:

$$P_b = p^2 = \frac{(N-1)^2}{4N^2}$$

$$P_l = 2p(1-p) = \frac{N^2-1}{2N^2}$$

$$P_t = (1-p)^2 = \frac{(N+1)^2}{4N^2}$$

Then

$$DB = \frac{P_b + P_t}{P_b + P_l + P_t} = \frac{N^2+1}{2N^2} \text{ when } N \rightarrow \infty, DB = 50\%$$

The fact that the measured DB of 47% was slightly smaller than 50% indicated that the condensation of 5-acetoxyisophthalic acid was close to an ideally random process and chemical reactivities of the units, such as the steric effect, played an insignificant role in this structure-forming process. Molecules with the size of a monomer have good accessibility to the structure. This point will be further illustrated by the fact that the inner units of the structure were quite accessible to other probes.

#### Effect of Lanthanide Shift Reagent

In the search for the limit of the openness of the structure,  $^1\text{H}$  NMR experiment in the presence of tris-(6,6,7,7,8,8,8-heptafluoro-2,2-dimethyl-3,5-octanedione) europium(III), shorthand as  $\text{Eu}(\text{fod})_3$ , was conducted on an EhHP sample ( $M_n=21,400$ ).  $\text{Eu}(\text{fod})_3$  is a commonly used Lanthanide Shift Reagent<sup>18</sup> (LSR) which interacts with electron donating groups on a molecule through strong dipolar force. In our case, the electron donor was mainly the oxygen atom of the carbonyl group on the ester linkage. The metal ion, because of its paramagnetic properties was able to affect both the chemical shift and the relaxation behavior of the nuclei nearby. LSRs have found extensive applications in organic and polymer chemistry, such as the identification of stereoisomers and chain sequence<sup>18</sup>.  $\text{Pr}(\text{III})$  and  $\text{Eu}(\text{III})$  are the two commonly used Lanthanide ions because of their capability of generating sufficient shift while maintaining the integrity of spectra.  $\text{Eu}(\text{III})$  was chosen in our case because it could create the downfield shift which fits our purpose of observing aromatic protons. Figure 3.4 shows a series of  $^1\text{H}$  NMR spectra with different  $[\text{LSR}]/[\text{carbonyl}]$  ratios. As this ratio increased, the peaks  $\delta_1$  and  $\delta_i$ , corresponding to  $\text{H}_1$  and  $\text{H}_i$  respectively, all shift downfield while  $\delta_b$  remained at the same position. This was because the steric effect at branch unit prohibited the access of LSR molecule to this unit. For the same reason,  $\delta_i$  shifted with a faster rate than  $\delta_1$ . The more important discovery of this

experiment was the splitting of  $\delta_t$ . As the majority of  $\delta_t$  shifted downfield, a small portion of it ( $\delta_t'$ ) remained at the original position. Similar phenomenon also seemed to occur to  $\delta_1$ . Thus, it appeared that most of the structure was open to the interaction with LSR. There was indeed a portion of the cluster that the LSR probe could not get access to. However, this portion was rather small. According to X-ray crystallography data<sup>19,20</sup>, the diameter of  $\text{Eu}(\text{fod})_3$  molecule is about 8 Å. Therefore, hyperbranched polyarylate was still porous up to this scale. Unfortunately, all LSRs are about the same size. Probes with larger size were not available to test the upper limit of the “pore” size.

### Static Light Scattering

To study the structural parameters in detail, light scattering experiments were conducted on the fractionated MeHP and PhHP under different conditions. Figure 3.5 shows the dependence of the mean square root of radius of gyration  $\langle R_g^2 \rangle^{1/2}$  on weight average molecular weight  $M_w$  of the two polymers in the same solvent, dioxane.

$R_g \sim M^V$  relation was valid for both polymers up to very high molecular weight. The deviations from this scaling law at the high molecular weights were due to the high PDI value of the samples since  $\langle R_g^2 \rangle^{1/2}$  as measured by light scattering is  $\langle R_g^2 \rangle_z^{1/2}$  which is always greater than  $\langle R_g^2 \rangle_w^{1/2}$ . The sizes of both polymers followed the same relation within experimental error. Figure 3.6 shows the results of MeHP in two different solvents which are dioxane and benzonitrile. The size of MeHP did not change significantly with solvent. The above two experiments presented the dimensional behavior of hyperbranched polyarylates under different polymer-solvent interactions. Table 3.2 presents the estimated polymer-solvent interaction parameters<sup>21</sup>( $\chi$ ) of all the polymer-solvent pairs involved in this experiment. The estimations were made from group contribution method. Although the thermal interactions between the polymer and the solvent are different, the polymers showed a size stability.

Table 3.2: Polymer-solvent interaction parameters

$\chi$ (estimated)	MeHP	PhHP
benzonitrile	0.002	0.007
dioxane	0.27	0.33
cyclohexane	0.74	0.81

The highly branched structure of the polymer limited the number of configurations polymer chain could assume to be swelled. Unfortunately, exact linear analogs of these two polymers were not soluble in the solvent employed. Direct comparison with linear polymers was not possible. Figure 3.5 includes the statistical mechanics analysis result of poly(1-hydroxy-3-benzoic acid) at  $\theta$  condition<sup>22</sup>. The calculation was based on the rotational isomeric state (RIS) theory. Considering that the dimension of a linear polymer chain is always smaller in a  $\theta$  solvent than in a good solvent, this result is only a conservative estimation of the dimension of a linear polyarylate. Compared with linear polyarylate of the same molecular weight,  $\langle R_g^2 \rangle^{1/2}$  of hyperbranched polymer is even smaller. In this respect, the hyperbranched polymer was more compact than linear polymers.

The slope of the linear part of the relation gave a power  $\nu=0.41\pm0.03$ . This finding could be understood with the scaling treatment and the percolation theory<sup>9,23</sup>. Generally, the size of a polymer  $R$  is determined by the competition between an elastic energy,  $F_{el}$ , tending to keep  $R$  at its free or Gaussian value,  $R_0$ , and a repulsive energy,  $F_{rep}$ , tending to swell the polymer. The expression for  $F_{el}$  is simply that of a Gaussian chain,

$$F_{el} \sim \frac{R^2}{R_0^2}$$

$R_0$  increases as a power of the degree of polymerization  $N$ ,

$$R_0 \sim N^{v_0}$$

where  $v_0=0.5$  for linear polymers and 0.25 for branched polymers with a fixed probability for branching.  $F_{rep}$  is determined by short range two monomer units interactions in good solvents. In dilute solutions,

$$F_{rep} \sim \frac{N^2}{R^d}$$

where  $d$  is the dimension of the system of interest. In dense solutions or melt, the screening factor comes in. The degree of screening is determined by the weight average degree of polymerization, and we have

$$F_{rep} \sim \frac{N^2}{R^d} \frac{1}{N_w} \text{ and } N_w \sim N^\rho .$$

Minimizing  $F = F_{el} + F_{rep}$ , we have

$$v = \frac{2(1 + v_0) - \rho}{d + 2}$$

For dilute branched polymers or swelled gels,  $v_0=0.25$ ,  $\rho=0$ ,  $d=3$  which leads to  $v=0.5$ .

To determine the  $\rho$  value for highly concentrated branched polymer solution and melt, percolation theory goes into effect after a critical point<sup>24</sup>  $\alpha_c = \frac{1}{f-1}$  in which  $\alpha$  is the extent of the reaction and  $f$  is the functionality of the monomer. According to the theory,  $\rho=0.5$  regardless of the branching topology after the critical point. Thus  $v$  should be 0.4 for such case. For a randomly branched polymer, the critical point is the start of gelation. For a hyperbranched system, due to its unique topology, gelation in terms of a crosslinking network can not exist. However, for hyperbranched polyarylates,  $f=3$ , so  $\alpha_c$  is 0.5. When the polymerization goes to completion,  $\alpha$  is 0.66

which is well beyond the critical point. Thus, percolation theory should apply to hyperbranched polymers.

Figure 3.4 shows the power to be  $0.41 \pm 0.03$  which is close to the value of unswelled gel, indicating a limited degree of swelling of the polymer in solution. Thus, from this respect, hyperbranched polyarylates were proved to be dimensionally stable.

The second virial coefficient  $A_2$  followed the relation  $A_2 = KM^c$  as shown in Figure 3.7 and Figure 3.8 where  $c = -0.81 \pm 0.04$  for all experiments. Generally, the  $A_2$  values were positive but very small for polyarylates in dioxane and benzonitrile, indicating the power of these solvents are limited. The scattering of data at high molecular weights were due to errors created by these small values. Depending on the interaction parameter difference,  $K$  showed a range of values indicating different thermodynamic interactions between solvent and polymer. When cyclohexane was used as solvent, no stable scattering data could be obtained, presumably because cyclohexane was a poor solvent for both polymers so that aggregation of polymers occurred in the solution.

It has been established<sup>25</sup>, for particles in dilute solution

$$A_2 = 4\pi^{\frac{3}{2}} N_A \Psi \frac{R^3}{M^2} \quad (1)$$

where  $N_A$  is Avogadro's constant and  $\Psi$  is the segment interpenetration function, a measure of the degree of interpenetration of polymer molecules in dilute solution. Polymer chains in very good solvent may be regarded as a thermodynamically noninterpenetrable sphere. On the other hand, polymer molecules are completely interpenetrable at the theta temperature, at which  $\Psi$  vanishes.  $\Psi$  is also a function of segment density. The higher the segment density is, the higher  $\Psi$  is. For a rigid sphere,  $\Psi = 1.61$ <sup>26</sup>. If we bring  $v = 0.41 \pm 0.03$ ,  $c = -0.81 \pm 0.04$  into (1),  $\Psi$  may be considered

independent of the size of the molecule. This is universally true for polymers when the molecular weight exceeds a certain value. From the measured value of  $R_g$  and  $A_2$ ,  $\Psi$  of all solvent-polymer pairs were calculated and listed in Table 3.3. The values ranged from 0.12 to 0.20. These results strengthened the notion that hyperbranched polyarylates in these solvents behaved more like open, free- draining particles than dense, compact ones, allowing free penetration through the structure by solvent molecules. This was in agreement with the conclusion from other experiments.

Table 3.3:  $\psi$  values for different polymer-solvent interactions

$\Psi$	dioxane	benzonitrile
MeHP	0.12	0.19
PhHP	0.14	0.20

### Molecular Simulation

Based on the DB data from  $^1\text{H}$  NMR, we constructed a model of hyperbranched polyarylate with carboxylic acid end groups by using the Dreiding II<sup>27</sup> program. This program, over other available programs, had the advantage of predicting accurate geometries with less difficulty for large molecules. Due to the limited power of the computer, the calculation was conducted up to 64 units ( $M=10,500$ ). Figure 3.9 shows the result of the simulation. The same model is displayed from two different observation angles. Compared with the published simulation results of dendritic polyamidoamine by the same program, where inner generations were hardly recognizable after generation 4, one interesting feature of our results is that the structure was not as globular as we had expected, apparently due to the stiffness of the polyarylate chain. Secondly, there is no tendency of backfolding of the chain, which seemed to be the case for dendritic polymers<sup>5,6</sup>. Instead, every branch reached out to find more open space so that the structure was able to grow uniformly and infinitely. Most importantly, this space-filling structure was quite open with almost every unit

identifiable and accessible. This result was apparently in agreement with previous results from NMR and light scattering.

### Dynamic Mechanical Analysis

Although porous on the dimensions of solvents and LSR, hyperbranched polyarylates were still more compact than linear polymers as shown by light scattering experiment. Their highly branched topology should hinder the entanglement between polymer chains. This feature was examined by dynamic mechanical measurement on the melt of hyperbranched polyarylate.

Mastercurves of  $G'$ ,  $G''$  vs.  $\omega a_T$  were obtained by applying the time-temperature superposition principle. Zero-shear viscosity ( $\eta_0$ ) was calculated following the relation

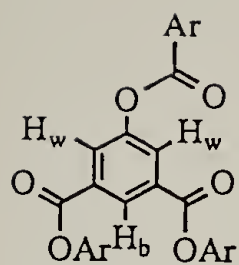
$$\eta_0 = \lim_{\omega \rightarrow 0} \eta' = \lim_{\omega \rightarrow 0} \frac{G''}{\omega}$$

Figure 3.10 shows the results for BuHP of  $M_w=16,500$  and PBuI of  $M_w=18,300$ . The reference temperature was taken as  $50^\circ\text{C}$  above the  $T_g$  of each sample. Although the two samples have comparable molecular weight, the viscoelastic behavior of BuHP was apparently different from that of PBuI. The mastercurve of BuHP looked very similar to the one of an unentangled polymer in the sense that below the glass transition frequency, the spectrum went directly to a standard Newtonian flow region without experiencing a plateau zone. However, the plateau showed up for the linear polymer PBuI manifested by the crossover between  $G'$  and  $G''$  around  $\omega=2500\text{rad/s}$ . As a result of this difference,  $\eta_0$  of BuHP was lower than that of PBuI by a magnitude, as shown in Figure 3.11. The relaxation spectra of these two polymers are shown in Figure 3.12. The apparent difference was the short relaxation time region where PBuI displayed a plateau and BuHP did not, indicating the relaxation mechanisms of the two polymers in this region were different.

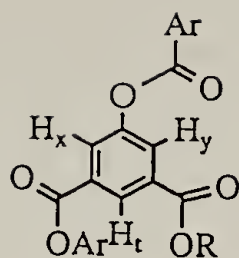
Even for linear polymers, it is necessary for the polymer to have enough chain length to form entanglement. Thus, the lack of entanglement found in the experiment described above might simply be a molecular weight effect instead of the result of molecular topology since BuHP of  $M_w=16,500$  had only approximately 80 units. Figure 3.13 shows the mastercurves of BuHP of  $M_w=16,500$  and 283,000. For the high molecular weight sample, the emergence of plateau zone was still not evident. Therefore, we can conclude that the absence of this region was due to the topology of hyperbranched structure rather than the low molecular weight effect.

### Conclusion

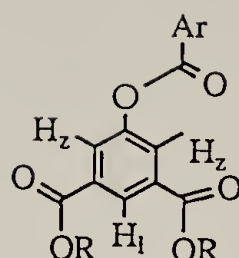
Because of their highly branched structure and the stiffness of the aryl ester bond, hyperbranched polyarylates had smaller molecular size than linear polymers and certain dimensional stability. However, the structure was still penetrable by small molecules such as solvents and LSR. Thus, in general, they may be perceived as hard porous particles. As a result, melt behavior of the hyperbranched polyarylate showed low viscosity and lack of entanglement between polymer chains.



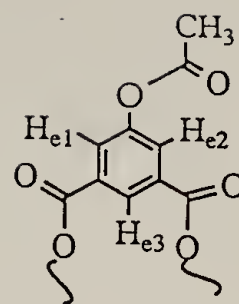
branch unit



linear unit



terminal unit



initial unit

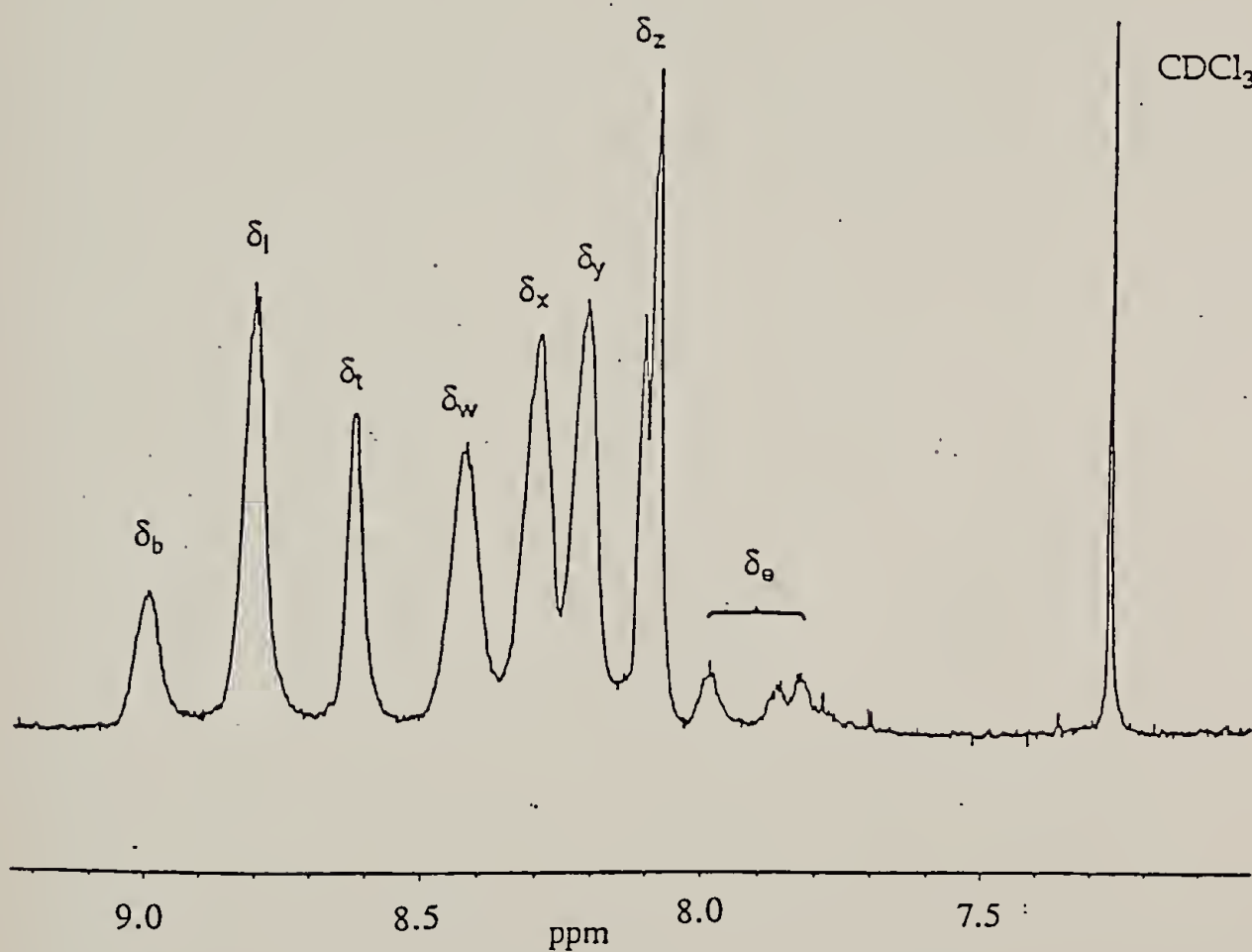


Figure 3.2:  $^1\text{H}$  NMR peak identification of aromatic protons of EhHP

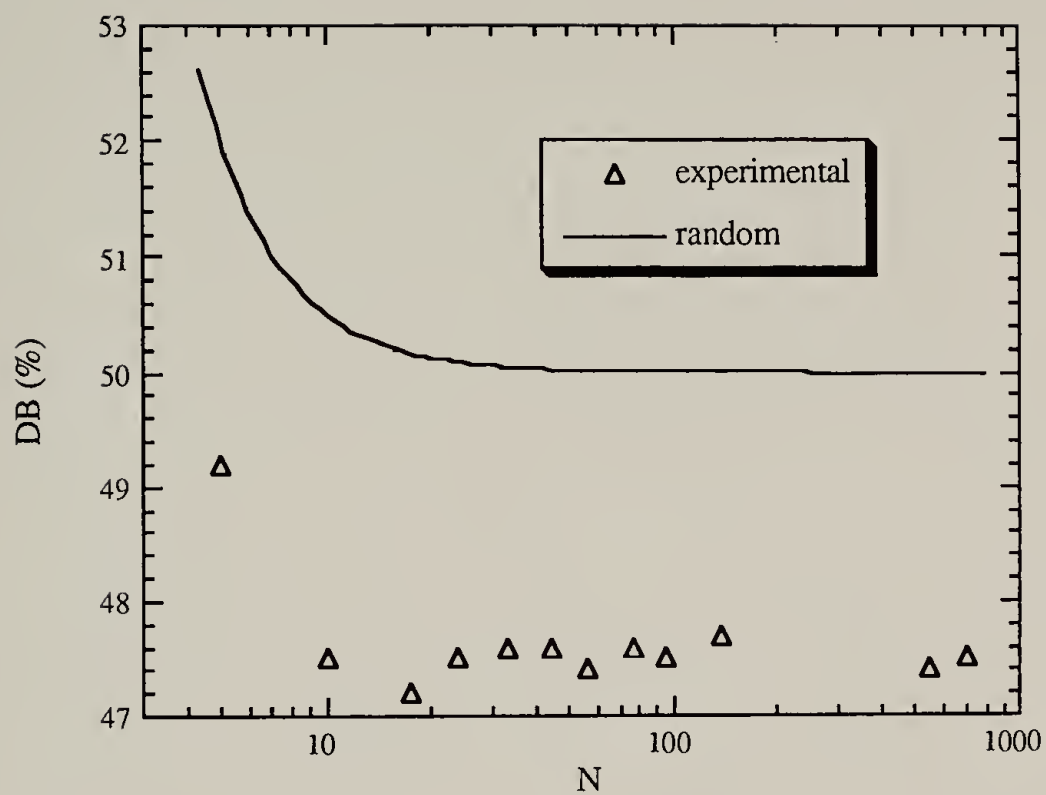


Figure 3.3: Dependence of degree of branching on degree of polymerization

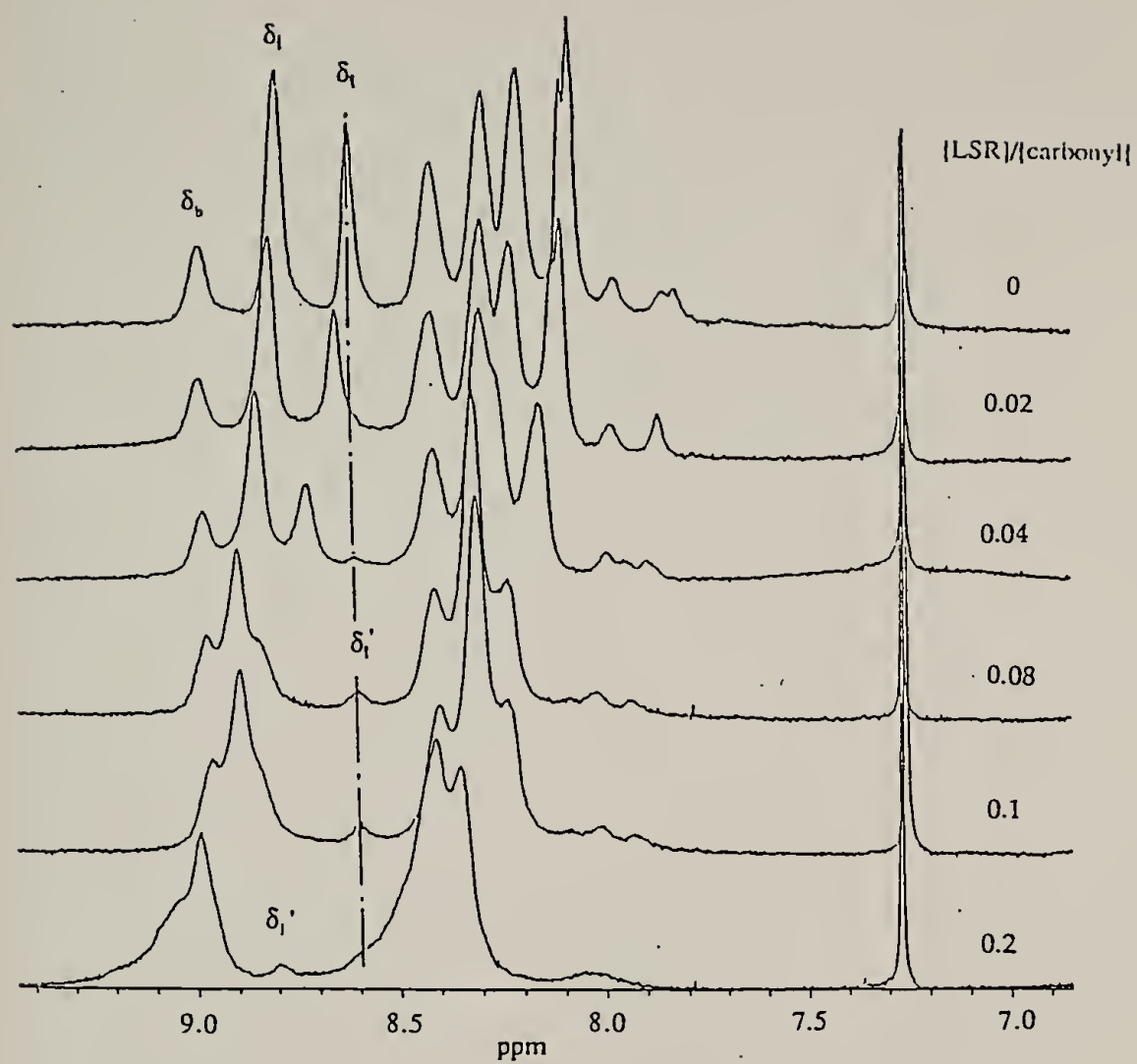


Figure 3.4: Effect of LSR on  $^1\text{H}$  NMR of EhHP ( $M_n=21,400$ )

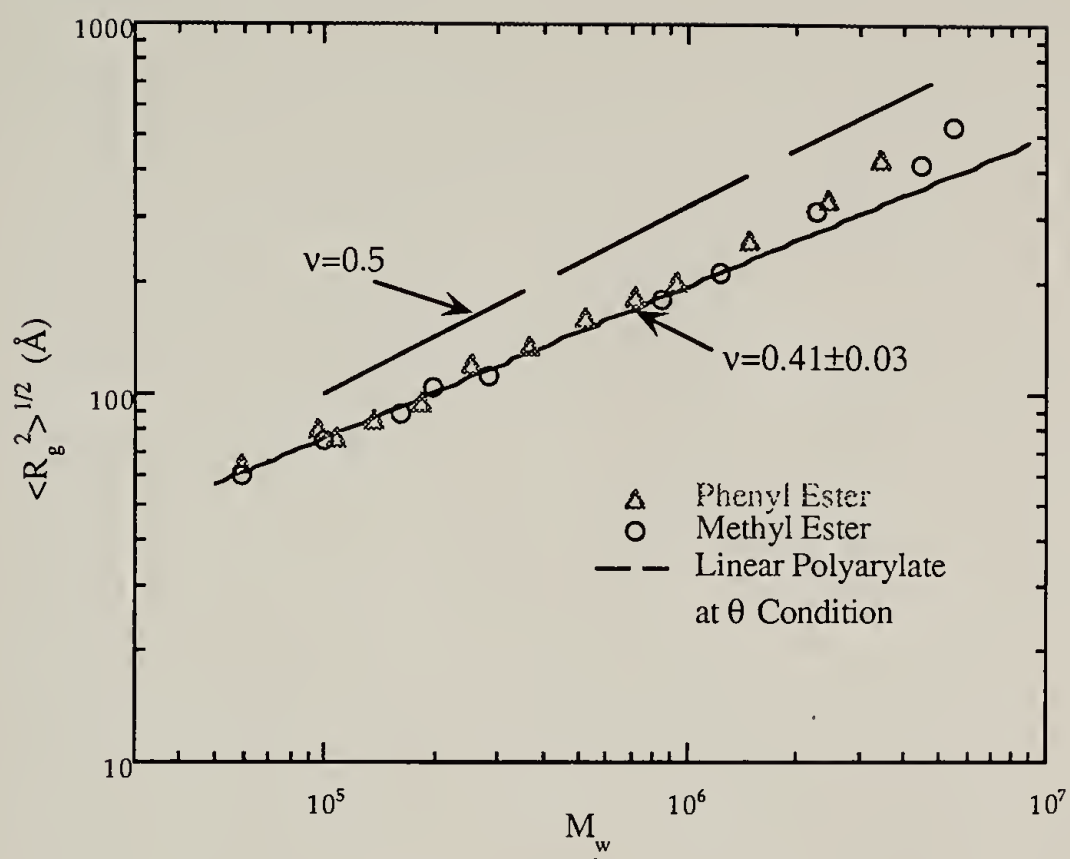


Figure 3.5: Dependence of root mean square radius of gyration  $\langle R_g^2 \rangle^{1/2}$  on weight average molecular weight ( $M_w$ ) (measured in dioxane at 15°C)

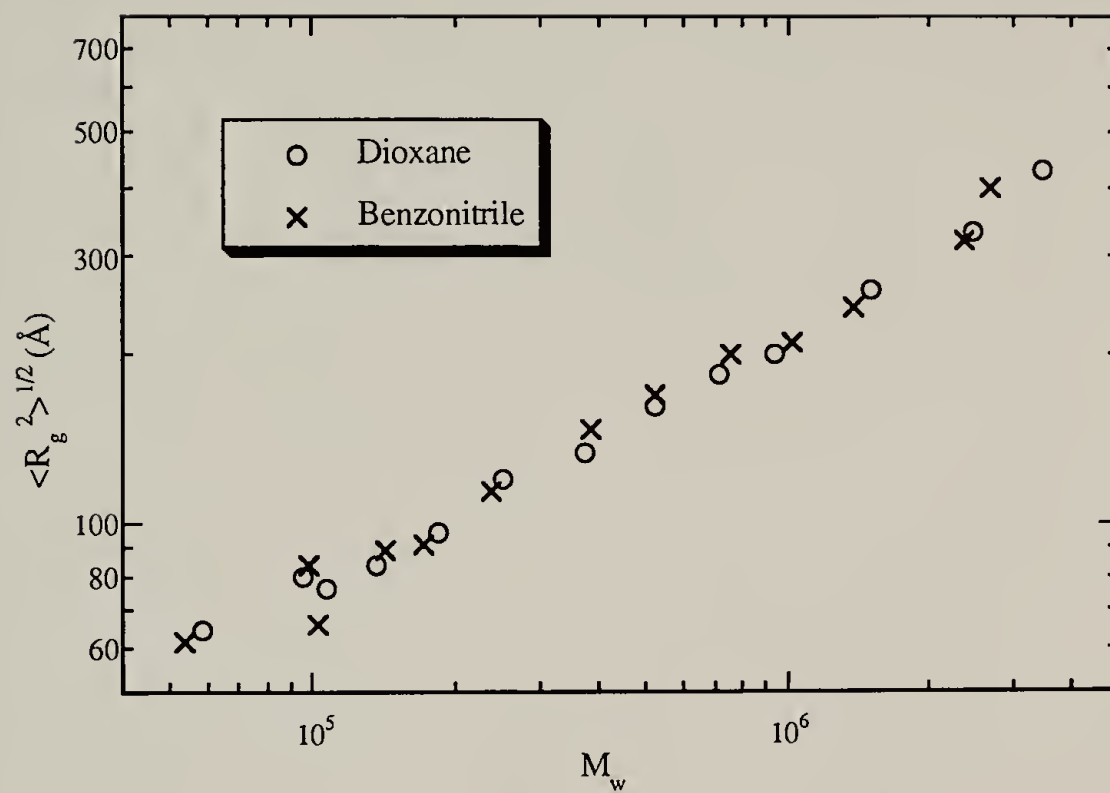


Figure 3.6: Dependence of root mean square radius of gyration  $\langle R_g^2 \rangle^{1/2}$  on weight average molecular weight ( $M_w$ ) (Measured with MeHP at 15°C)

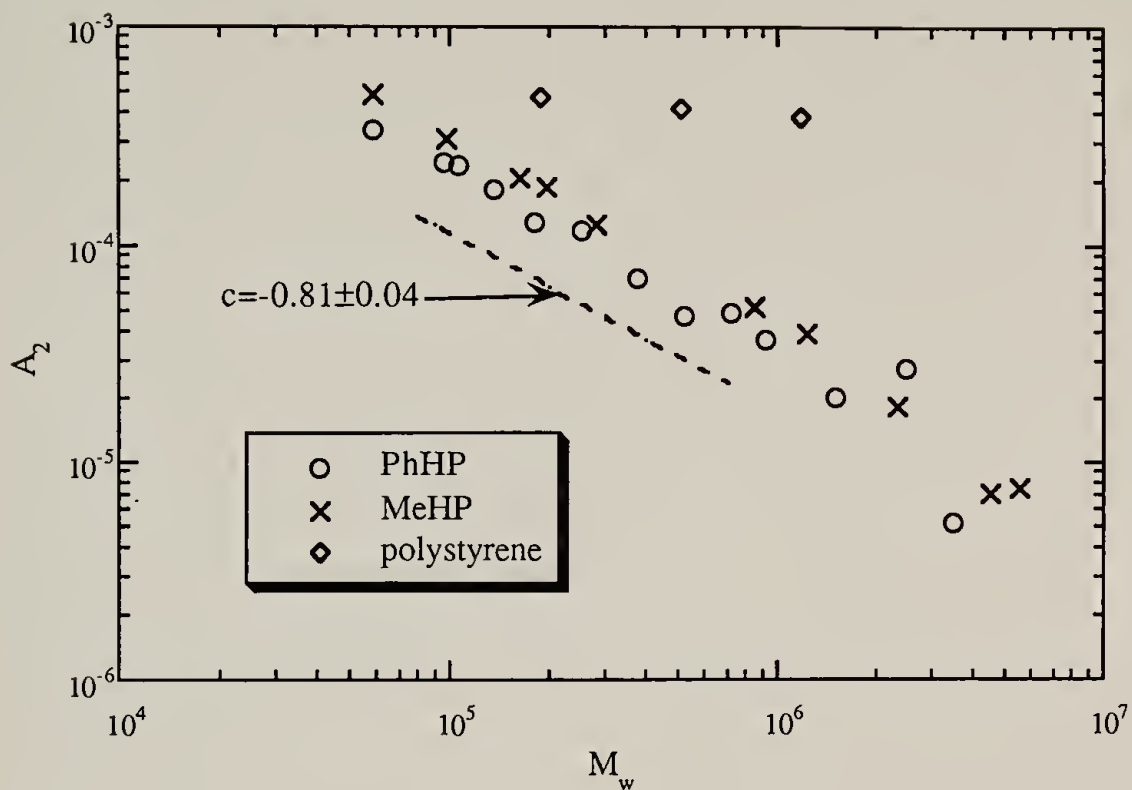


Figure 3.7: Dependence of the second virial coefficient ( $A_2$ ) on weight average molecular weight ( $M_w$ ) (measured in dioxane at 15°C)

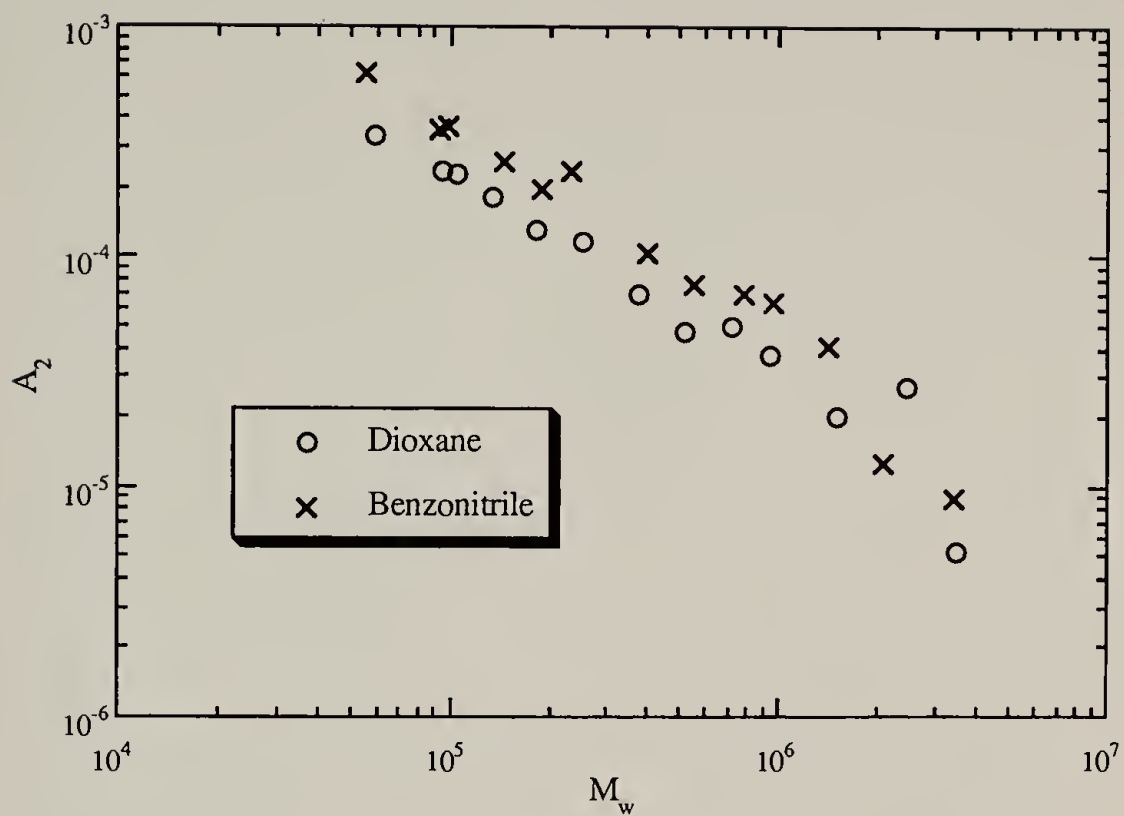


Figure 3.8: Dependence of the second virial coefficient ( $A_2$ ) on weight average molecular weight ( $M_w$ ) (measured with MeHP at 15°C)

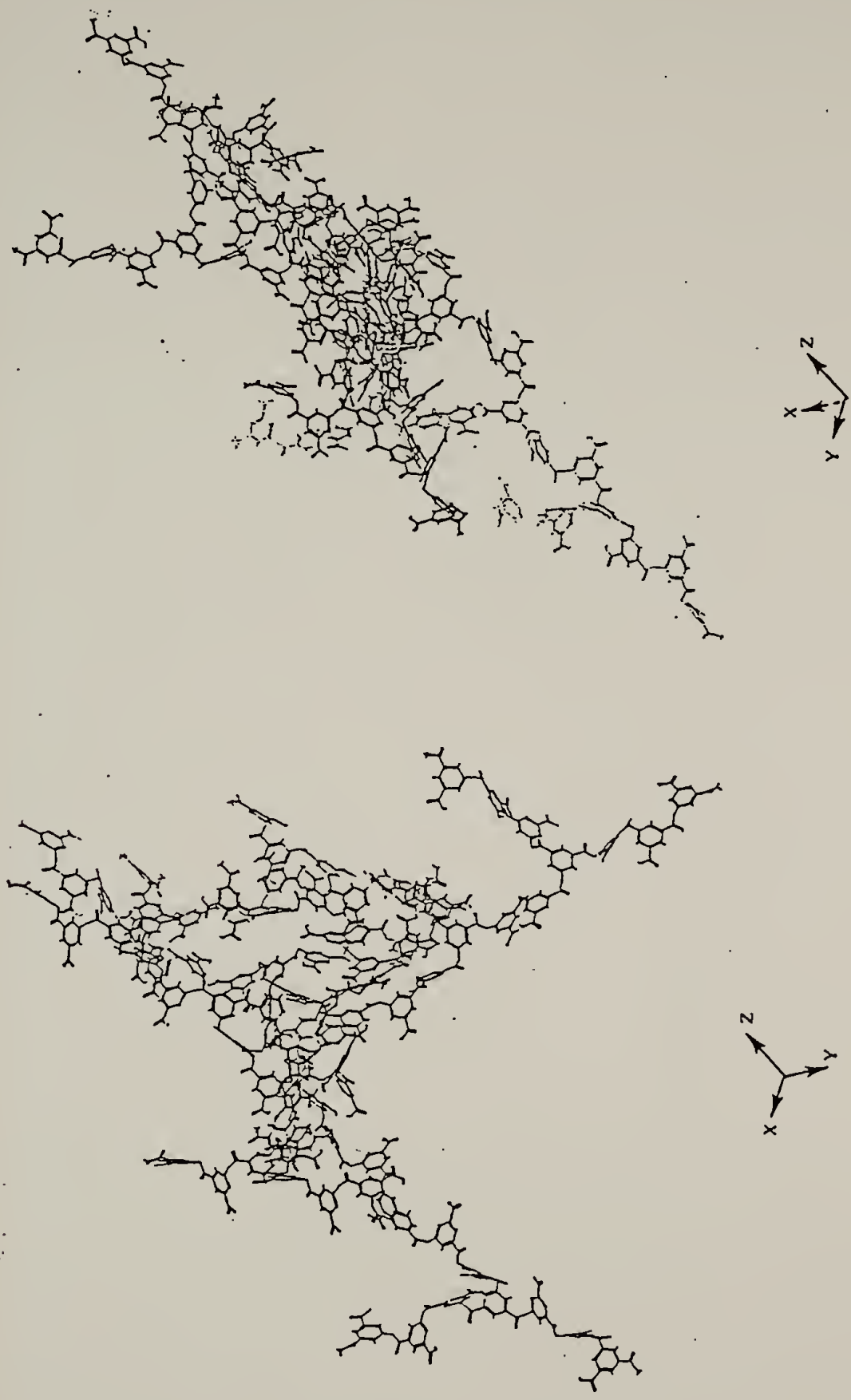


Figure 3.9: Molecular simulation results

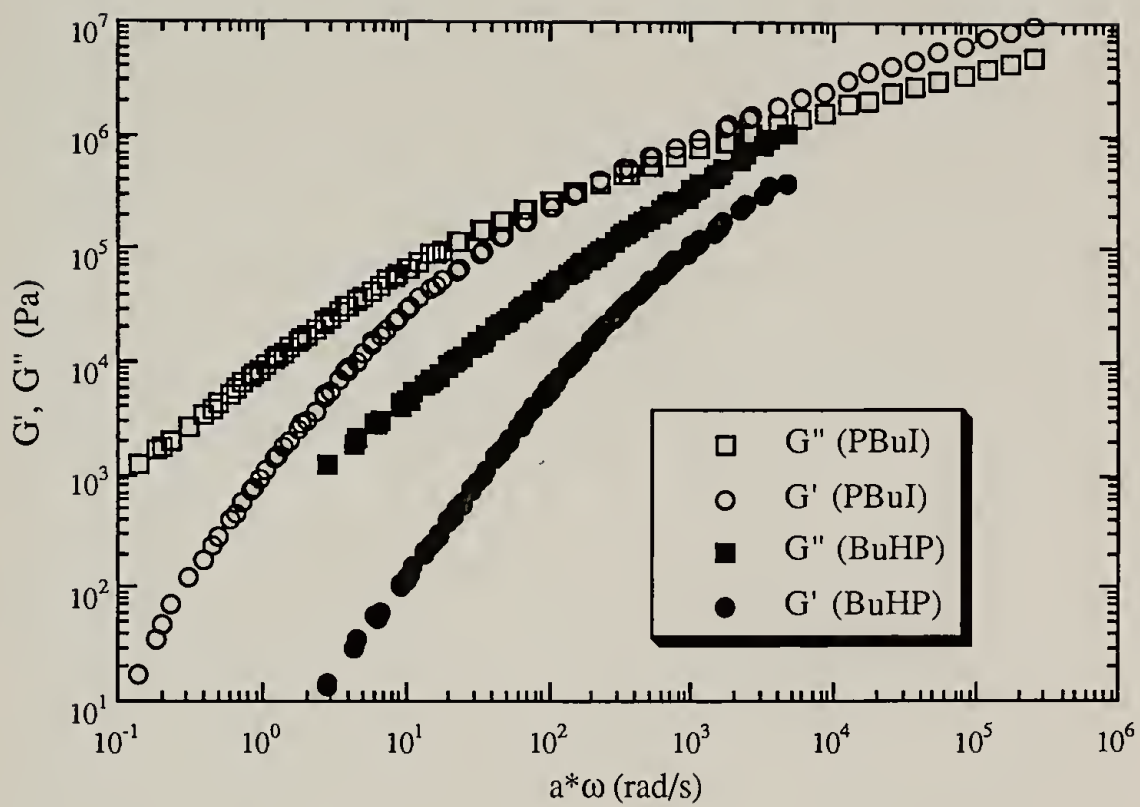


Figure 3.10: Mastercurves of BuHP and PBuI ( $T_{\text{ref}}=T_g+80^\circ\text{C}$ )

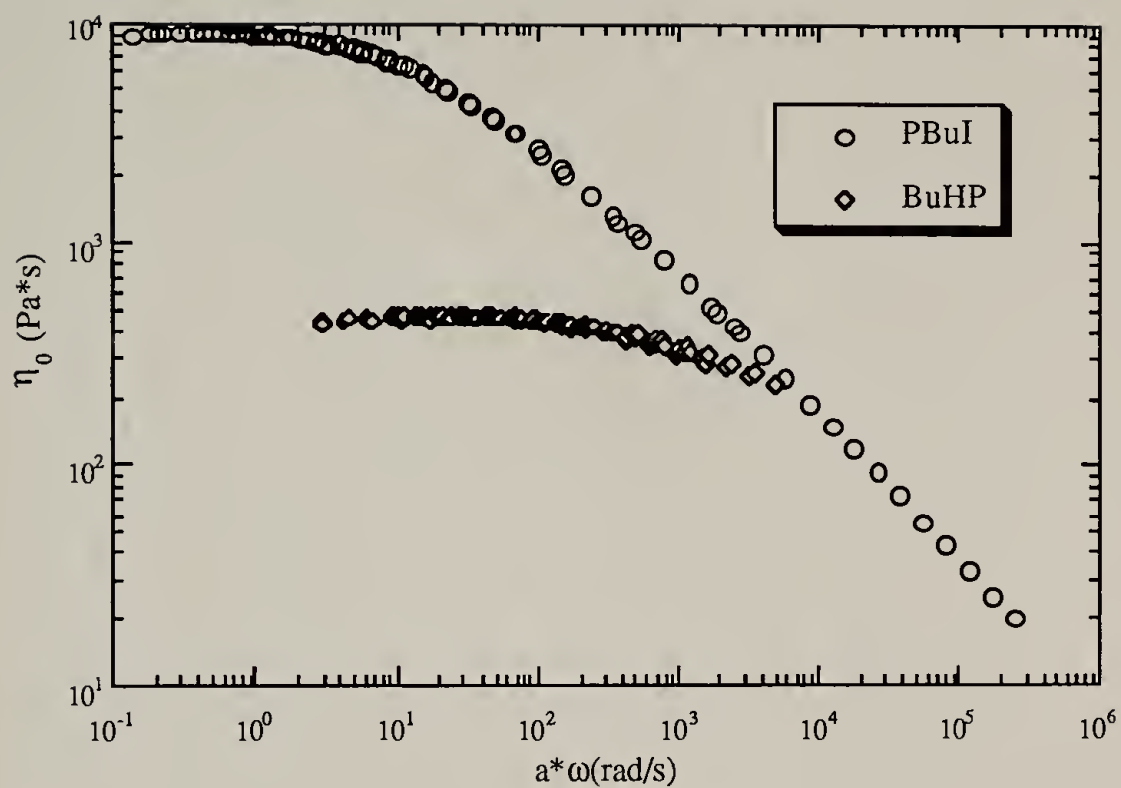


Figure 3.11: Dynamic viscosity of BuHP and PBuI ( $T_{\text{ref}} = T_g + 80^\circ\text{C}$ )

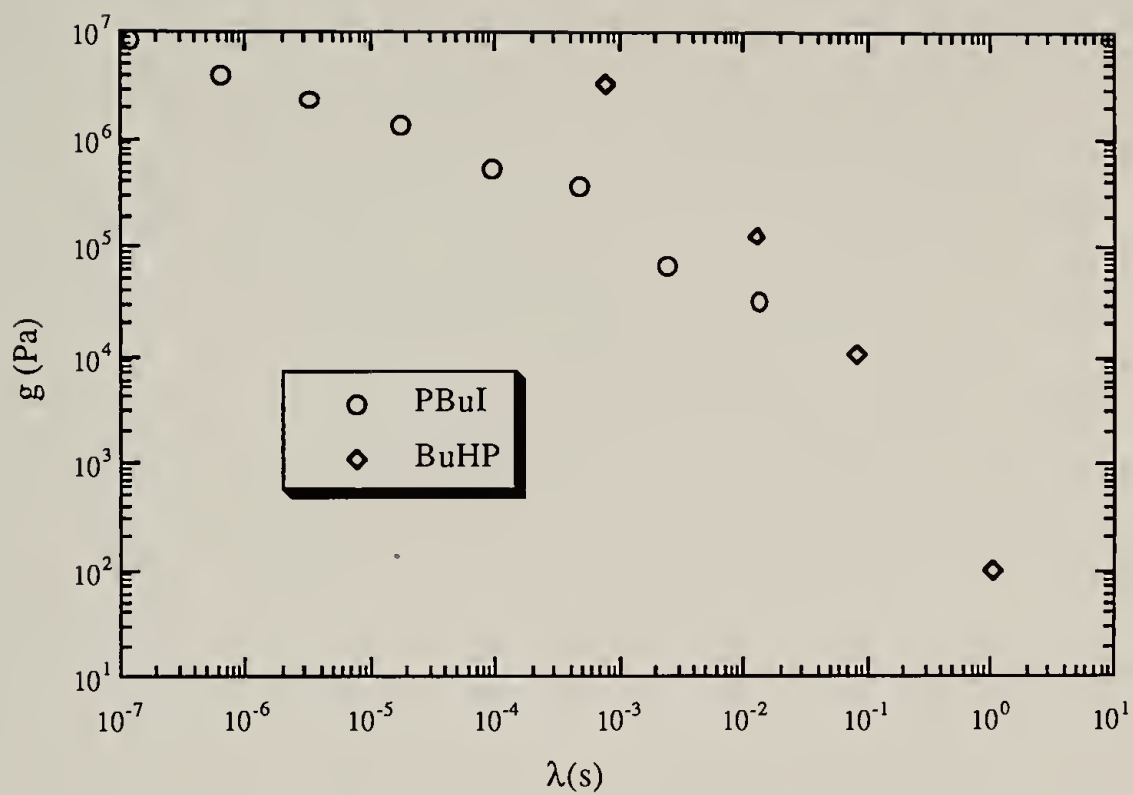


Figure 3.12: Relaxation spectra of BuHP and PBuI

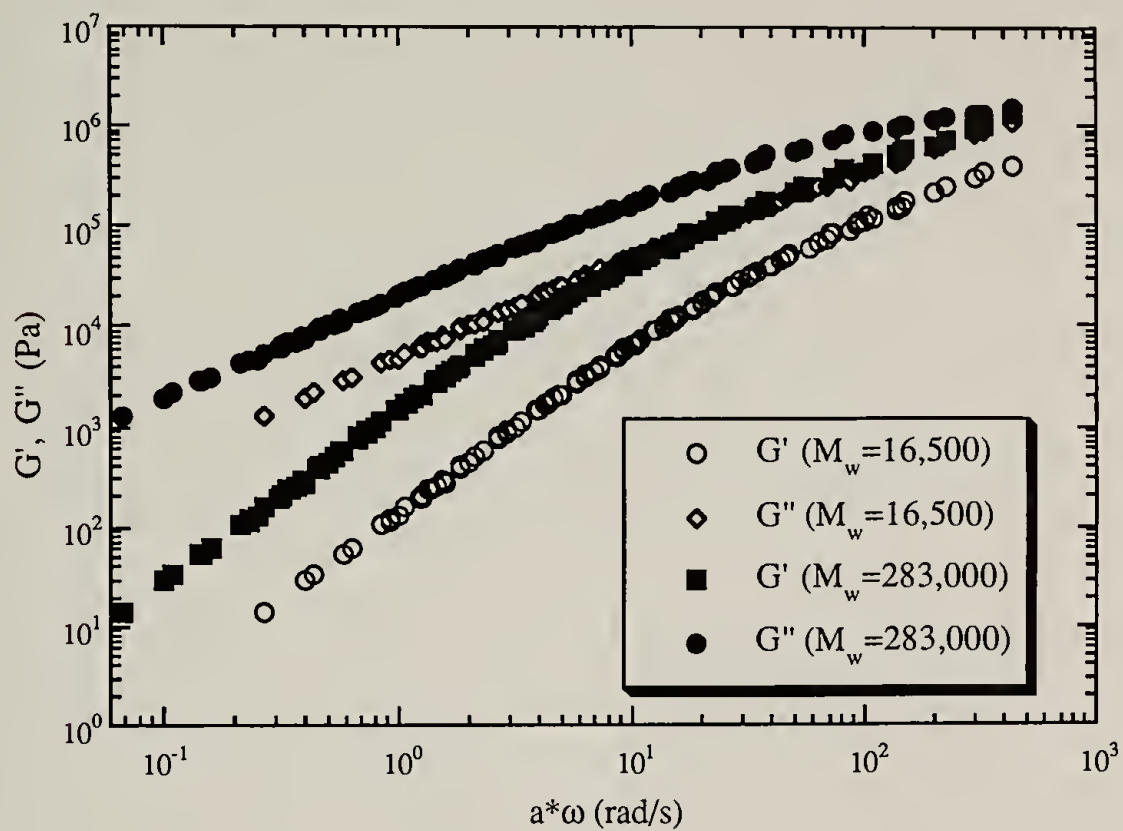


Figure 3.13: Mastercurves of BuHP of  $M_w=16,500$  and  $283,000$  ( $T_{ref}=120^\circ\text{C}$ )

## References

1. de Gennes, P. G., Hervet, H., J. Phys., Lett., **44**, L351 (1983)
2. Maciejewski, M., Macromol. Sci., Chem., , **A17** (4), 689 (1982)
3. Lescanec, R. L. and Muthukumar, M., Macromol., **24**, 4892 (1991)
4. Meltzer, A. D., Tirrell, D. A., Jones, A. A., Inglefield, P. T., Hedstrand, D. M. and Tomalia, D. A., Macromol., **25**, 4541 (1992)
5. Meltzer, A. D., Tirrell, D. A., Jones, A. A. and Inglefield, P. T., Macromol., **25**, 4549 (1992)
6. Mansfield, M. L. and Klushin, L. I., private communication.
7. Bauer, B. J., Briber, B. M. and Hammouda, B., Polym. Prep., **2**, 476 (1992)
8. Briber, B. M., Bauer, B. J. and Hammouda, B., Polym. Prep., **2**, 478 (1992)
9. Stauffer, D., Introduction to Percolation Theory; (Taylor and Francis: London) (1985)
10. de Gennes, P. G., Scaling Concepts in Polymer Physics , (Cornell University: Ithaca) (1979)
11. Zimm, B. H. and Stockmayer, W. H., J. Chem. Phys., **17**, 1301 (1949)
12. Bauer, J. and Burchard, W., Macromol., **26**, 3103 (1993)
13. Antonietti, M., Basten, R. and Lohmann, S., Macromol. Chem. Phys., **196**, 441 (1995)
14. Wachenfeld-Eisele, E. and Burchard, W., Macromol., **22**, 2496 (1989)
15. Ferry, J. D., Viscoelastic Properties of Polymers, (Wiley: New York) (1980)
16. Antonietti, M., Pakula, T. and Bremser, W., Macromol., **28**, 4227 (1995)
17. Hawker, C. J., Frechet, J. M. J., J. Am. Chem. Soc., **112**, 7638 (1990)
18. Wenzel, T. J., NMR Shift Reagents, (CRC Press: Boca Raton) (1987)
19. de Villiers, J. P. R. and Boeyens, J. C. A., Acta Cryst., **B27**, 692 (1971)
20. Cramer, R. E. and Seff, K., Acta Cryst., **B28**, 3281 (1972)
21. Small, P. A., J. Appl. Chem., **3**, 71 (1953)
22. Rutledge, G. C., Macromol., **25**, 3984 (1992)

23. Isaacson, J. and Lubensky, T. C., J. Phys., Lett., **41**, L469 (1980)
24. Flory, P., Principle of Polymer Chemistry, (Cornell University: Ithaca) (1971)
25. Yamakawa, H., Modern Theory of Polymer Solution, (Harper and Row: New York) (1971)
26. Lang, P., Burchard, W., Wolfe, M. S., Spinelli, H. J. and Page, L., Macromol., **24**, 1306 (1991)
27. Mayo, S. L., Olafson, B. D. and Goddard, W. A., III., J. Phys. Chem., **94**, 8897 (1990)

## CHAPTER 4

### BLEND OF N-BUTYL HYPERBRANCHED POLYARYLATE AND POLY(1,4-BUTYLENE ISOPHTHALATE)

#### Introduction

As has been shown in Chapter 3, n-butyl hyperbranched polyarylate (BuHP) had a much lower melt viscosity than its linear analog, poly(1,4-butylene isophthalate) (PBuI). This feature opened a window of application for hyperbranched polymers as rheology modifiers. In the meantime, hyperbranched polymers are intrinsically isotropic so that they can also function as an anisotropy reducer when blended with linear polymers. To realize both of these application potentials, blends of hyperbranched polymer and linear polymer need to be investigated in terms of miscibility, morphology and mechanical properties.

The miscibility of polymer blend is defined<sup>1,2</sup> in terms of equilibrium thermodynamics, e.g. if the free energy of mixing is negative ( $\Delta G_m < 0$ ), the blend is miscible and the material is homogeneous on the segmental scale. Otherwise, if the free energy of mixing is positive ( $\Delta G_m > 0$ ), the blend is immiscible and phase-separated. Most polymer blends are immiscible due to the unfavorable enthalpy contribution. Among the few immiscible blends, the properties of their homopolymer components are often too similar to have any practical advantage for blending. Properties of immiscible blends not only depend on those of their constituent polymers but also on the morphology of phase separation. Among them is a special class of blends called compatible blends. The domain size of phase separation in such blends is submicron. These blends are generally homogeneous to eye and frequently offer improved physical properties over the constituent polymers.

The effect of hyperbranching topology on the miscibility and the compatibility of blends has hardly been addressed. Massa et al<sup>3</sup> studied the blends of hyperbranched

polyarylates with linear polymers such as polycarbonate, polyesters and polyamides. They found that none of the blends was miscible. However, they did not mention the morphology of these phase separated blends. Moreover, because the chemical compositions of their model polymers were different, they failed to pin point the contribution of the hyperbranching topology on miscibility.

The free energy of mixing ( $\Delta G_m$ ) consists of an entropy term ( $\Delta S_m$ ) and an enthalpy term ( $\Delta H_m$ ), e.g.

$$\Delta G_m = \Delta H_m - T\Delta S_m$$

According to Flory-Huggins theory,  $\Delta H_m$  can be expressed as

$$\Delta H_m = RT(V/V_0)\chi\phi_1\phi_2$$

where  $\chi$  is the Flory-Huggins interaction parameter,  $\phi_h$  and  $\phi_l$  are the volume fractions of hyperbranched and linear polymer respectively,  $V$  is the total volume of the blend and  $V_0$  is a reference volume. For polymers without specific interaction,  $\chi$  may be expressed in terms of the solubility parameters of the two constituent polymers, e.g.

$$\chi = \frac{V_0}{RT}(\delta_1 - \delta_2)^2$$

where,  $R$  is the gas constant and  $\delta_1, \delta_2$  are the solubility parameters of the two constituent polymers.

According to the theory, for a blend of two linear polymers

$$\Delta G_m = RT(V/V_0)[(\phi_1/x_1)\ln\phi_1 + (\phi_2/x_2)\ln\phi_2 + \chi\phi_1\phi_2]$$

where  $x_1$  and  $x_2$  are the degree of polymerization of the two polymers. For the above relationship, there exists a critical value of  $\chi_c$  below which phase separation can not occur and  $\chi_c$  is  $0.5(x_1^{-0.5} + x_2^{-0.5})^2$ .

In this chapter, we'll examine the validity of the above theory in the hyperbranched -linear polymer system by selecting chemically similar BuHP and PBuI as model polymers whose solubility parameters are 10.6 and 10.4 (cal/ml)<sup>0.5</sup> respectively. The estimated  $\chi$  value for the polymer pair is 0.007.

Fractionated BuHP samples with different molecular weights were used to investigate the molecular weight effect on miscibility. The miscibility of BuHP and PBuI was observed by Differential Scanning Calorimetry (DSC). The morphology of the blends was analyzed by Transmission Electron Microscopy. Finally, the effects of introducing the hyperbranched polymer on the rheological properties were investigated.

## Experimental

### Sample Preparation

n-Butyl hyperbranched polyarylate (BuHP) was synthesized and fractionated according to the procedures described in Chapter I. Poly(1,4-butylene isophthalate) (PBuI) was purchased from Sp<sup>2</sup> Scientific Polymer Product, Inc.  $M_w=18,300$  according to the product report. All blends were prepared by the solution casting method in combination with press molding. Thus a 5% solution of the two polymers was made by using a common solvent, m-cresol, with subsequent evaporation of the solvent under nitrogen at 150°C for 48 hours. 3 torr vacuum was then applied and the temperature was raised to 160°C to dry the films to a constant weight. The casted film was then press molded under 200 psi at 160°C for 10min. GPC showed the molecular weight distribution of BuHP did not change after the above procedure.

### Differential Scanning Calorimetry (DSC)

The thermal analysis of blends was determined by a Perkin-Elmer DSC7 instrument at a 20°C/min heating rate. The temperature and power ordinates of the DSC were calibrated with respect to the known melting point and heat of fusion of high purity indium and mercury standards supplied by Perkin-Elmer. The glass transition temperature ( $T_g$ ) was defined as the midpoint of the change in the specific heat.

Although poly(1,4-butylene isophthalate) was a semicrystalline material ( $T_m = 145^\circ\text{C}$ ), the rate of crystallization was extremely slow. If annealed at any temperature between  $T_g$  and  $T_m$ , no crystallization was detectable within 4 hours. This feature allowed us to focus the attention on the amorphous phase behavior of the blends. To avoid crystallization, all PBuI containing blends were first heated to  $170^\circ\text{C}$  before being annealed at programmed temperatures. Samples were annealed at the annealing temperature for 30 minutes before being quenched in liquid nitrogen to preserve the phase properties.

#### Transmission Electron Microscopy (TEM)

The morphology of blends was observed by using TEM. To enhance the contrast between phases, 5mol% of allyl alcohol was added with n-butanol to make BuHP. DSC showed no change of  $T_g$  from 100% n-butanol modified BuHP. Blends were prepared by the same method for the thermal measurement. Approximately 700 Å thick sections of sample were cut by cryoultramicrotomy using a diamond knife at  $-50^\circ\text{C}$ . These sections were collected on copper TEM grids and stained in  $\text{OsO}_4$  vapor for 5 hours. The stain reacted preferentially with the double bonds in BuHP, rendering the BuHP microdomain dark via mass-thicken contrast in TEM micrographs. The samples were then observed in a JEOL 100CX TEM operated at 100 KV.

#### Dynamic Mechanical Analysis

Measurements were carried out on a Rheometrics RMS800 rheometer. By compression molding at  $170^\circ\text{C}$ , disks with a diameter of 30mm were prepared to fit the geometry of a 25mm plate/plate rheometer. This treatment and the subsequent measurement did not affect the original molecular weight distribution as checked by GPC. The temperature of testing ranged from  $80^\circ\text{C}$  to  $170^\circ\text{C}$  and the frequency from 1 rad/s to 464 rad/s.

## Results and discussion

### Miscibility of BuHP/PBuI Blends

DSC experiments covered blends of BuHP content from 0 to 100% with 10% increments and the annealing temperature ranged from 80 to 200°C. PBuI was a semicrystalline material with  $T_m=145^\circ\text{C}$ . However, the rate of crystallization was so slow that within the time scale of the experiment, the crystallization was undetectable. This feature provided some convenience for the explanation of data because it allowed us to focus our attention on the glass transitions of the two polymers.

Shown as the bottom curve in Figure 4.1, the glass transition of BuHP covered a wide temperature range. In the case of linear polymers, this is usually attributed to the wide molecular weight distribution of sample. However, the BuHP samples employed in this experiment were well fractionated and had PDIs lower than 2. We attributed this phenomenon to the structural polydispersity of hyperbranched polymer as has been mentioned in Chapter I.

For the blends that were composed of BuHP of  $M_w=16,500$  and PBuI of  $M_w=18,300$ , all blends were found immiscible at any annealing temperature. Figure 4.1 shows a typical example of the thermograms of different compositions at the annealing temperature of 160°C. Thermograms at other annealing temperatures were essentially identical to this example. Although at low BuHP content, the  $T_g$  of BuHP was hard to recognize, the  $T_g$  of PBuI always maintained the same value. The change of heat capacity ( $\Delta C_p$ ) of the transition also stayed the same. This is a clear evidence of phase separation. Blend samples were also prepared by using BuHP with different molecular weight. Figure 4.2 shows the thermograms of blends composed of 50% of PBuI of  $M_w=18,300$  and 50% of some fractions of BuHP of low molecular weight. The  $T_g$  of PBuI phase did not shift until BuHP of  $M_w=8,860$  was blended. Below this molecular weight, the  $T_g$  of PBuI phase started to shift slightly to a higher value indicating partial miscibility. This shift continued until the BuHP of the lowest molecular weight

available ( $M_w=3,270$ ) was blended. The  $T_g$  of this fraction was hardly recognizable. However, judging from the slight shift of PBuI transition, this blend was still immiscible. As a result, we were not able to detect the lower molecular weight limit below which the blend was miscible. Thus, from DSC data, no miscibility window could be found.

If we apply the Flory-Huggins theory for linear-linear polymer blend to the blend of polymer 1 of  $M_w=3,270$  ( $x_1=17$ ) and polymer 2 of  $M_w=18,300$  ( $x_2=83$ ), the critical interaction parameter  $\chi_c$  for the system is

$$\chi_c = 0.5(x_1^{-0.5} + x_2^{-0.5})^2 = 0.5(17^{-0.5} + 83^{-0.5})^2 = 0.062$$

For the system we have chosen,  $\chi=0.007$  which is far smaller than  $\chi_c$ . Thus, immiscibility should not have been observed if the two polymers had been both linear polymers. Apparently, in our case, the hyperbranching topology contributed unfavorably to the free energy change of mixing,  $\Delta G_m$ . To take the hyperbranching topology into account, the entropy change of mixing,  $\Delta S_m$ , has to be reconsidered. Unfortunately, the exact calculation or simulation of  $\Delta S_m$  of the similar system is not currently available. From the results of chapter III, we can roughly consider hyperbranched polymers as hard porous particles and design a lattice model as shown in Figure 4.3. According to Flory-Huggins theory<sup>1,4</sup>, the formation of polymer solution may be perceived to occur in two steps: disorientation of the homopolymer chains and the mixing of the disoriented chains.

For linear homopolymer, the configurational entropy is its disorientational entropy, e.g.

$$S_1 = S_{d1} = -R(V/V_0)(\phi_1/x_1)\{\ln(1/x_1) - (x_1-1)\ln[(z-1)/e]\}$$

where  $k$  is Boltzman constant,  $\phi_l$  is the volume fraction of linear polymer and  $x_l$  is the degree of polymerization of linear polymer and  $z$  is the coordination number of the lattice.

For a hard porous particles, there are so few ways to arrange themselves in the lattice that

$$S_h \approx 0$$

For the blend of linear polymer and hard porous particle,

$$S_b = S_{mb} + S_{db}$$

where  $S_b$  is the configurational entropy of the blend,  $S_{mb}$  is the mixing entropy and  $S_{db}$  is the disorientational entropy.

$S_{mb}$  is universal for all blends and

$$S_{mb} = -R(V/V_0)[(\phi_l/x_l)\ln\phi_l + (\phi_h/x_h)\ln\phi_h]$$

where  $\phi_l$ ,  $\phi_h$  are the volume fractions of linear and hyperbranched polymer respectively.

As for the disorientational entropy of the blend  $S_{db}$ , the most contribution is from the linear polymers that are outside of the pores and are not restricted by the pores.

Assuming  $\rho$  is the pore content in the hard particles, then

$$S_{db} \approx -(1-\rho\phi_h)S_{dl} = -(1-\rho\phi_h) R (V/V_0)(\phi_l/x_l) \{ \ln(1/x_l) - (x_l-1)\ln[(z-1)/e] \}$$

Thus,

$$S_b \approx - R(V/V_0) \{ [(\phi_l/x_l)\ln\phi_l + (\phi_h/x_h)\ln\phi_h] + (1-\rho\phi_h)(\phi_l/x_l) \{ \ln(1/x_l) - (x_l-1)\ln[(z-1)/e] \} \}$$

The entropy change of mixing is then,

$$\Delta S_m = S_b - (S_l + S_h)$$

$$\approx - R(V/V_0) \{ [(\phi_l/x_l)\ln\phi_l + (\phi_h/x_h)\ln\phi_h] - \rho\phi_h(\phi_l/x_l) \{ \ln(1/x_l) - (x_l-1)\ln[(z-1)/e] \} \}$$

Thus,  $\Delta G_m = RT(V/V_0)\{[(\phi_l/x_l)\ln\phi_l + (\phi_h/x_h)\ln\phi_h]$

$$- \rho\phi_h(\phi_l/x_l)\{\ln(1/x_l) - (x_l-1)\ln[(z-1)/e]\} + \chi\phi_l\phi_h\}$$

From this relation, the critical interaction parameter for hyperbranched-linear polymer blend can be calculated by taking the third differential of  $\Delta G_m$  over  $\phi_h$  as zero.

Thus,  $\chi_c = 0.5(x_l^{-0.5} + x_h^{-0.5})^2 + (\rho/x_l)\{\ln(1/x_l) - (x_l-1)\ln[(z-1)/e]\}$ . The second term in this equation is the effect of hyperbranching topology and is always negative. In order to guarantee miscibility, the real  $\chi$  value of the hyperbranched-linear polymer pair has to be much smaller than that of the linear-linear polymer pair. Assuming  $\rho=0.2$ , i.e. 20% of the volume of hyperbranched polymer can be considered as pores. Taking  $x_l=83$ ,  $x_h=17$  into this equation, we get the result  $\chi_c = -0.06$ . Therefore, there has to be a specific interaction between the two polymers in order to guarantee the miscibility.

Although this proposed model is crude in many senses, it explains well qualitatively the experimental results.

#### Morphology of BuHP/PBuI blends

TEM was used to observe the morphologies of blends. For annealed samples, phase separation was observable even at low BuHP content. Figure 4.4 shows the micrograph of the blend of 20wt% BuHP. Small spherical domains of BuHP phase of 400 to 600Å were present and these domains tended to aggregate without coalescing. Considering that the repeating units of the two polymers had similar solubility parameters, this phenomenon was possibly due to the low interfacial tension between the two phases. As BuHP content increased (as shown in Figure 4.5 of blend of 40wt% BuHP content), the separated phase spread though the whole observed section in a percolative manner similar to the morphology of early stage spinodal decomposition.

With BuHP content higher than 60%, the material became so brittle that high quality microtoning was not possible. Figure 4.6 shows the morphology of this blend. Phase inversion was still not observable at this content. Thus, within the experimentally observable composition range, although BuHP/PBuI blends were not miscible in the thermodynamic sense, they could be considered compatible morphologically.

#### Dynamic mechanical analysis

The time-temperature superposition principle was applied to all blends to construct the master curves. Figure 4.7 shows the master curve of blends of 50% BuHP as an example. Because time-temperature superposition was theoretically valid only for homopolymers<sup>5</sup>, cautions had to be taken when applying this principle to immiscible blend systems. According to Han and Kim<sup>6</sup>, the superposition could be applied to blends if  $\log G'$  and  $\log G''$  have linear relationship over the whole experimental frequency range. Figure 4.8 displays this relationship for BuHP/PBuI blends of all compositions. For each individual composition, the linear relation was valid. Thus, superposition could be applied to each blend. However, the fact that all data did not collapse as one line indicated that structural changes other than viscoelasticity happened in the material. This point can be further illustrated by the different  $\log a_T \sim T$  relationships of the blends as shown in Figure 4.9.  $a_T$  is the temperature reduction factor.

The most interesting finding of the rheological properties was the zero-shear viscosities of the blends as shown in Figure 4.10. Over the whole range of composition,  $\eta_0$ s of the blends showed negative deviations from the log-additivity rule which represented ideal athermal mixing of the two components without volume change. To understand the reasons for the observed changes, it is important to compare the relaxation characteristics with changes in the free volume of the system.

For this purpose, we carried out the calculation of free volume based on the William-Landel-Ferry (WLF) equation<sup>5,7,8</sup>, e.g.

$$\log a_T = - \frac{[b/Rf(T_0)](T - T_0)}{f(T_0)/\alpha + (T - T_0)}$$

where  $b$  is a constant,  $R$  is the gas constant,  $\alpha$  is the thermal expansion coefficient of free volume,  $f(T_0)$  is the fractional free volume at reference temperature  $T_0$ . Assuming  $b=1$ ,  $\alpha$  and  $f(T_0)$  can be calculated from  $\log a_T \sim T$  relationships.  $f(T_0)$  data and the additive values are plotted in Figure 4.11. It is seen that extra free volume is created upon blending. The experimentally observed drop in the viscosity of the blend may be connected to this free volume change. From the observation of blend morphology, the extra free volume is likely to exist in the interfacial region between the two phases.

### Conclusion

Blends of *n*-butyl hyperbranched polyarylate and its linear analog poly(1,4-butylene isophthalate) were found immiscible. Because the enthalpy effect had been minimized by the careful choice of this model system, the deciding factor for immiscibility was attributed to the unfavorable entropy change of mixing. Apparently, it is essential in the future to introduce specific interactions between the two polymer components to form a miscible blend. However, blends can be compatible if the chemical compositions of the two constituent polymers are similar. As a result of the compatibility, the viscosities of the blends showed negative deviations from the additive relation. This property has presented an application potential for hyperbranched polymers to be used as rheology modifiers.

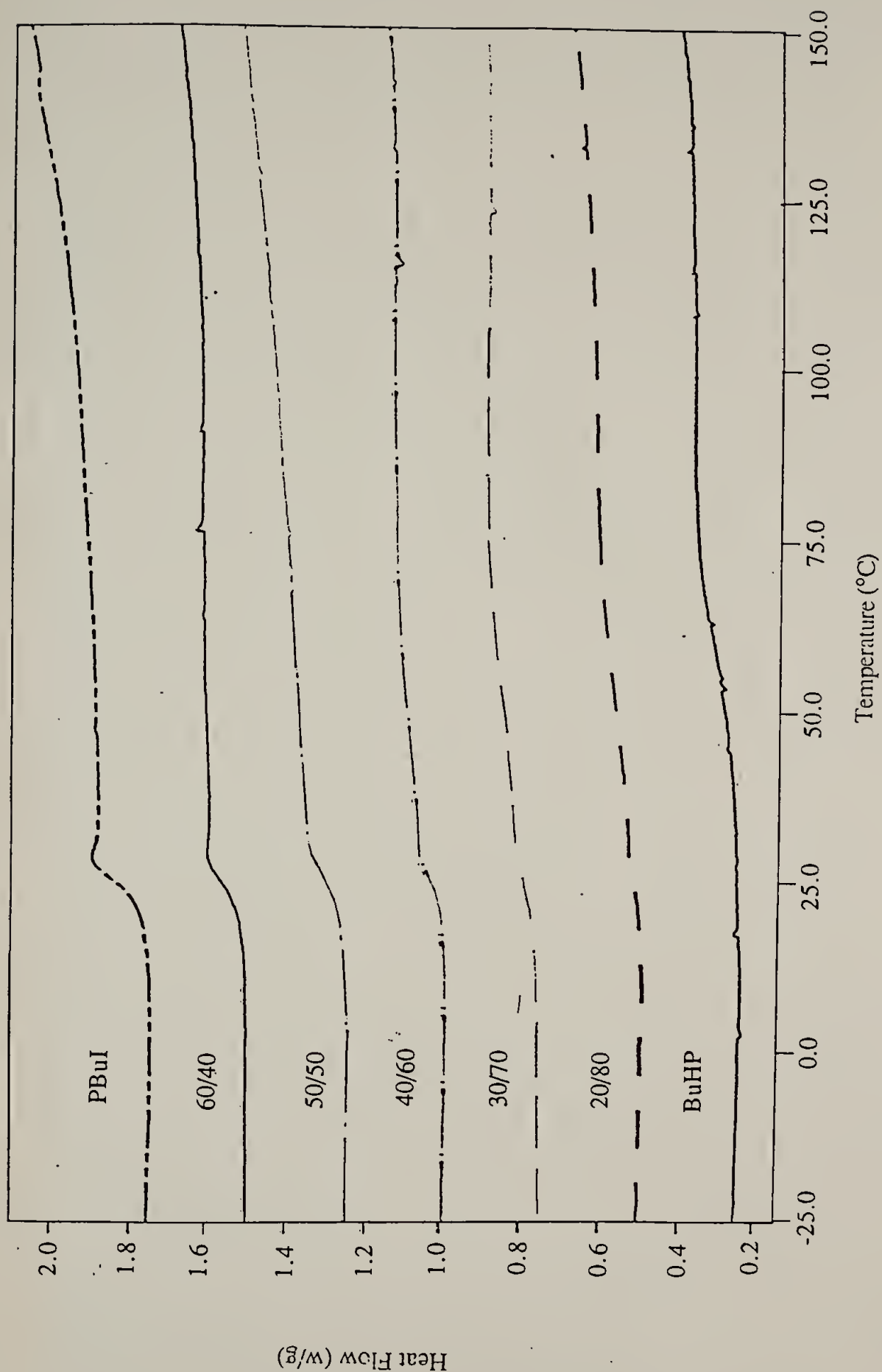


Figure 4.1: DSC traces for BuHP/PBuI blends of different compositions

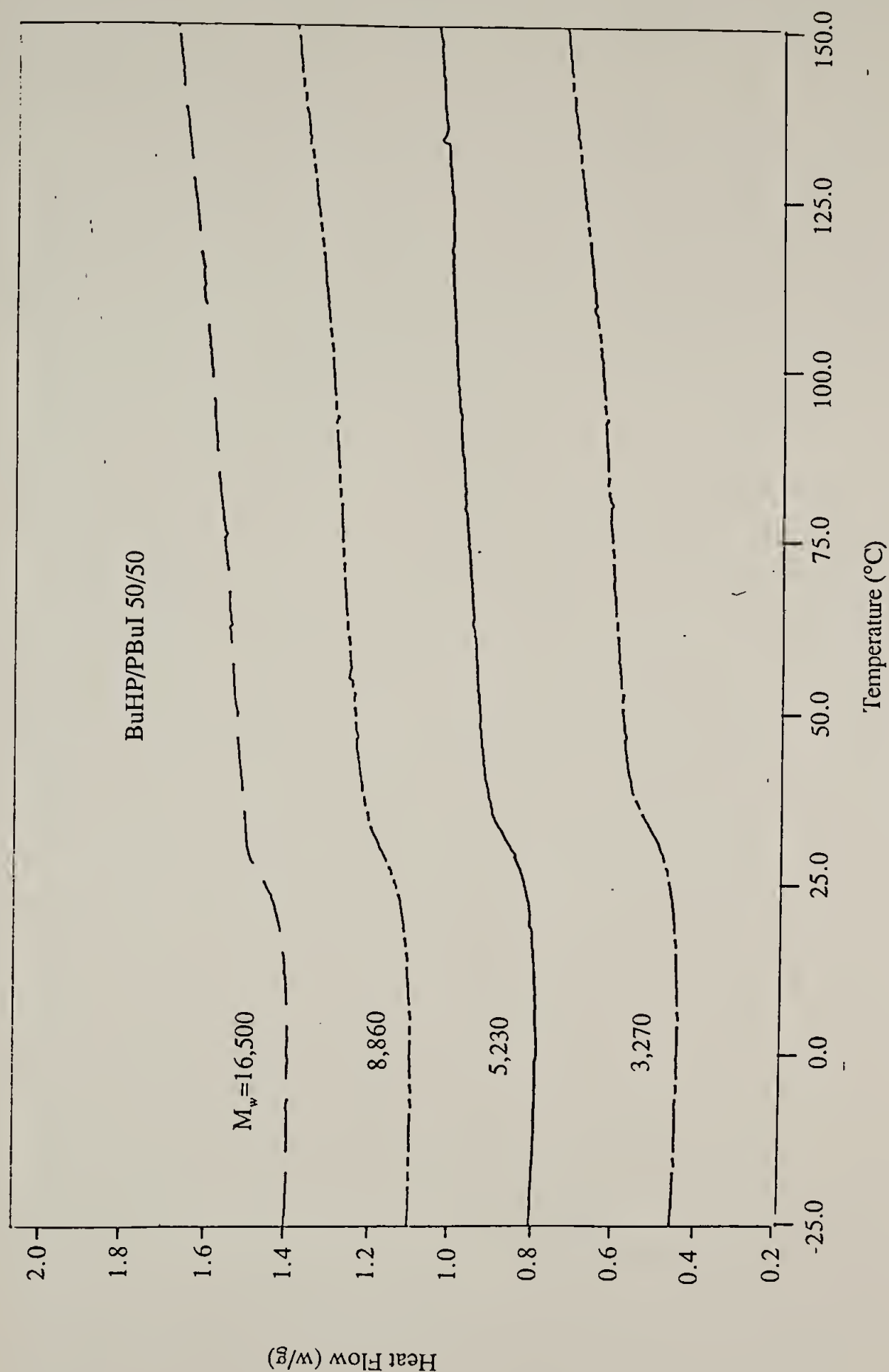


Figure 4.2: DSC traces for BuHP/PBuI (50/50) blend with BuHP of different molecular weight

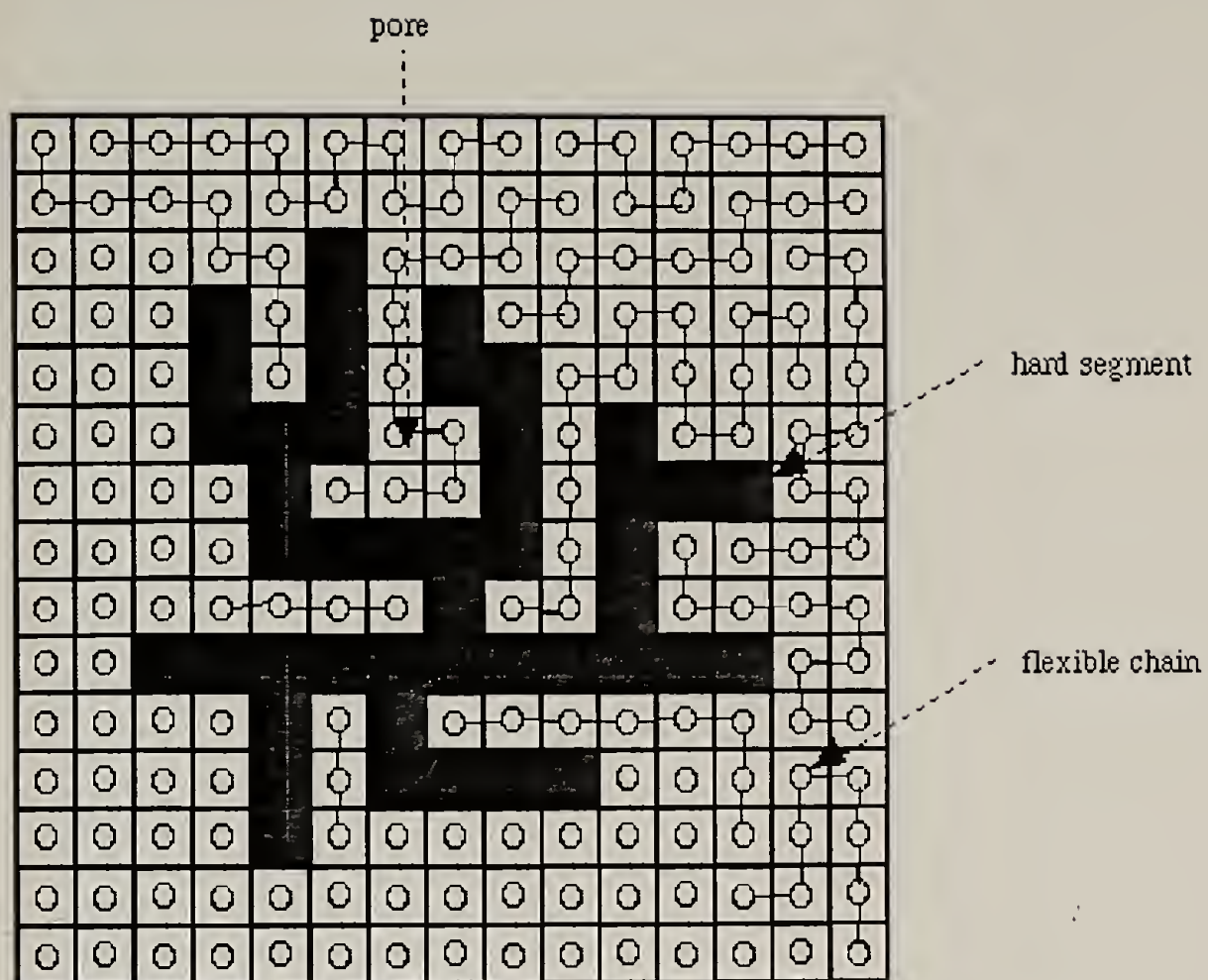


Figure 4.3: Modified lattice model



1 $\mu$ m

Figure 4.4: Micrograph of BuHP/PBuI 20/80 (wt%) blend



1 $\mu$ m

Figure 4.5: Micrograph of BuHP/PBuI 40/60 (wt%) blend



1 $\mu$ m

Figure 4.6: Micrograph of BuHP/PBuI 60/40 (wt%) blend

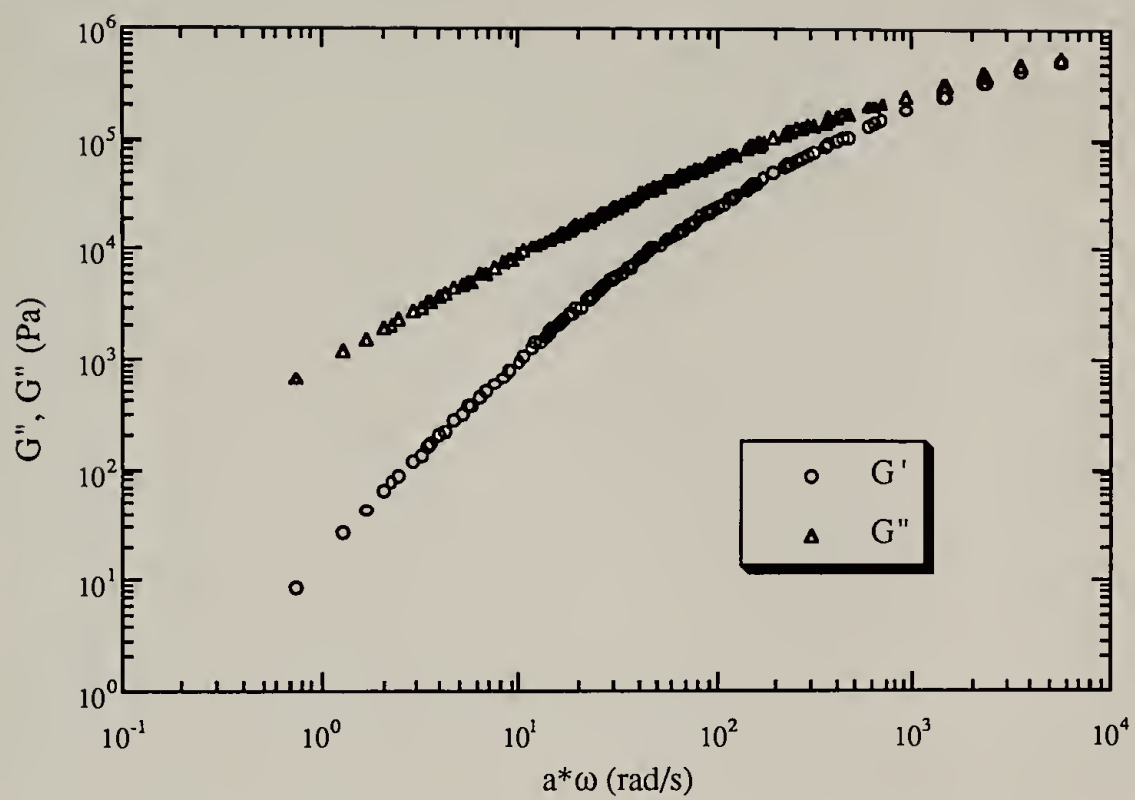


Figure 4.7: Mastercurve of BuHP/PBuI 50/50 (wt%) blend

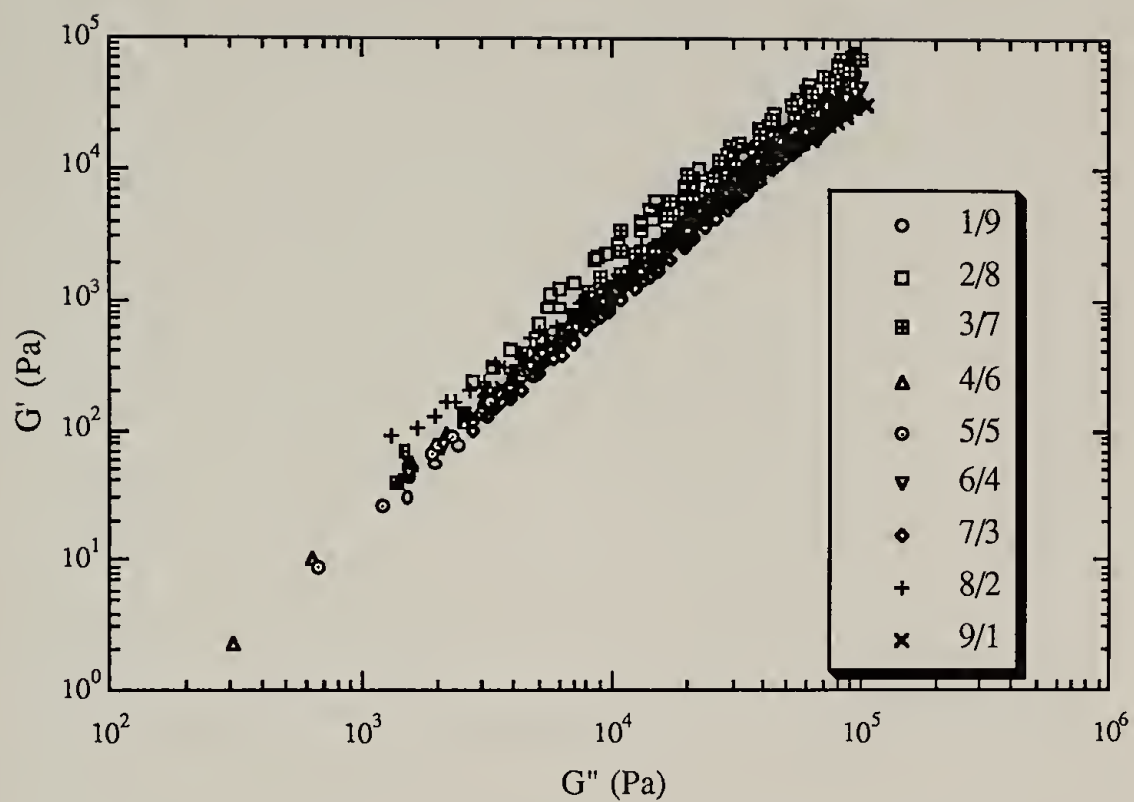


Figure 4.8: Relationship between  $G'$  and  $G''$

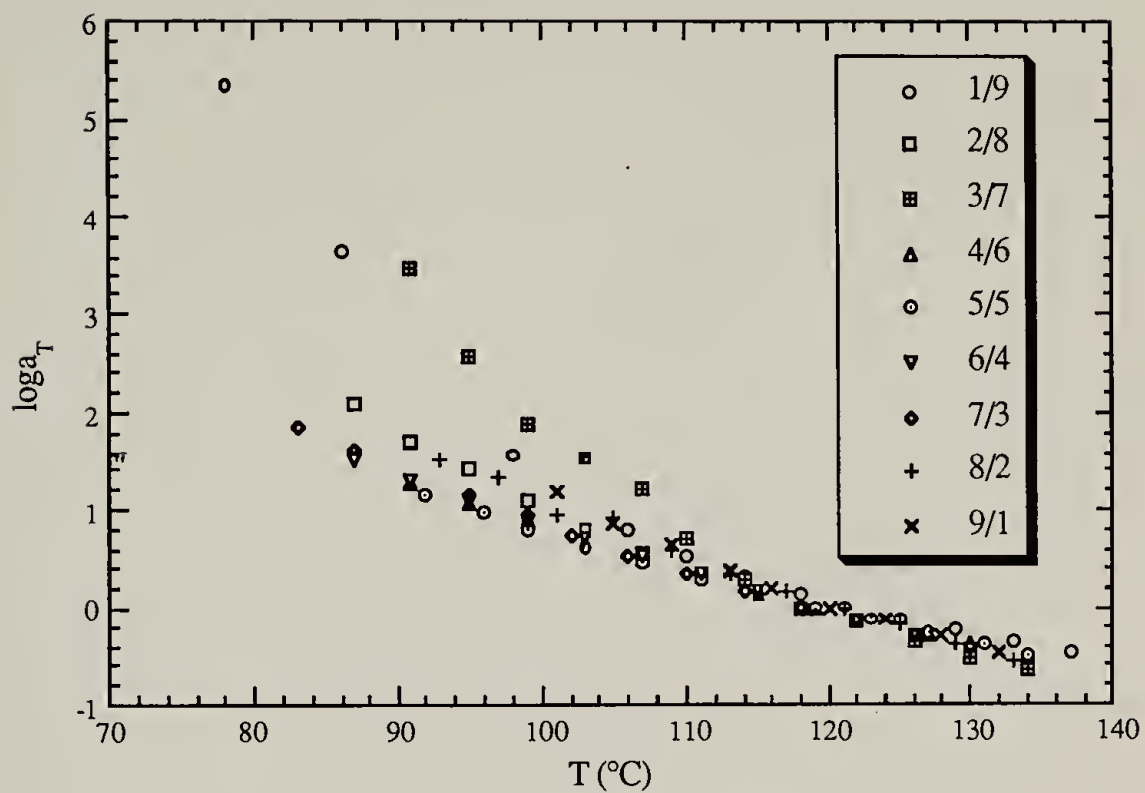


Figure 4.9: Dependence of frequency reduction parameter  $a_T$  on temperature  $T$

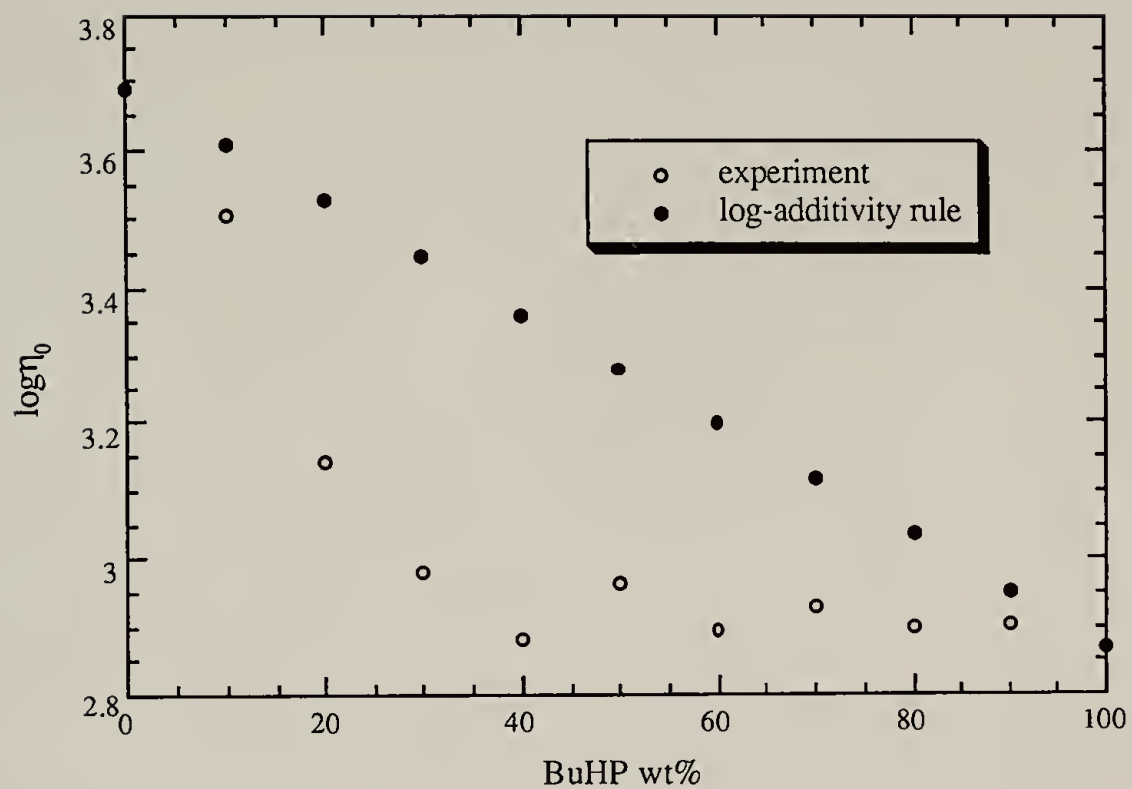


Figure 4.10: Dependence of  $\eta_0$  on blend composition

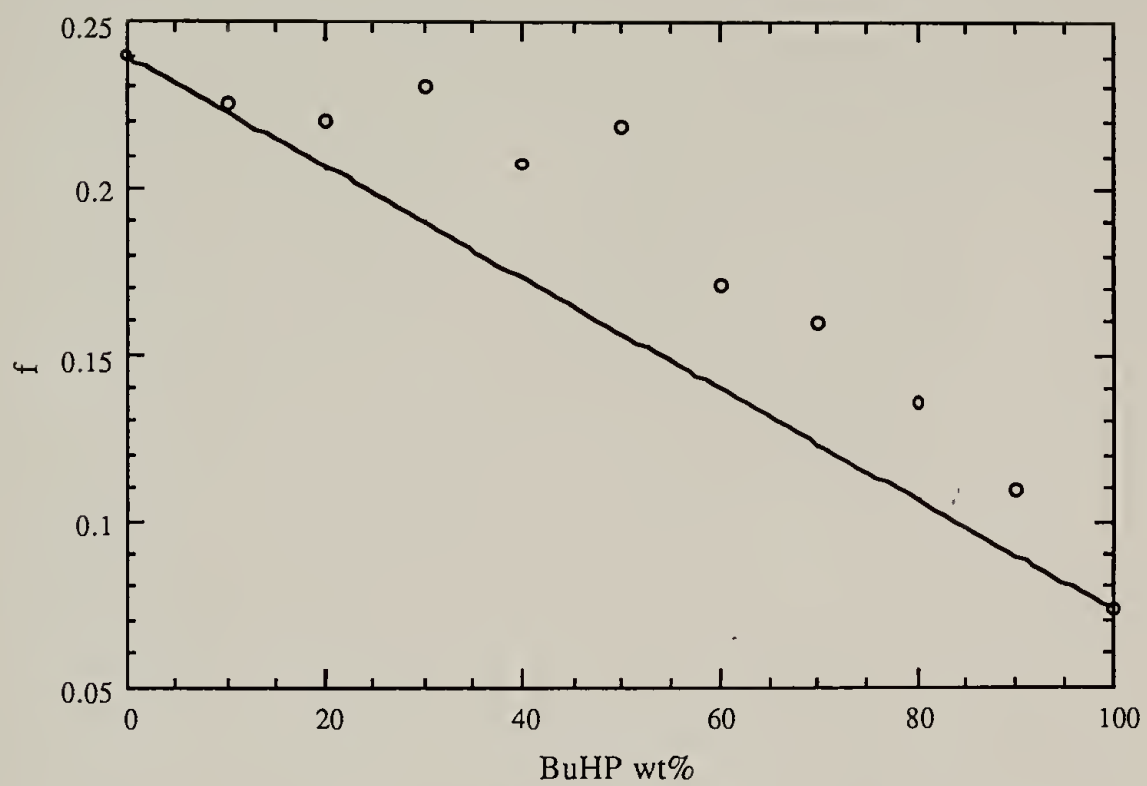


Figure 4.11: Dependence of fractional free volume  $f$  on blend composition

## References

1. Paul, D. R. and Newman, S., Polymer Blends, (New York: Academic Press), (1978)
2. Utracki, L. A., Polymer Alloys and Blends: Thermodynamics and Rheology, (New York: Hanser) (1989)
3. Massa, D. J., Shriner, K. A., Turner, S. R. and Voit, B. I., Macromol., **28**, 3214 (1995)
4. Flory, P. J., Principle of Polymer Chemistry , (Cornell University: Ithaca) (1971)
5. Ferry, J. D., Viscoelastic Properties of Polymers, (Wiley: New York) (1980)
6. Han, C. D. and Kim, J. K., Polym., **34(12)**, 2533 (1993)
7. McCrum, N. G., Read, B. E. and Williams, G., Anelastic and Dielectric Effects in Polymeric Solids, (Dover: New York) (1991)
8. Aklonis, J. J. and Macknight W. J., Introduction to Polymer Viscoelasticity, 2nd ed., (Wiley: New York) (1983)

## CHAPTER 5

### ETHERIMIDE MODIFIED HYPERBRANCHED POLYARYLATE

#### Introduction

It has been demonstrated in the previous chapters that hyperbranched polymers indeed have some interesting properties that present application potentials. The most striking feature among them is the low melt viscosity. This characteristic, together with the high functionality of the macromolecule, offers the possibility of making low viscosity adhesives and flocculants. By doing so, the need for solvent will be greatly reduced. In addition, hyperbranched polymers can be made compatible with linear polymers and act as rheology modifiers by tailoring their chemistry. They have tremendous advantage over conventional plasticizers in the sense that hyperbranched polymers reduce melt viscosity without lowering the glass transition temperature of the material. High functionality and permeability by small molecules also make hyperbranched polymers good candidates for catalytic group carriers. These catalysts have large surface to volume ratio which brings high catalytic efficiency. Finally, hyperbranched polymers are intrinsically isotropic and dimensionally stable, which allows them to be anisotropy reducers.

The structure and properties of hyperbranched polymers can be modified with ease. Thermal properties such as glass transition temperatures can be adjusted by changing end units or introducing soft segments between branch units. The viscosity can be adjusted by modification with long chain terminal groups and introducing AB monomers to change the degree of branching. Compatibility of hyperbranched polymer blends can also be tailored by changing modifying groups of different solubility parameters.

In order to explore the potential of the above mentioned applications, we studied an etherimide modified hyperbranched polyarylate in terms of its synthesis and the effect on the mechanical properties, when this polymer was added to a commercial

linear polyetherimide. Polyetherimide<sup>1</sup> is a unique engineering plastics developed first by General Electric in the 1980s. It has superb mechanical performances with good thermal and chemical stability. When it is spin-coated onto electronic circuit boards, polymer chains tend to orient along the shear field. This is responsible for the film anisotropy which is the cause for stress related failure. Introducing intrinsically isotropic hyperbranched material into this process can certainly reduce the anisotropy.

As has been shown in chapter III, the lack of entanglement between molecules is a characteristic of hyperbranched polymer. In addition to reduction of viscosity, it is going to have impacts on other mechanical properties of material, such as tensile strength and toughness. These aspects will be examined in this chapter.

### Results and Discussion

#### Synthesis of [AB] Type Polyetherimide

To make hyperbranched polyarylate compatible with polyetherimide, etherimide segments were synthesized to modify the polyarylate. Commercial polyetherimides were produced through the following AA+BB type nucleophilic substitution reaction<sup>1</sup> as shown in Figure 5.1, with AA, BB being dianion of Bisphenol-A (BPA) and bis-nitroimide comonomers respectively. Molecular weight was controlled by adding sodium phenoxide at the final stage of the reaction. It would be nice if we could directly transfer the above chemistry and make some segments of AA[BBA]<sub>n</sub>BB which has unreacted anionic group A (phenoxide) and carry out the coupling between A and the acyl chloride polyarylate intermediate. However, AA+BB type condensation polymerization inevitably generates AA[BBA]<sub>m</sub>BBA type segments which have anionic A groups on both chain ends. These dianion segments will crosslink the multifunctional hyperbranched polyarylate, causing insolubility of the final product. Thus, a strategy was designed to form segments with the phenoxide group exclusively on one end. This was realized by the polymerization of AB type monomer in which A is an aromatic hydroxyl group and B is the nitro group on the imide.

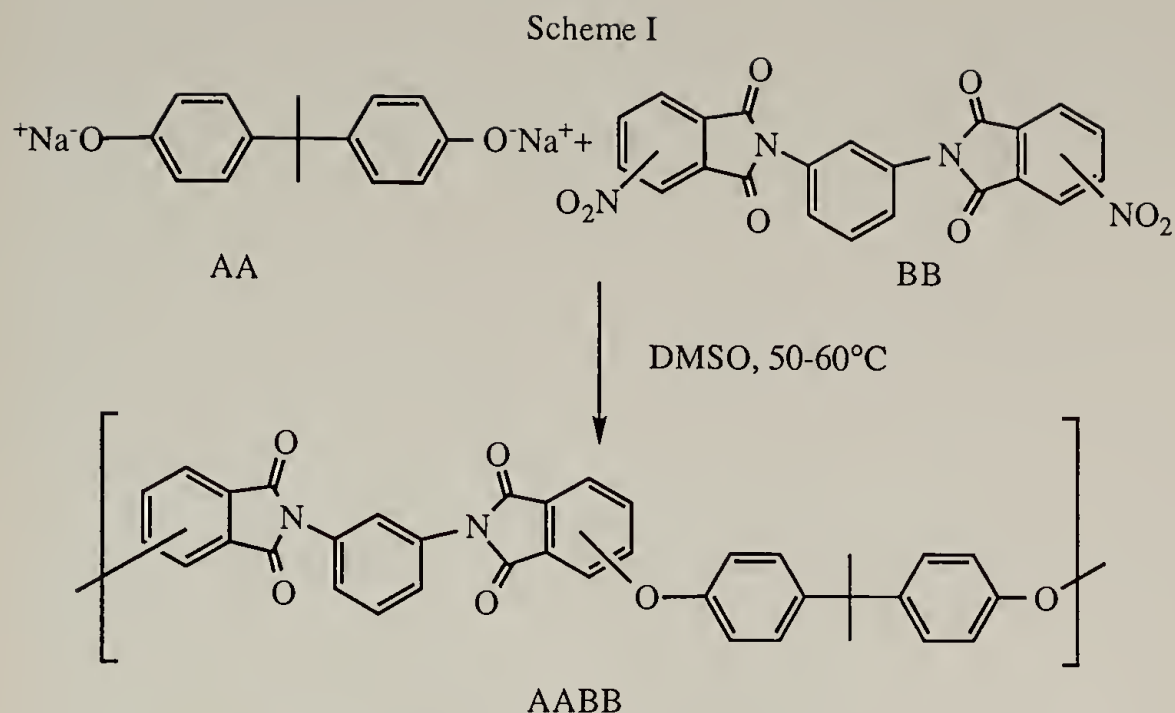


Figure 5.1: Scheme I, commercial polyetherimide and its synthesis

In this work, two AB type monomers were synthesized as shown in Figure 5.2. Monomer I had the simplest form and served as a model reaction for monomer II. The synthesis of monomer I was carried out by using 4-aminophenol and 3-nitrophthalic anhydride refluxing in acetic acid for 4 hours. This method was based on a model reaction reported by White et al<sup>1</sup> on the condensation between aniline and 3-nitrophthalic anhydride.

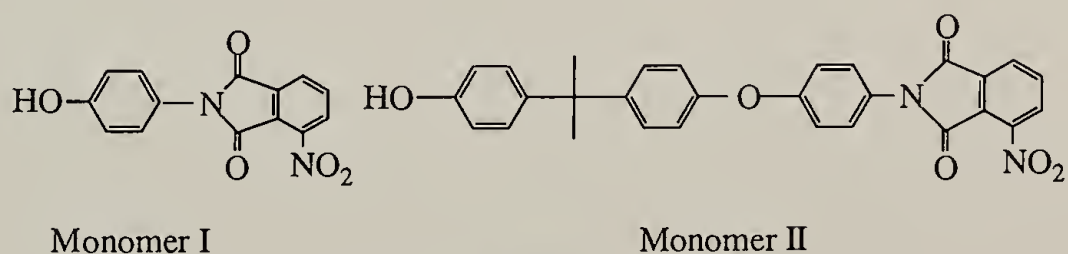


Figure 5.2: Structures of monomer I and monomer II

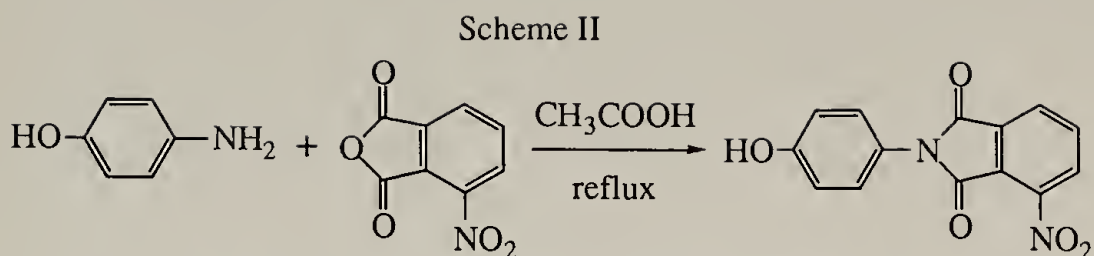


Figure 5.3: Scheme II, synthesis of monomer I

The existence of a hydroxyl group in our case did not affect the imidization significantly. The product was in light yellow crystalline form with a melting point of 342~5°C. The yield was 75%.

The substitution of the nitro group required the hydroxyl group to be transformed to anionic form. The other requirement was the exclusion of any trace of water in the system because of the possible imide ring opening caused by  $[\text{OH}^-]$  which was generated by water under basic conditions. An in-situ polymerization was carried out by using  $\text{Na}_2\text{CO}_3$  as the base to form the anion.

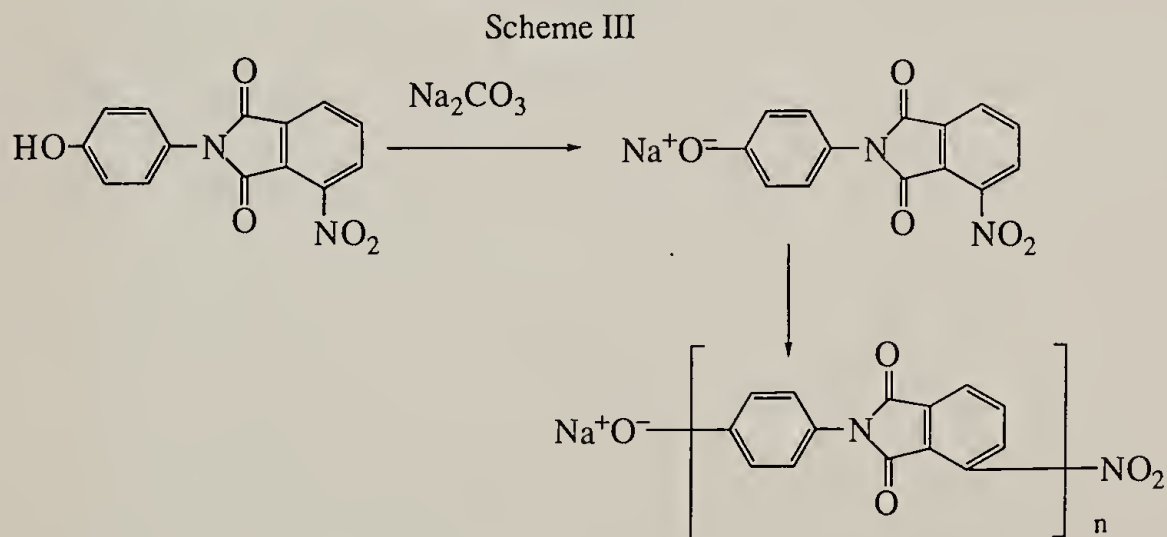


Figure 5.4: Scheme III, in-situ condensation polymerization of monomer I

The reaction temperature was maintained at 60°C. The polymer based on this monomer was not soluble in any solvent and precipitated from DMSO/toluene (50/50). NMR was not performed on this polymer due to the insolubility.

With the imidization and polymerization steps proven feasible, we proceeded to synthesize monomer II which had a structure similar to the repeating unit of commercial polyetherimide. The synthesis route is Scheme IV, as shown in Figure 5.5.

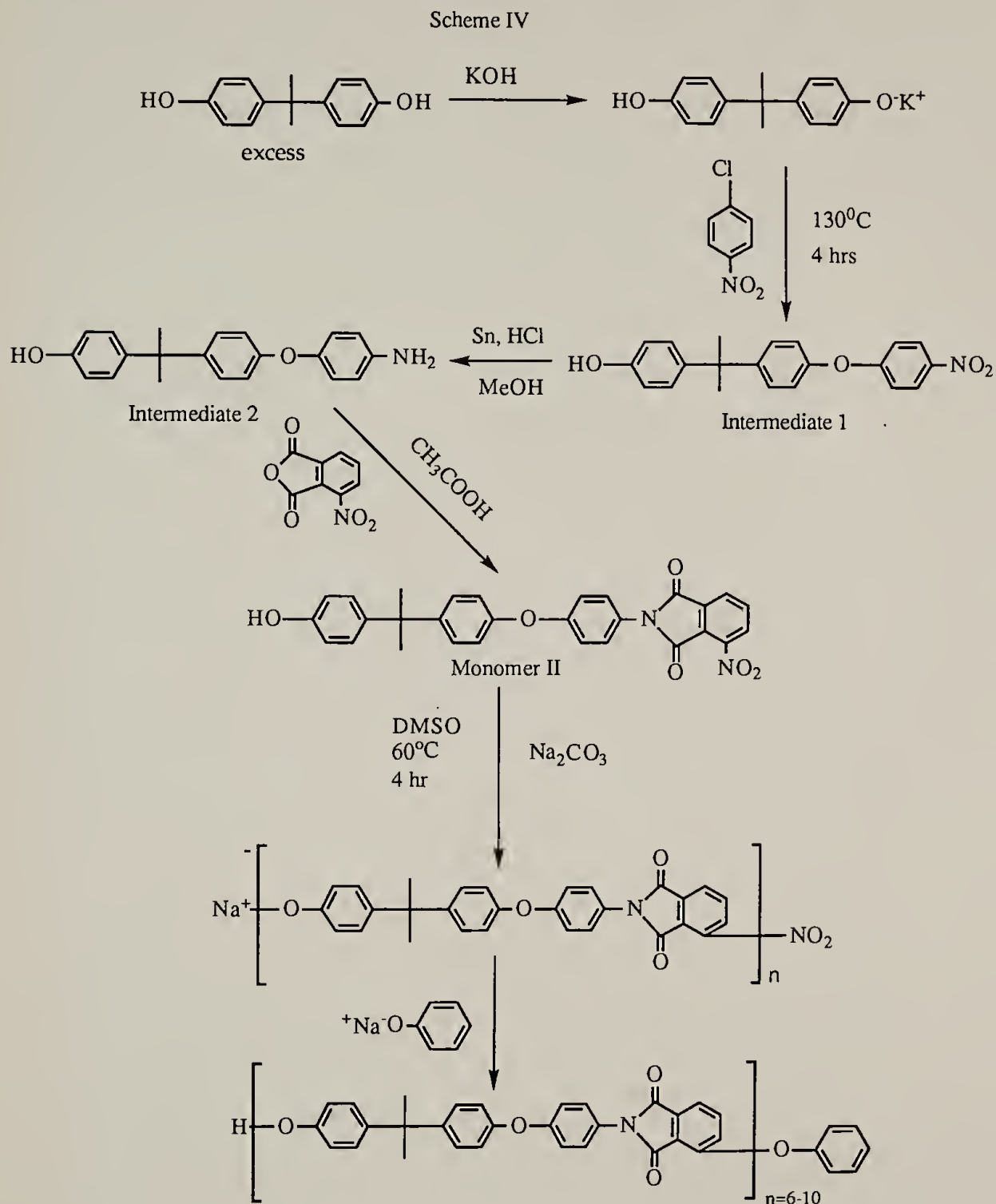


Figure 5.5: Scheme III, synthesis of AB type polyetherimide

Intermediate (1) was formed by the formation of mono potassium salt of BPA and the subsequent substitution of the chloro group on 4-nitro-chlorobenzene. The [BPA]/[KOH] ratio was optimized to maximize the outcome of intermediate 1. Side product (1') (of which structure is shown in Figure 5.6) was precipitated in MeOH. Most of the excess of BPA could be recrystallized in CH<sub>2</sub>Cl<sub>2</sub>. Intermediate (1) was further purified using column chromatography. It was a light yellow crystalline material with a melting point of 154~156°C.



Figure 5.6: Structure of side product (1')

Intermediate (1) was reduced to intermediate (2) with Sn and HCl in MeOH. The product was white crystalline with a yield of 85%. Because it could be oxidized in air and light over prolonged time but it was stable under acidic conditions, it was stored in acetic acid. The imidization of intermediate (2) followed the same condition of the synthesis of monomer I. The conversion was close to 80%.

The polymerization was carried out successfully. The unreacted nitro groups were capped with anhydrous sodium phenoxide. An excess amount of acetic acid was used to transform all O<sup>-</sup>Na<sup>+</sup> back to OH. Polymer with molecular weight up to 12,700 was obtained. Because the compact nature of hyperbranched polymer determined that the degree of its modification was limited by the size of the modifying agent, the molecular weight of [AB] polyetherimide was usually controlled at around 4,000 with DP of 6 to 8.

The coupling of the above oligomer to the acyl chloride of hyperbranched polyarylate was conducted in chloroform with pyridine as the catalyst. The curing of acyl chloride with only etherimide segment could not be higher than 38% after 24hr even with etherimide in excess. The residual acyl groups were capped with methanol/allyl alcohol 10/1 mixture. The coupled product was fractionated from the

solution by precipitation method. GPC showed a significant molecular weight increase of hyperbranched polyarylate after the coupling.

### Thermal Analysis

Glass transition temperature of purified EIHP was found to be 188°C. At all blend compositions and annealing temperatures below 200°C, there existed two glass transition temperatures indicating phase separation. At high annealing temperatures, prolonged annealing time tended to merge the two  $T_g$ s into one, as shown in Table 5.1 of 50wt% EIHP content. However, this process was not reversible when the annealing was repeated at low temperature. A solubility test after the thermal scan found insoluble polyarylate indicating chemical change in the system. Thus, the blends were immiscible. This finding was consistent with our study on other blends involving hyperbranched polymers. The highly compact nature of hyperbranched polymer restricted the two blend components from mixing on the segmental level.

Table 5.1: DSC of EIHP/PEI 50/50 wt% blend

Annealing temperature (°C)	$T_g$ (°C) of EIHP phase	$T_g$ (°C) of PEI phase
190	188	217
200	190	217
210	204	204
220	204	204
230	204	204

### Morphology of Blend

Figure 5.7 shows TEM micrograph of EIHP/PEI blend with 40% EIHP content. The morphology of this blend was quite similar to that of BuHP/PBuI blend. However in this case, the domain size of 800~1000Å was larger than that of the model blend. Judging from the domain size, the blend could still be considered compatible.

### Mechanical Properties

The mechanical property of PEI/EIHP blends are shown in Table 5.2. Due to the highly brittle nature of EIHP, the preparation of a standard sample of this material was not successful. Only the data of blends with less than 40% EIHP content are

presented here. Young's modulus increased with increasing EIHP content. However, the elongation at break of the material dropped significantly. This drawback of the hyperbranched polymer could be improved in the future by reducing the degree of branching and introducing longer modifying segment.

Table 5.2: Tensile properties of EIHP/PEI blend

EIHP/PEI (wt%)	Young's Modulus E (MPa)	Elongation at Break (%)
0/100	2710	60
10/90	3240	43
20/80	3690	25
30/70	4150	11
40/60	4860	<5

Although the modulus of pure EIHP can not be known directly, it can be estimated based on polymer composite theory. The modulus for a polymer blend can be expressed as the Lewis-Nielson<sup>2</sup> equation:

$$\frac{M_b}{M_1} = \frac{1 + AB\phi_2}{1 - B\psi\phi_2}$$

where  $M_b$  and  $M_1$  are the moduli of the blend and the matrix, respectively.

$A=k_E-1$ ,  $k_E$  being Einstein's ratio, which is 2.5 for spherical particles. Other terms in the equation are given as follows:

$$B = \frac{M_2/M_1 - 1}{M_2/M_1 + A}$$

$$\psi \approx 1 + \left( \frac{1 - \phi_m}{\phi_m^2} \right) \phi_2$$

where  $M_2$  and  $M_1$  are the moduli of the dispersed phase and the matrix, respectively,  $\phi_2$  is the volume fraction of the dispersed phase and  $\phi_m$  is the maximum possible volume fraction of the dispersed phase, which is limited by particle packing and geometry. From the above relations,

$$E_2 = \frac{\frac{E_b}{E_1}(A + \psi\phi_2) + A(\phi_2 - 1)}{\frac{E_b}{E_1}(\psi\phi_2 - 1) + A\phi_2 + 1} E_1$$

$E_b$ ,  $E_1$  were measured,  $\phi_2$  was taken as the weight fraction of the hyperbranched phase,  $\psi$  was calculated using  $\phi_m=0.64$  for spherical particles,  $A$  being taken as 1.5 for polyetherimide. The calculated Young's modulus for etherimide modified hyperbranched polyarylate was  $18600 \pm 2500$  MPa. The highly restricted structure apparently was responsible for the tremendous increase in modulus. However, the lack of entanglement between macromolecules could not supply the strength for large deformation.

## Experimental

### Synthesis

Monomer I. 10.9g (0.1mol) of 4-aminophenol and 19.3g (0.1mol) 3-nitrophthalic anhydride were dissolved in 120ml of glacial acetic acid. The solution was heated at reflux for 4 hours. After this heating period, the system was concentrated by distillation of 50ml of acetic acid and allowed to cool to room temperature. The light yellow solid was separated by filtration, washed with 100ml cyclohexane and dried in vacuum. The yield of the imide was 20.9g (74%).  $^{13}\text{C}$  NMR ( $\text{DMSO}-d_6$ ) spectrum: a, 154.4; b, 120.1; c, 129.6; d, 127.5; e, 166.0; f, 134.2; g, 129.5; h, 137.5; i, 128.0; j, 145.8; k, 124.4; l, 164.0 as shown in Figure 5.8. Elemental analysis for  $\text{C}_{14}\text{H}_8\text{N}_2\text{O}_5$ : C, 59.15; H, 2.82; N, 9.86. Found: C, 59.22; H, 2.77; N, 9.80.

Polymerization of Monomer I. 10g (0.035mol) of monomer I was added to 40 ml of DMSO and the mixture was stirred for 15min. The solution was then canulated to a mixture containing 40ml dried toluene and 15g pulverized anhydrous sodium carbonate. The system was steadily stirred and maintained at  $60^\circ\text{C}$  overnight. The full operation was under dry nitrogen atmosphere. The mixture was then cooled down to

room temperature. 30ml glacial acetic acid was added gradually to the mixture to eliminate solid sodium carbonate. Additional 50ml of DMSO was used to dilute the mixture. The insoluble polymer was filtered and washed with methanol. It was dried at 60°C in vacuum and ground into fine powder. The powder was further washed with water/acetic acid (10/1) to eliminate all residual sodium carbonate and dried in vacuum. The polymer was not soluble in all available solvents. FTIR was performed as shown in Figure 5.9.

Intermediate (1). 91.2g BPA (0.4mol) was dissolved in 200ml methanol. The solution was strongly stirred while 56g of 10% KOH aqueous solution was added dropwise. After all the base was added. The methanol and water were evaporated on a rotavap. The white solid was further dried in vacuum. 200 ml of DMSO was used to dissolve the above potassium salt of BPA and 15.8g (0.1mol) 4-nitro-chlorobenzene. The solution was heated at 130°C for 4hr before the solution was concentrated by distillation of DMSO under reduced pressure. Unreacted BPA and side product (1') were crystallized in methylene chloride and methanol respectively. High purity intermediate 1 was finally obtained by using methylene chloride/silica gel column chromatography. The yield of was 19.9g (57%). Melting point was 154~156°C.  $^{13}\text{C}$ -NMR (DMSO- $d_6$ ) spectrum: 13, 153.9; 14, 114.7; 15, 123.4; 16, 141.6; 17, 30.7; 18, 42.8; 19, 147.8; 20, 128.9; 21, 119.6; 22, 154.9; 23, 156.0; 24, 120.5; 25, 129.3; 26, 141.7, as shown in Figure 5.10. Elemental analysis for  $\text{C}_{21}\text{H}_{19}\text{NO}_4$ : C, 72.21; H, 5.44; N, 4.01. Found: C, 72.10; H, 5.38; N, 4.15.

Intermediate (2). 6.98g (0.02mol) of intermediate (1) was dissolved in 150ml of methanol, 6.0g (0.051mol) tin powder was added to the system and steady stirring was applied. 20ml concentrated hydrochloric acid was added gradually to the suspension. The reaction was kept at 40°C by occasional cooling with ice water. After the reaction stopped, the mixture was cooled to room temperature and the solution was neutralized with 1N NaOH solution. Care was taken at this step to prevent the solution turning

basic. Tin hydroxide precipitation was filtered. The filtrate was then extracted with ether three times. The ether was then distilled and the product dried in vacuum. It was a white crystalline material. The yield was 4.02g (63%).  $^{13}\text{C}$ -NMR ( $\text{DMSO}-d_6$ ) spectrum: 13, 153.9; 14, 114.7; 15, 123.4; 16, 141.6; 17, 30.7; 18, 42.8; 19, 147.8; 20, 128.9; 21, 119.6; 22, 154.9; 27, 156.5; 28, 120.7; 29, 127.2; 30, 114.6, as shown in Figure 5.11. Elemental analysis for  $\text{C}_{21}\text{H}_{21}\text{NO}_2$ : C, 79.00; H, 6.58; N, 4.39. Found: C, 79.12; H, 6.77; N, 4.50.

Monomer II. Imidization of intermediate (2) followed the same procedure of the synthesis of monomer I. The product was a greenish yellow noncrystalline material.  $^{13}\text{C}$ -NMR ( $\text{DMSO}-d_6$ ) spectrum: 13, 153.9; 14, 114.7; 15, 123.4; 16, 141.6; 17, 30.7; 18, 42.8; 19, 147.8; 20, 128.9; 21, 119.6; 22, 154.9; 31, 158.5; 32, 119.0; 33, 129.6; 34, 127.2; 35, 165.9; 36, 134.8; 37, 129.0; 38, 136.9; 39, 127.5; 40, 146.0; 41, 124.0; 42, 163.3, as shown in Figure 5.12. Elemental analysis for  $\text{C}_{29}\text{H}_{22}\text{N}_2\text{O}_6$ : C, 70.45; H, 4.45; N, 5.67. Found: C, 70.52; H, 4.50; N, 5.55.

Polymerization of Monomer II. This polymerization was similar to that of monomer I. In the late stage of the reaction the mixture became viscous so additional 50ml of DMSO was added and sodium phenolate was used to control the molecular weight. After the elimination of sodium carbonate, the polymer was precipitated in water, taken up in methylene chloride and reprecipitated in methanol.  $M_n=4,200$  (GPC, PS standard).  $^{13}\text{C}$ -NMR ( $\text{DMSO}-d_6$ ) spectrum: 13, 153.9; 14, 114.7; 15, 123.4; 16, 141.6; 17, 30.7; 18, 42.8; 19, 147.8; 20, 128.9; 21, 119.6; 22, 154.9; 31, 158.5; 32, 119.0; 33, 129.6; 34, 127.2; 43, 166.4; 44, 136.8; 45, 130.3; 46, 136.8; 47, 128.2; 48, 155.0; 49, 118.6; 50, 164.7; 51, 152.6; 52, 118.6; 53, 126.5; 54, 114.6, as shown in Figure 5.12.

Modification of Polyarylate with Etherimide. 1g acyl chloride of poly(5-acetoxyisophthalic acid) and 20g AB etherimide were dissolved in 200 ml dry THF. 10g pyridine was added gradually to the solution and the reaction was kept at  $50^\circ\text{C}$

overnight after the addition of pyridine. 11ml methanol/allyl alcohol 10/1 mixture was then added to the solution and the reaction was kept for another 1hr. The polymer was precipitated in methanol and filtered. The high molecular weight fraction was fractionated in dioxane/water mixture. The molecular weight distribution before and after the fractionation is shown in Figure 5.13.

#### Blend Sample Preparation

Blends of EIHP and polyetherimide (PEI) were prepared by dissolution of both components in DMAC with subsequent evaporation of the solvent in 48hr at 120°C and then to constant weight and pressure of 3 torr.

#### Thermal Analysis

The thermal analysis of blends was determined by a Perkin-Elmer DSC7 instrument at a 20°C/min heating rate. The temperature and power ordinates of the DSC were calibrated with respect to the known melting point and heat of fusion of high purity indium and mercury standards supplied by Perkin-Elmer. Glass transition temperature ( $T_g$ ) was defined as the midpoint of the change in the specific heat. Blends were first heated to 240°C before being annealed at programmed temperatures. Samples were annealed at the annealing temperature for 30 min before being quenched in liquid nitrogen to preserve phase properties.

#### Transmission Electron Microscopy

The morphology of blends was observed by using TEM. Blends were prepared by the same method for thermal measurement. Approximately 700 Å thick sections of sample was cut by cryoultramicrotomy using a diamond knife at room temperature. These sections were collected on copper TEM grids and stained in OsO<sub>4</sub> vapor for 5 hours. The stain reacted preferentially with the double bonds in EIHP, rendering the EIHP microdomain dark via mass-thicken contrast in TEM micrographs. The samples were then observed in a JEOL 100CX TEM operated at 100 KV.

### Mechanical Testing

The tensile properties of the blends were determined using the ASTM-III Tensile Test (Small Dogbone) on a Instron Universal Testing Instruments, Model 4201. The engineering stress was calculated using the average cross-sectional area, and the strain was calculated using an effective gauge length of 20.5 mm. Young's modulus was calculated using a linear regression of the initial slope of the stress-strain curve, from approximately 0 to 3% strain.

### Conclusion

It has been demonstrated that by modifying hyperbranched polyarylate with etherimide segments, hyperbranched polyarylate can form an optically transparent blend with a linear polyetherimide, Ultem 1000. The tensile strength of the material was increased by the addition of hyperbranched polymer. However, the toughness of the material was seriously compromised. This drawback was intrinsically related to the lack of entanglement between hyperbranched molecules. In order to improve the performance, a balance has to be reached between branching and entanglement. For hyperbranched polyarylate, it is desirable to reduce the degree of branching by introducing more linear units and longer terminal groups. In other words, the optimum material should be of a structure in between hyperbranched polymer and branch polymer.



1 $\mu$ m

Figure 5.7: TEM micrograph of 40/60 EIHP/PEI blend

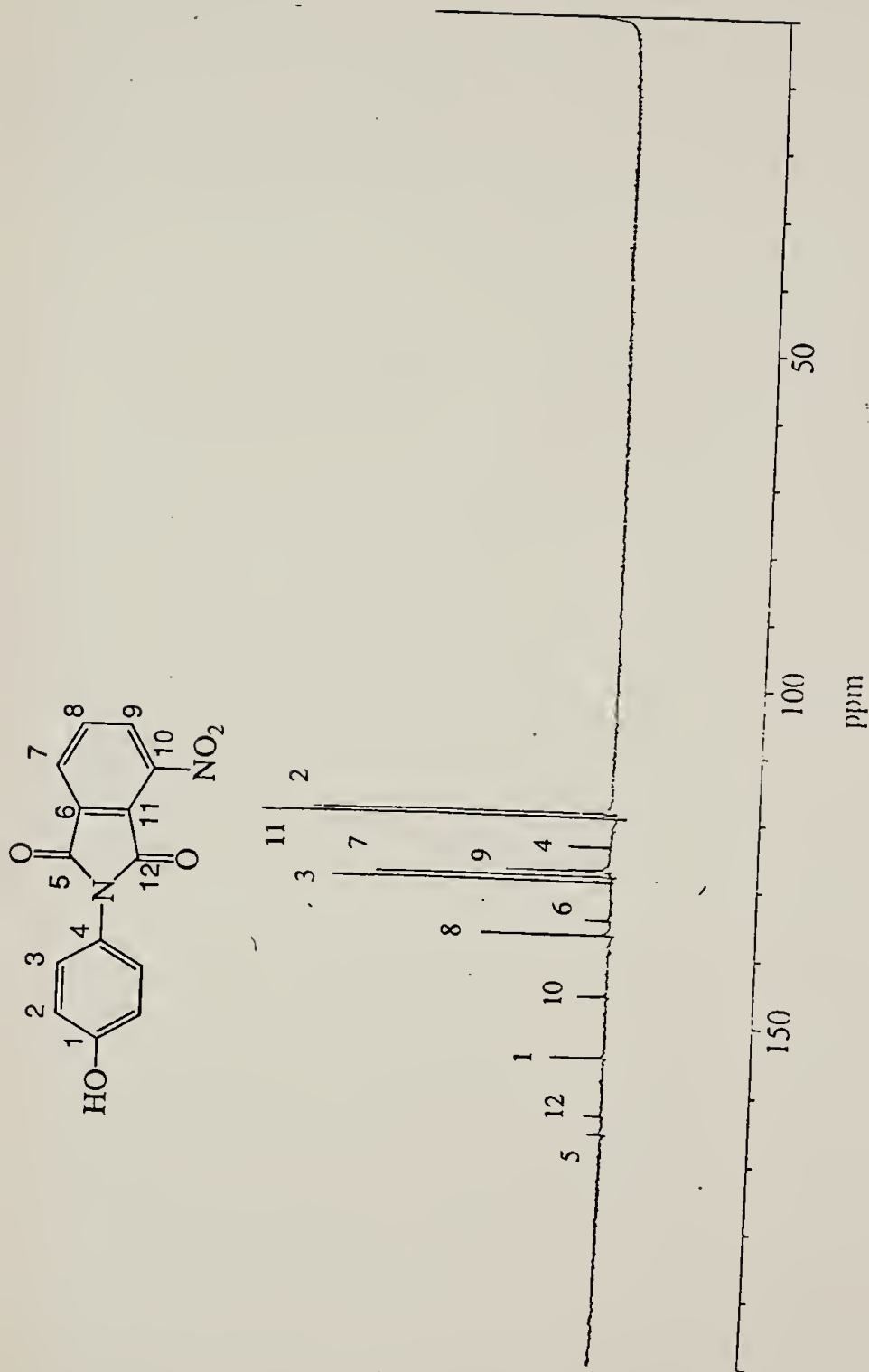


Figure 5.8:  $^{13}\text{C}$  NMR of monomer I

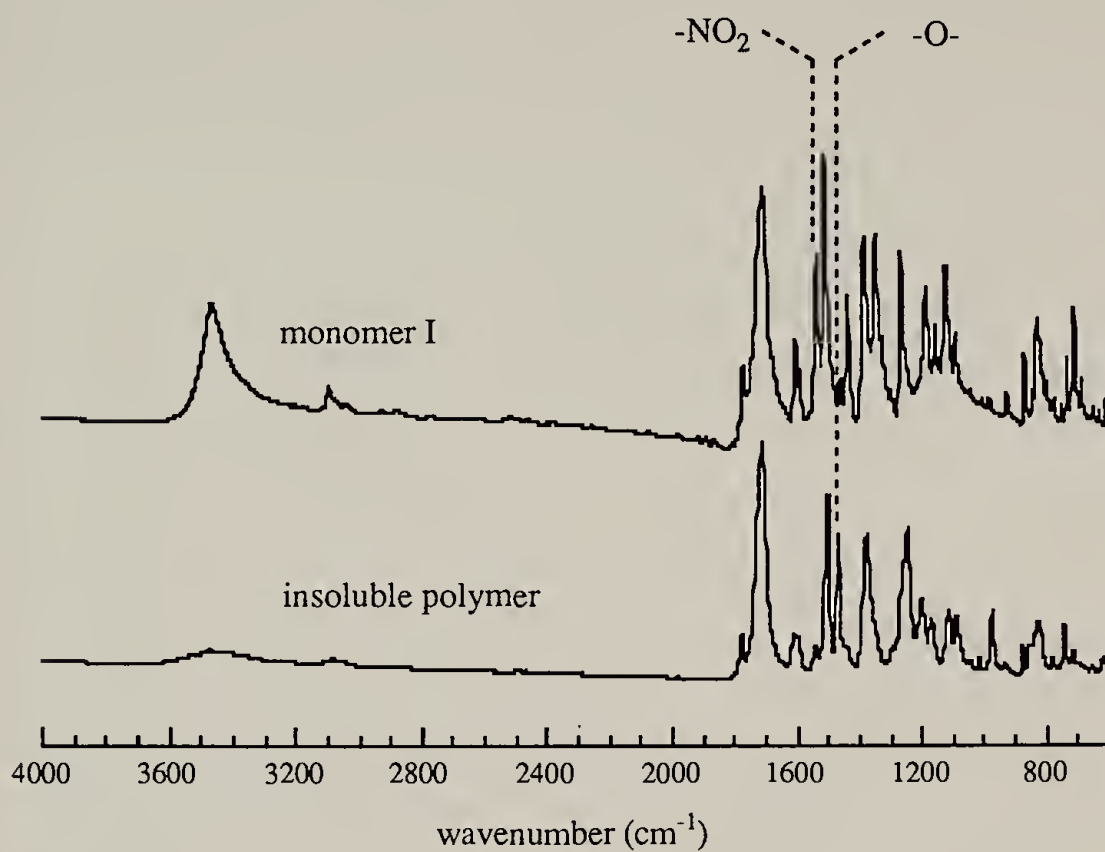


Figure 5.9: FTIR of polymerization of monomer I

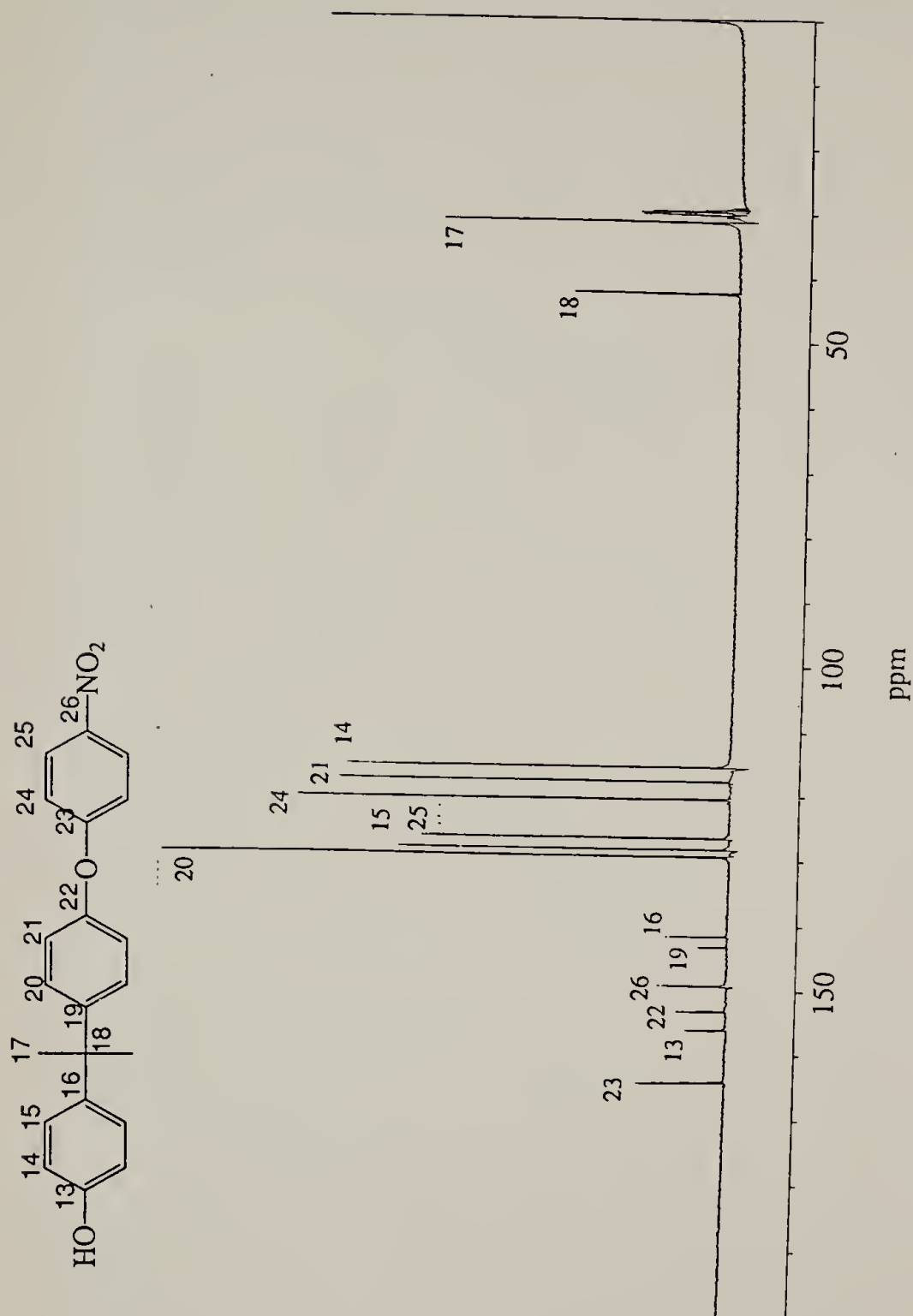


Figure 5.10:  $^{13}\text{C}$  NMR of intermediate (1)

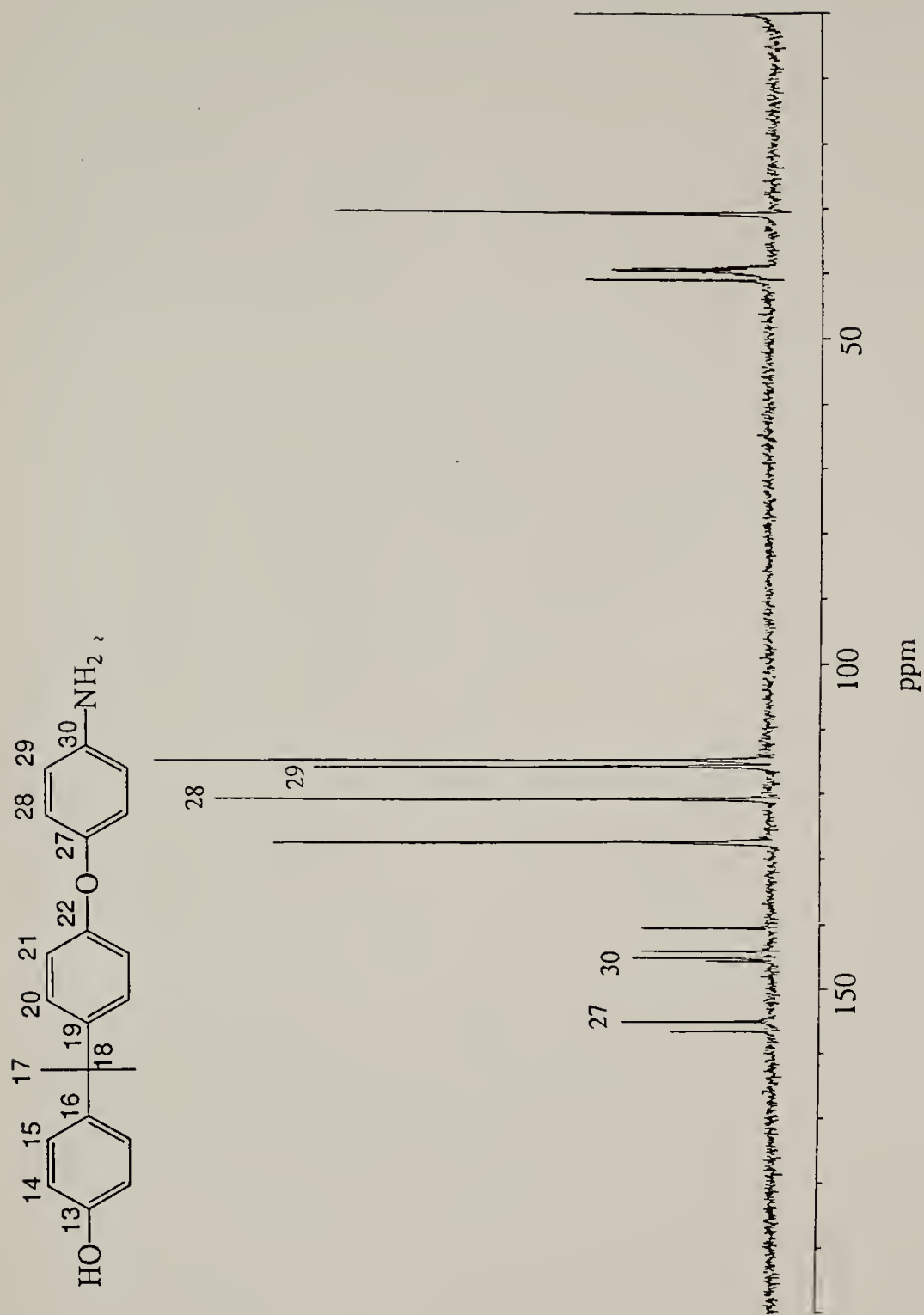


Figure 5.11:  $^{13}\text{C}$  NMR of intermediate (2)

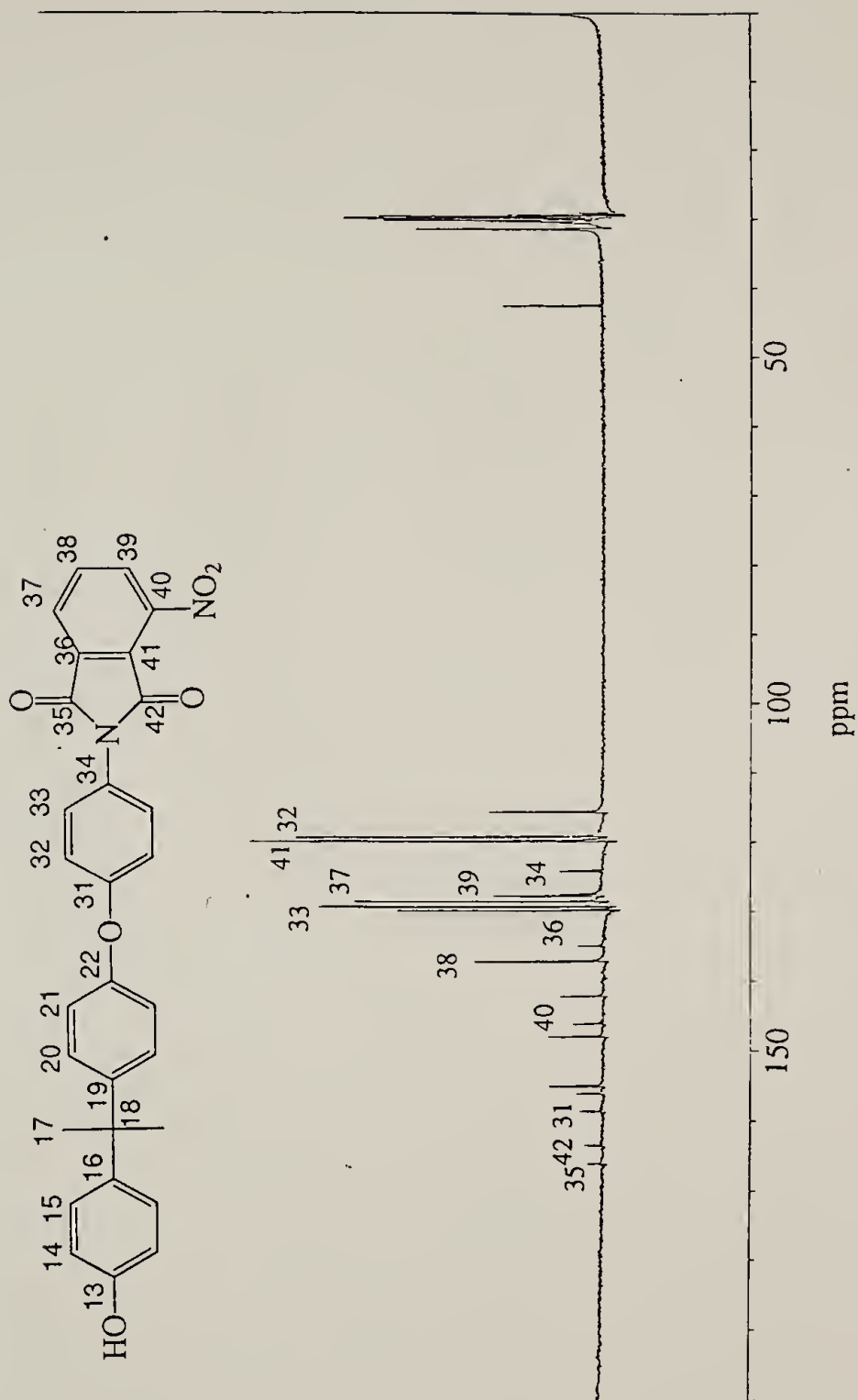


Figure 5.12:  $^{13}\text{C}$  NMR of monomer II

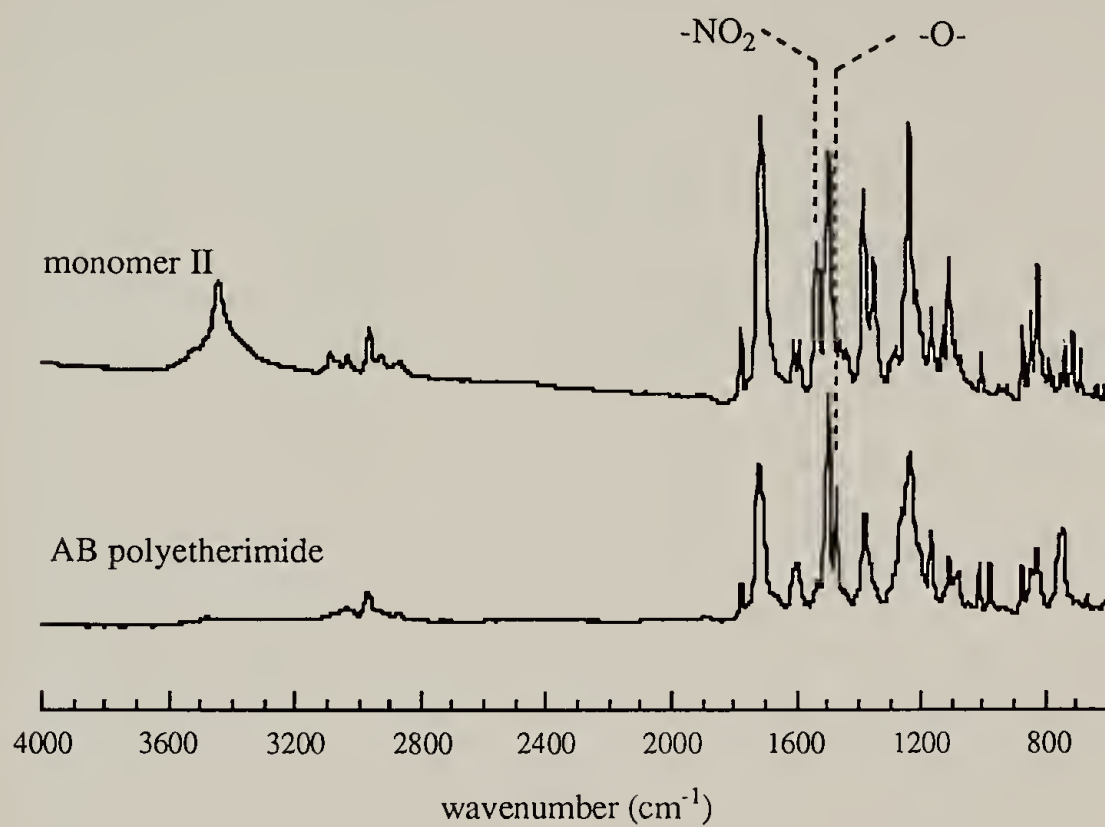


Figure 5.13: FTIR of polymerization of monomer II

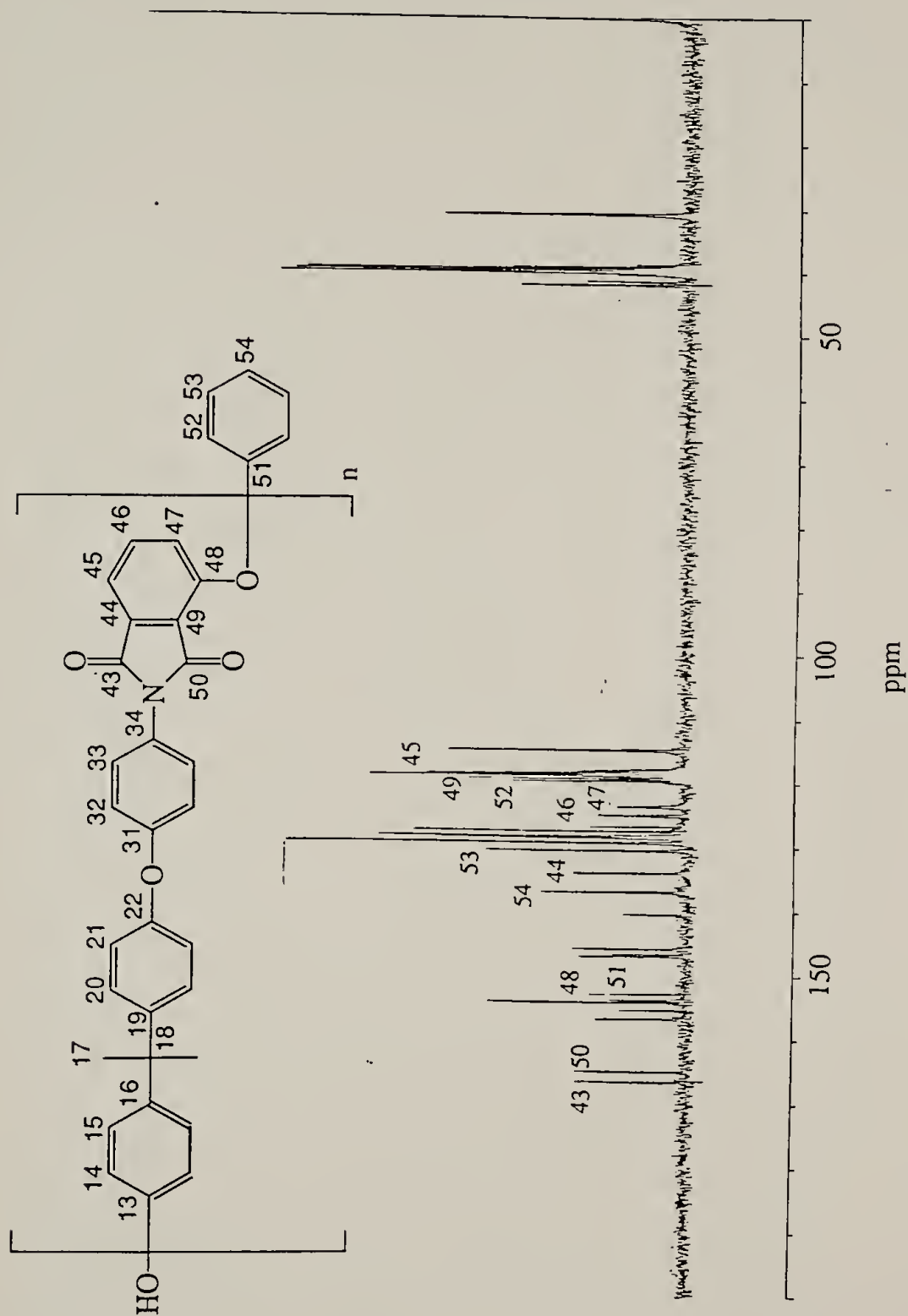


Figure 5.14:  $^{13}\text{C}$  NMR of AB type polyetherimide

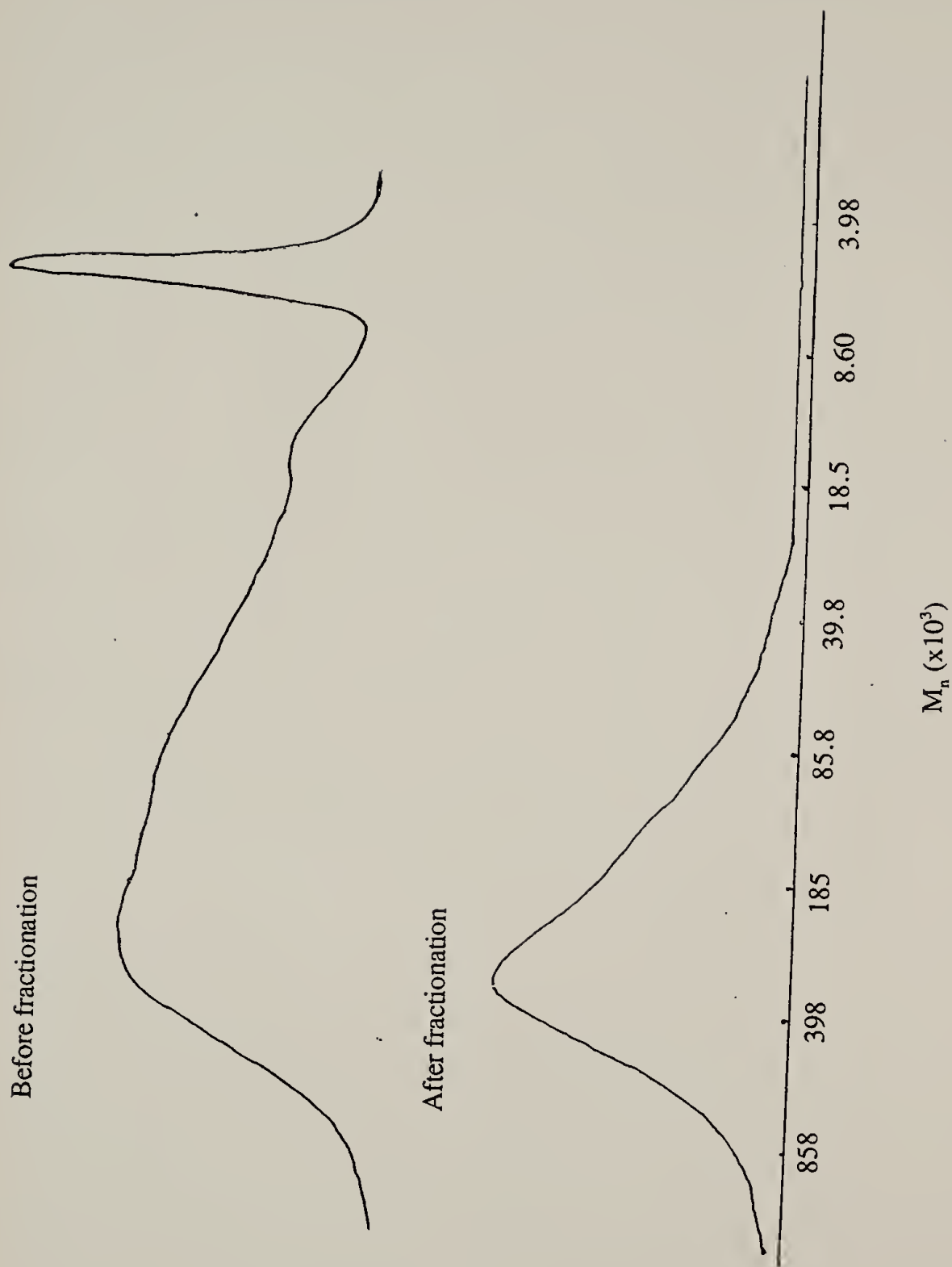


Figure 5.15: GPC trace of fractionation of EIHP

## References

1. White, D. M., Takekoshi, T., Williams, F. J., Relles, H. M., Donahue, P. E., Klopfer, H. J., Loucks, G. R., Manello, J. S., Matthews, R. O. and Schlunz, R. W., J. Polym. Sci., Polym. Chem. Ed., **19**, 1635 (1981)
2. Nielsen, L. E. and Landel, L. E., Mechanical Properties of Polymers and Composites, 2nd Ed., (Marcel Dekker: New York) (1994)

## CHAPTER 6

### CONCLUSIONS AND SUGGESTED FUTURE WORK

#### Conclusions

In this work, the existing laboratory polymerization procedure was scaled up by a suspension method to synthesize hyperbranched poly(5-acetoxyisophthalic acid) of high molecular weight. High boiling point silicone oil was chosen as the suspension fluid so that a stable suspension of 5-acetoxyisophthalic acid melt could be obtained and polymerized at a high temperature. Hyperbranched poly(5-acetoxyisophthalic acid) of wide molecular weight distribution and high molecular weight was produced at large quantity. A method of modifying the above polymer with different end groups was also established. Specifically, the acyl groups were transformed into esters through an acyl chloride intermediate. All modified polymers were characterized by FTIR,  $^1\text{H}$  and  $^{13}\text{C}$  NMR, elemental analysis and DSC. Through this modification route, hyperbranched polymers with glass transition temperatures ( $T_g$ ) ranging from  $-50^\circ\text{C}$  to  $188^\circ\text{C}$  were prepared. The  $T_g$  of the final polymer depended on the stiffness of the modifying group. For the purpose of further investigation, methyl, n-butyl, phenyl and 2-ethylhexyl esters of hyperbranched poly(5-acetoxyisophthalic acid), shorthanded as MeHP, BuHP, PhHP and EhHP respectively, were fractionated by using precipitation and chromatography techniques. Samples with polydispersity indexes ranging from 1.16 to 4.57 were obtained.

The structural profiles of hyperbranched polyarylates were investigated. The degree of branching was found invariant of the degree of polymerization indicating these macromolecules had uniform chemical structures, i.e. a monomer attached to a polymer of low molecular weight experienced the same environment as one attached to a polymer of high molecular weight. This feature was significantly different from that of dendritic polymer in which new monomers experienced a more and more steric hindrance as the polymer grew larger. Solution static light scattering of hyperbranched polyarylates

probed the behavior of these polymers under different polymer-solvent interactions. The radius of gyration, i.e. the dimension of hyperbranched polyarylate, remained stable under a variety of experimental conditions. The dimensions of these hyperbranched polymers were also smaller than linear polymers revealing that the polymer had a compact structure. The power  $\nu$  in the relation  $R_g \sim M^\nu$  was  $0.41 \pm 0.03$  in good agreement with the percolation theory. Small second virial coefficients ( $A_2$ ) indicated that the configuration of the polymer in solution was close to that in melt, i.e. there is only limited swelling of the structure by the solvent. On the other hand, light scattering also revealed a small polymer-polymer interpenetration parameter  $\Psi$ , indicating that hyperbranched polyarylate could still be treated as free draining particles on the dimension of solvent. Lanthanide Shift Reagent (LSR), specifically  $\text{Eu}(\text{fod})_3$  of 8 Å in diameter, could penetrate the hyperbranched structure to interact with most of the polar groups so that a large portion of the related peak in  $^1\text{H}$  NMR shifted downfield. Thus, the structure was still porous at this scale. Molecular simulation showed the space filling tendency of the growth of hyperbranched polyarylate. Voids could be clearly identified in the structure which was in agreement with light scattering and LSR experiments. Although larger probes were not available, modification with a large modifying agent, such as etherimide oligomer could not be completed above 50% indicating limited access of the structure for large particles. Furthermore, the dynamic mechanical data of both low and high molecular weight BuHPs showed clear indication of a lack of entanglement between hyperbranched polymers. Thus, we concluded that hyperbranched polyarylates could be treated as hard porous particles with small pore sizes.

Due to the poor toughness caused by the lack of chain entanglement, hyperbranched polyarylate as a solid state material may only find application in blends as either rheology modifiers or other functional components. n-Butyl hyperbranched polyarylate and its linear analog poly(1,4-butylene isophthalate) were employed to

investigate the effect of the hyperbranching topology on blend properties. Although the enthalpic effect was kept at minimum by the choice of the above model polymers, under all experimental conditions, including a wide range of annealing temperature, molecular weight of the hyperbranched polymer and blend composition, the blends were found always immiscible by the observation of glass transitions using DSC. A simplified model based on Flory-Huggins entropy calculation was introduced by utilizing the “hard, porous” profile of hyperbranched component. Entropically, the compact nature of hyperbranched polymer prevented itself from mixing with its linear analog at segmental scale. Unlike linear-linear polymer blends where entropic effect always offers a positive contribution to the miscibility, entropy is not favorable to the mixing of a hyperbranched polymer and a linear polymer. Although immiscible, due to the chemical similarity between the two model polymers, the blends were compatible as revealed by TEM that the domain size of the phase separation was around 400 to 600 Å. The possibility of compatibilization of hyperbranched polymer-linear polymer blends was encouraging from the perspective of future application.

The rheological properties of hyperbranched polymers and their blends presented the most promising aspect for future application. The relaxation spectrum of n-butyl hyperbranched polyarylate did not exhibit a plateau zone which was the indication of chain entanglement for linear polymers. This observation was true even for samples with molecular weight over  $10^5$ . Zero shear viscosity of hyperbranched polyarylate was one magnitude lower than that of its linear analog with comparable molecular weight. Furthermore, the viscosities of their blends showed negative deviations from the so-called “log-additivity rule”. This phenomenon was attributed to the extra free volume created upon microphase separation.

To explore the possibility of using the hyperbranched polyarylate as an anisotropy reducer, an etherimide modified hyperbranched polyarylate (EIHP) was synthesized for the purpose of compatibilization with linear polyetherimide. An AB type etherimide

oligomer which resembled commercial polyetherimide was synthesized and characterized. The modification of poly(5-acetoxyisophthalic acid) with this oligomer could not be completed at 100% due to the compact nature of the hyperbranched polymer. Finally, the mechanical property of blends EIHP and polyetherimide was investigated. While the tensile modulus of the material was enhanced, the toughness was drastically reduced due to the brittle nature of hyperbranched polymer.

In summary, hyperbranched polyarylates are a unique family of materials. Their high functionality, good solubility and hard, porous structure present tremendous potential for future application as the host of catalytic groups or other functional groups. Their special rheological properties make them good candidates as plastisizers that do not compromise the thermal properties of material. However, due to lack of entanglement between macromolecules, hyperbranched polyarylates are intrinsically brittle materials. However, a balance has to be reached to utilize the unique features of these polymers while maintaining the mechanical integrity of material.

#### Suggested future work

All the physical property characterizations done in this thesis were based on a polymer with a hyperbranched backbone of polyarylate. Besides topology of the chain, the bulkyness of aromatic functionality also played a role in determining the “hard and porous particle” profile of the polymer. Effort should be given in the future to characterize hyperbranched polymers with shorter linkages to focus solely on the effect of hyperbranching topology.

As has been mentioned, a balance has to be reached to utilize the unique features of hyperbranched polymer while maintaining the mechanical integrity of material. This should be accomplished by introducing a certain amount of entanglement into the system. To do this, the degree of branching of the polymer has to be reduced by inserting longer linear units in between branching points. It would be an interesting topic to study the

relationship between the mechanical properties and the degree of branching of the polymer.

To further verify the entropy calculation carried out in this thesis, low molecular weight and low PDI poly(1,4-butylene isophthalate) (PBuI) samples have to be obtained and their blends with butyl hyperbranched polyarylate (BuHP) should be examined. However, the glass transition of the linear polymer would be hard to detect at low molecular weight by means of DSC. Thus, solid state NMR technique will be utilized to study the miscibility.

## BIBLIOGRAPHY

- Aihara, T. and Nakayama Y., Prog. Org. Coat., **14**, 103 (1986)
- Aklonis, J. J. and Macknight W. J., Introduction to Polymer Viscoelasticity, 2nd ed., (Wiley: New York) (1983)
- Antonietti, M., Basten, R. and Lohmann, S., Macromol. Chem. Phys., **196**, 441 (1995)
- Antonietti, M., Pakula, T. and Bremer, W., Macromol., **28**, 4227 (1995)
- Bauer, B. J., Briber, B. M. and Hammouda, B., Polym. Prep., **2**, 476 (1992)
- Bauer, J. and Burchard, W., Macromol., **26**, 3103 (1993)
- Briber, B. M., Bauer, B. J. and Hammouda, B., Polym. Prep., **2**, 478 (1992)
- Bromley, C. W. A., J. Coat. Tech., **61**, 768 (1989)
- Cantow, M. J. R., Polymer Fractionation, (Academic Press: New York) (1967)
- Clarson, S. J., Siloxane Polymers, (New Jersey: PTR Prentice Hall) (1995)
- Connolly, J. M., Ma, B. and Karasz, F. E., to be published.
- Connolly, J. M., Ma, B., Wedler, W., Winter, H. H. and Karasz, F. E., to be published.
- Cramer, R. E. and Seff, K., Acta Cryst., **B28**, 3281 (1972)
- de Gennes, P. G., Hervet, H., J. Phys., Lett., **44**, L351 (1983)
- de Gennes, P. G., Scaling Concepts in Polymer Physics, (Cornell University: Ithaca) (1979)
- de Villiers, J. P. R. and Boeyens, J. C. A., Acta Cryst., **B27**, 692 (1971)
- Duan, R. G., Miller, L. L. and Tomalia, D. A., J. Am. Chem. Soc., **117**, 10783 (1995)
- Evans D. J., Kanagasooriam, A., Williams, A. and Pryce, R. J., J. Molecul. Catal., **85**, 21 (1993)
- Ferry, J. D., Viscoelastic Properties of Polymers, (Wiley: New York) (1980)
- Flory, P. J., J. Am. Chem. Soc., **74**, 2718 (1952)
- Flory, P. J., Principle of Polymer Chemistry, (Cornell University: Ithaca) (1971)
- Friedel, and Crafts, Bull. Soc. Chim., **43**, 53 (1885)

- Gitsov, I. and Frechet, J. M. J., Macromol., **26**, 6536 (1993)
- Gitsov, I., Wooley, K. L., Hawker, C. J., Ivanova, P. T. and Frechet, J. M. J., Macromol., **26**, 5621 (1993)
- Han, C. D. and Kim, J. K., Polym., **34**(12), 2533 (1993)
- Harun, G. and Williams, A., Polymer, **22**, 916 (1981)
- Hawker, C. J. and Frechet, J. M. J., J. Am. Chem. Soc. **112**, 7638 (1990)
- Hawker, C. J., Lee, R. and Frechet, J. M. J., J. Am. Chem. Soc., **113**, 4583 (1991)
- Hawker, C. J., Wooley, K. L. and Frechet, J. M. J., J. Am. Chem. Soc., **115**, 4375 (1993)
- Hawker, C. J., Wooley, K. L. and Frechet, J. M. J., J. Chem. Soc., Chem. Commun., **8**, 925 (1994)
- Isaacson, J. and Lubensky, T. C., J. Phys., Lett., **41**, L469 (1980)
- Jacobson, R. A., J. Am. Chem. Soc., **54**, 1513 (1932)
- Kawaguchi, H., Colloid Polym. Sci., **270**, 53 (1992)
- Kawaguchi, T. K., Walker, K. L., Wilkins, C. L. and Moore, J. S., J. Am. Chem. Soc., **117**, 2159 (1995)
- Kim Y. H. and Beckerbauer, R., Macromol., **27**, 1968 (1994)
- Kim, Y. H. and Webster, O. W., Macromol., **28**, 3214 (1995)
- Kremers, J. A. and Meijer, E. W., J. Org. Chem., **59**, 4202 (1994)
- Kricheldorf, H. R. and Stober, O., Macromol. Rapid Commun., **15**, 87 (1994)
- Kricheldorf, H. R., Stober, O. and Lubers, D., Macromol., **28**, 2118 (1995)
- Lang, P., Burchard, W., Wolfe, M. S., Spinelli, H. J. and Page, L., Macromol., **24**, 1306 (1991)
- Lange, P., Schier, A. and Schmidbaurm H., Inorg. Chem., **35**, 637 (1996)
- Lapierre, J., Skobridis, K. and seebach, D., Helvetica Chimica Acta, **76**, 2419
- Lee, J. J., Ford, W. T., Moore, J. A. and Li, Y. F., Macromol., **27**, 4632 (1994)
- Lescanec, R. L. and Muthukumar, M., Macromol., **24**, 4892 (1991)
- Maciejewski, M., Macromol. Sci., Chem., **A17** (4), 689 (1982)

- Mansfield, M. L. and Klushin, L. I., private communication.
- Mark, H. F., Bikales, R. M., Overburger, C. G. and Menges, G., ed., Encyclopedia of Polymer Science and Engineering, 2nd ed., (Wiley: New York) (1990)
- Massa, D. J., Shriner, K. A., Turner, S. R. and Voit, B. I., Macromol., **28**, 3214 (1995)
- Mathias, L. J. and Carothers, T. W., J. Am. Chem. Soc., **113**, 4043 (1991)
- Mayo, S. L., Olafson, B. D. and Goddard, W. A., III., J. Phys. Chem., **94**, 8897 (1990)
- McCrum, N. G., Read, B. E. and Williams, G., Anelastic and Dielectric Effects in Polymeric Solids, (Dover: New York) (1991)
- Mekelburger, H., Rissanen, K. and Vogtle, F., Chem. Ber., **126**, 1161 (1993)
- Meltzer, A. D., Tirrell, D. A., Jones, A. A. and Inglefield P. T., Macromol., **25**, 4549 (1992)
- Meltzer, A. D., Tirrell, D. A., Jones, A. A., Inglefield, P. T., Hedstrand, D. M. and Tomalia, D. A., Macromol., **25**, 4541 (1992)
- Meyer, K. H., Natural and Synthetic Polymers, 2nd ed., pp.456 ff.(Interscience Publishers, New York-London, 1950)
- Miller, T. M. and Neenan, T. X., Chem. Mater., **2**, 346 (1990)
- Miller, T. M., Kwock, E. W. and Neenan, T. X., Macromol., **25**, 3143 (1992)
- Miller, T. M., Neenan, T. X., Kwock, E. W. and Stein, S. M., J. Am. Chem. Soc., **115**, 356 (1993)
- Moore, J. S. and Xu, Z., Macromol., **24**, 5894 (1991)
- Morikawa, A., Kakimoto, M. and Imai, Y., Macromol., **24**, 3469 (1991)
- Morikawa, A., Kakimoto, M. and Imai, Y., Macromol., **25**, 3247 (1992)
- Morikawa, A., Kakimoto, M. and Imai, Y., Macromol., **26**, 6324 (1993)
- Mourey, T. H., Turner, S. R., Rubinstein, M., Frechet, J. M. J., Hawker, C. J. and Wooley, K. L., Macromol., **25**, 2401 (1992)
- Murry, M. J. and Snowden, M., J. Adv. Colloid Interface Sci., **54**, 73 (1995)
- Newkome, G. R. and Lin, X., Macromol., **24**, 1443 (1991)
- Newkome, G. R., Behera, R. K., Moorefield, C. N. and Baker G. R., J. Org. Chem., **56**, 7162 (1991)

- Newkome, G. R., Hu, Y., Saunders, M. J. and Fronczek, F. R., Tetrahedron Lett., **32**, 1133 (1991)
- Newkome, G. R., Moorefield, C. N., Baker, G. R., Johnson, A. J. and Behera, R. K., Angew. Chem., Int. Ed. Engl., **30**, 1176 (1991)
- Newkome, G. R., Yao, Z., Baker, G. R., Gupta, V. K., J. Org. Chem., **50**, 2004 (1985)
- Newkome, G. R., Young, J. K., Baker, G. R., Potter, R. L., Audoly, L., Cooper, D. and Weis, C. D., Macromol., **26**, 2394 (1993)
- Nielsen, L. E. and Landel, L. E., Mechanical Properties of Polymers and Composites, 2nd Ed., (Marcel Dekker: New York) (19
- Pankasem, S., Thomas, J. K., Snowden, M. J. and Vincent B., Langmuir, **10**, 3023 (1994)
- Paul, D. R. and Newman, S., Polymer Blends, (New York: Academic Press) (1978)
- Percec, V. and Kawasami, M., Macromol., **25**, 3843 (1992)
- Percec, V., Chu, P., Ungar, G. and Zhou, J., J. Am. Chem. Soc., **117**, 11440 (1995)
- Rao, C. and Tam, J. P., J. Am. chem. Soc., **116**, 6975 (1994)
- Seyferth, D., Son, D. Y., Rheingold, A. L. and Ostrander, R. L., Organometallics, **13**, 2682 (1994)
- Slany, M., Bardaji, M., Casanove, M., caminade, A., Majoral, J. and Chaudet, B., J. Am. Chem. Soc., **117**, 9764 (1995)
- Small, P. A., J. Appl. Chem., **3**, 71 (1953)
- Snowden, M. J. and Booty, M. T., in Karsa, D. (Ed.), Encapsulation and Cotrolled Release., Royal Society of Chemistry, p.141 (1993)
- Stacey K. A., Weatherhead R. H. and Williams, A., Makromol. Chem., **181**, 2517 (1980)
- Stauffer, D., Introduction to Percolation Theory; (Taylor and Francis: London) (1985)
- Suzuki, H., Kimata, Y., Satoh, S. and Kuriyama, A., Chem. Lett., **4**, 293
- Suzuki, M., Ii, A. and Saegusa, T., Macromol., **25**, 7071 (1992)
- Tomalia, D. A., Naylor, A. M. and Goddard, W. A., III., Angew. Chem. Int. Ed. Engl., **29**, 138 (1990)
- Tomalia, D.A., Baker, H., Dewald, J., Hall, M., Kallos, G., Martin, S., Roeck, J., Ryder, J. and Smith, P., Polym. J., **17**, 117 (1985)

- Turner, S. R., Voit, B. I. and Mourey, T. H., Macromol., **26**, 4617 (1993)
- Turner, S. R., Walter, F., Voit, B. I. and Mourey, T. H., Macromol., **27**, 1611 (1994)
- Uhrich, K. E., Hawker, C. J., Frechet, J. M. J. and Turner, S. R., Macromol., **25**, 4583 (1992)
- Utracki, L. A., Polymer Alloys and Blends: Thermodynamics and Rheology, (New York: Hanser) (1989)
- van Hest, J. C. M., delnoye, D. A. P., Baars, M. W. P. L., van Genderen. M. H. P. and Meijer, E. W., Science, **268**, 1592 (1995)
- Wachenfeld-Eisele, E. and Burchard, W., Macromol., **22**, 2496 (1989)
- Wenzel, T. J., NMR Shift Reagents, (CRC Press: Bocca Raton) (1987)
- White, D. M., Takekoshi, T., Williams, F. J., Relles, H. M., Donahue, P. E., Klopfer, H. J., Loucks, G. R., Manello, J. S., Matthews, R. O. and Schluez, R. W., J. Polym. Sci., Polym. Chem. Ed., **19**, 1635 (1981)
- Wooley, K. L., Hawker, C. J. and Frechet, J. M. J., J. Am. Chem. Soc., **113**, 4252 (1991)
- Xu, Z. and Moore, J. S., Angew. Chem. Int. Ed. Engl., **32**, 246 (1993)
- Yamakawa, H., Modern Theory of Polymer Solution, (Harper and Row: New York) (1971)
- Young, J. K., Baker, G. R., Newkome, G. R., Morris, K. F. and Johnson, C. S., Jr., Macromol., **27**, 3464 (1994)
- Zhang, Y., Wang, L., Wada, T. and Sasabe H., J. Polym. Sci., Part A: Polym. Chem., **34**, 1359 (1996)
- Zhou, Y., Bruening, M. L., Bergbreiter, D. E., Crooks, R. M. and Wells M., J. Am. Chem. Soc., **118**, 3773 (1996)
- Zimm, B. H. and Stockmayer, W. H., J. Chem. Phys., **17**, 1301 (1949)



